UFL/COEL-92/006

Sebastian Inlet Physical Model Studies
Final Report – Movable Bed Model

by

Hsiang Wang
Lihwa Lin
Gang Miao

May, 1992

Submitted to:

Sebastian Inlet District Commission
Sebastian Inlet, Florida.

REPORT DOCUMENTATION PAGE

1. Report No.	2.	3. Recipient's Accession No.

4. Title and Subtitle	5. Report Date
SEBASTIAN INLET PHYSICAL MODEL STUDIES Final Report -- Movable Bed Model	May 10, 1992 6.

7. Author(s)	8. Performing Organization Report No.
Hsiang Wang, Lihwa Lin, Gang Miao	UFL/COEL-92/006

9. Performing Organization Name and Address	10. Project/Task/Work Unit No.
Coastal and Oceanographic Engineering Department University of Florida 336 Weil Hall Gainesville, Fl.32611	11. Contract or Grant No.
	13. Type of Report Final
12. Sponsoring Organization Name and Address Sebastian Inlet District Commission Sebastian Inlet Tax District Office 134 Fifth Avenue Suite 103, Indialantic, FL 32903-3164	14.

15. Supplementary Notes

16. Abstract

A movable bed model study was conducted to investigate nine structural configurations to assess the sediment transport process in the vicinity of the Sebastian Inlet. The model has a vertical to horizontal scale distortion of 2 to 3. A horizontal scale of 1 to 60 was selected to cover approximately 2,500 ft of shoreline. The vertical scale is 1 to 40. Natural beach sand of finer grain than the native sand at the Sebastian Inlet was used to fulfill the scale requirement.

The nine tested structural configurations constitute various combinations of jetty extension, ebb shoal material removal and beach nourishment. The test conditions consisted of 6-day(prototype equivalent) storm waves from NE and SE; 8-day recovery waves from E and 8-day normal waves from NE direction.

The shoreline immediately south of south jetty (within 2000 ft south) suffers recession for all tested configurations under storm waves from NE and SE. The recovery is difficult in the vicinity of the south jetty. The ultimate shoreline position south of the south jetty appears to be dictated by the length and configuration of the south jetty. Significant bathymetric change also occurs in the nearshore zone on the south side of the south jetty, which is due to strong alongshore current.

Ebbshoal removal, extension of south jetty and beach nourishment all induce increased rate of downdrift transport. The last case is seen to have the mild shore erosion.

17. Originator's Key Words	18. Availability Statement
Erosion Sediment transport Shore erosion Structural alternative	

19. U. S. Security Classif. of the Report	20. U. S. Security Classif. of This Page	21. No. of Pages	22. Price
Unclassified	Unclassified	108	

PREFACE

This report presents results of the experiments of the existing inlet and eight structural alternatives to the Sebastian Inlet from a movable bed model. It is intended to find solutions for improvement of boating safety and protection of beaches adjacent to the inlet. Based upon the experimental results from here and the fixed bed model study, which is summarized in Part I report, an optimum structural modification plan was then recommended providing a general frame of improvement scheme.

The research in this report was authorized by the Sebastian Inlet District Commission of September 15, 1989. The University of Florida was notified to proceed on November 14, 1989. The study and report were prepared by the Department of Coastal and Oceanographic Engineering, University of Florida. Coastal Technology Corporation was the technical monitor representing the Sebastian Inlet District.

Special appreciation is due to Mr. Michael Walther of Coastal Tech. for his continuous technical assistance. Other personnel at Coastal Tech. and Inlet District Office including Dr. Paul Lin, Ms. Kathy FitzPatrick and Mr. Raymond K. LeRoux also provided their support at various stages of the experiment. Appreciation is also due to Mr. T. Kim and Mr. J. Lee, both graduate assistants in the Coastal Engineering Department, University of Florida, for their participation in laboratory and field experiments.

Contents

List of Figures

List of Tables

Sebastian Inlet Physical Model Studies
Final Report – Movable Bed Model

1 Introduction

1.1 Authorization

This study and report were authorized by the Sebastian Inlet District Commission of September 15, 1989. On November 14, 1989, the "University of Florida" was notified to proceed. This report was prepared by the Department of Coastal and Oceanographic Engineering, University of Florida. Coastal Technology Corporation was the technical monitor representing the Sebastian Inlet District.

On May 23, 1919, the original legislation establishing the Sebastian Inlet District (District) was passed by the State of Florida. In 1927 the Florida Legislature passed Chapter 12259, Laws of Florida, which amend the original governing legislation of the District. Chapter 12259 prescribes that "It shall be the duty of said Board of Commissioners of Sebastian Inlet District to construct, improve, widen or deepen, and maintain an inlet between the Indian River and the Atlantic Ocean..." [1].

1.2 Purpose

The main objective of the study aims to find solutions improving the inlet navigation as well as beach preservation at the Sebastian Inlet through physical model experiments. The study was concentrated in testing the hydrodynamic and littoral sediment drift properties for the existing inlet and several other structure configurations, including modification of the jetties and excavation of the ebb shoal.

Two physical models were conducted in the study: a fixed bed model for the hydrodynamic study and a movable bed model for the littoral sand process study. The results of the fixed-bed model study were summarized in the Part I report. The preliminary results of the movable-bed model experiment for the existing inlet and two other alternative structural configurations, which modify the existing jetties, were summarized in the Part II report. The final results of the complete movable-bed model study, which includes testing another six structure alternatives, were summarized in this report.

1.3 Background

Sebastian Inlet is located at the Brevard/Indian River County line approximately 45 miles south of Port Canaveral entrance and 23 miles north of Fort Pierce Inlet. It is a man-made cut connecting the Atlantic Ocean to the Indian River Lagoon (Figure 1). Its coordinates are as follows:

Latitude	Longitude
27° 51' 35" N	80° 26' 45" W

The First attempt to cut a man-made inlet in the Sebastian area was made in 1886 [2]. In the ensuing 60 years or so, the inlet closed, re-opened and shifted a number of times. The present configuration was maintained after a major dredging operation in 1947-48 to open a new channel. Since 1948, a series of dredging operations and jetty improvements have kept the inlet open in this existing configuration [3]. In 1962, a channel of 11 ft deep was excavated.

In 1965, the A1A bridge across the inlet was completed (State Project Number 88070-3501) and navigation guides were installed in the open section under the bridge which forms a natural throat of the inlet.

East of the bridge the dredged channel width was 200 ft and west of the bridge the width was 150 ft. In 1970, the north and south jetties were extended to their present configuration as shown in Figure 2, based on the results of a model study by the Department of Coastal and Oceanographic Engineering, University of Florida [4]. The present south jetty is a sand-tight rubble mound structure. The north jetty, on the other hand, is of composite nature; the original section completed before 1955 is rubble mound but the extension in 1970 with total length of 452 ft is a pier structure supported by concrete pilings. The rubble mound base only extends to the mean sea level.

The channel has a rocky bottom of marine origin. The cross section in the vicinity of the throat is about one-half that which would result in a stable inlet with sandy bottom. In other words, the tidal prism is about twice the value corresponding to the cross section. This has resulted in rather strong currents through the inlet, over 8 ft/sec during both flood and ebb. So far, the channel remains open with minimal maintenance dredging. Shoals were, however, gradually forming on both sides along the banks of the inlet. The navigation channel becomes narrower as a consequence. The ebb shoal from the south is also slowly encroaching into the inlet creating a cross shoal near the mouth. This shoal enhances the incoming waves and causes them to break. These combined effects have created a hazardous condition for small craft in the vicinity of the inlet entrance.

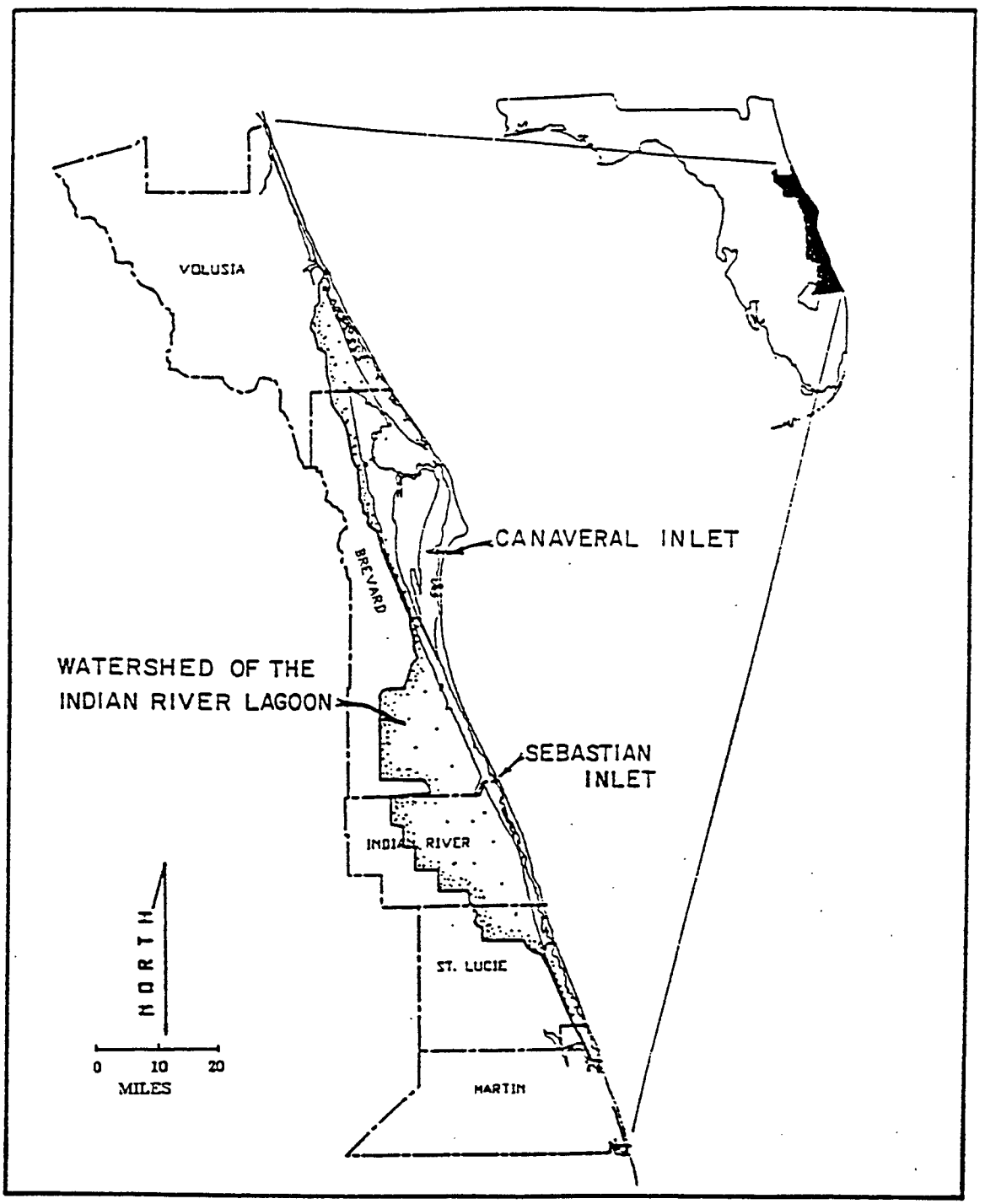

Figure 1: Location of Sebastian Inlet, Florida.

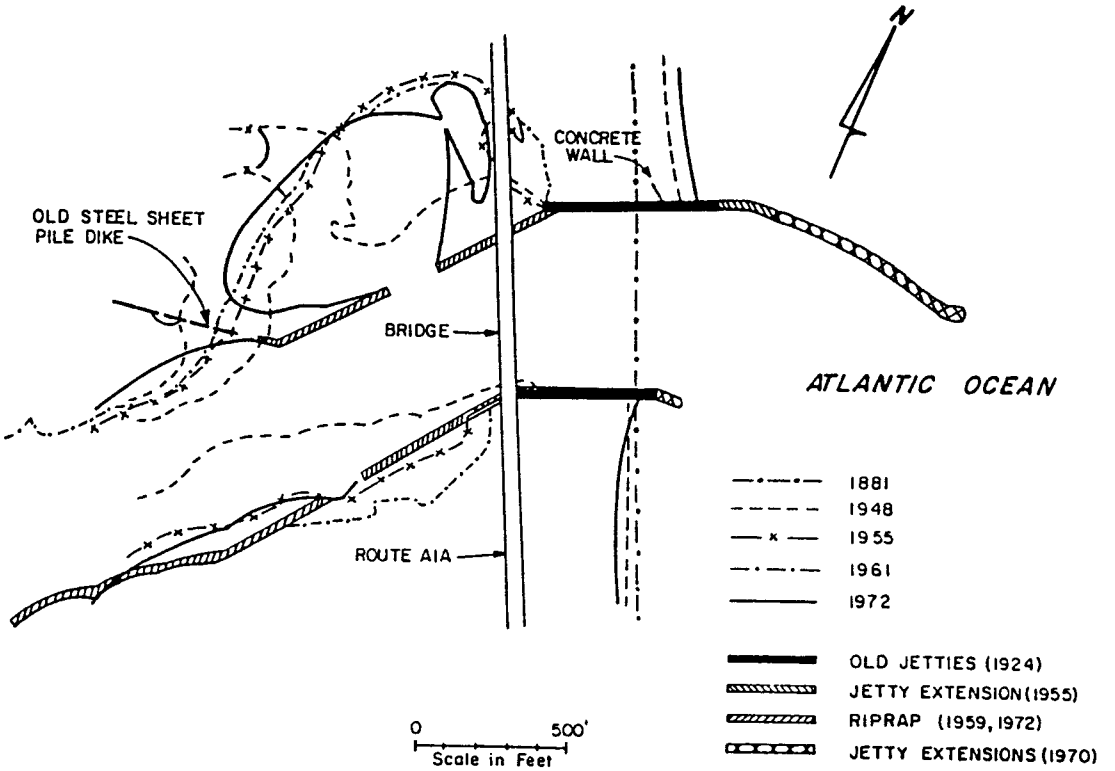

Figure 2: Jetty configuration and shoreline changes since 1881.

In 1987, Coastal Technology Corporation carried out a "Comprehensive Management Plan" study for the Sebastian Inlet District Commission [5]. In which, various engineering alternatives for maintenance and improvement of inlet navigation and beach preservation were presented. The present study is to evaluate these alternatives through physical model experiments.

1.4 Scope

The general purpose of this study is to conduct physical model investigation for inlet navigation improvement and sand transfer schemes; the former is a fixed-bed model study and the latter a movable-bed model study. The fixed-bed model experiments were completed in November, 1990, and the results were summarized in the Part I Report. The movable bed model was first tested for the existing inlet structure and two modified jetty configurations subject to the northeaster storm waves and the results were summarized in the Part II report. The model was then tested for another six structure alternatives subject to storm, normal and swell-dominated waves. The final results for the completed movable-bed model experiment are presented in this report.

The movable bed model was conducted in the three dimensional wave basin at the Coastal and Oceanographic Engineering Laboratory, University of Florida.

This model study includes testing the existing inlet and eight other structure alternatives. Through the model study, the littoral transport, onshore and offshore sand transport, shoreline changes, entrapment of sand by the inlet and ebb shoal system, etc., for the different structure alternatives were evaluated. The information is then synthesized to estimate the sediment balance as well as the sediment deficit of the inlet-beach system. From this analysis, the effects of different structure alternatives are evaluated.

In addition to the movable bed model study, a Sediment budget analysis was perform based upon the combined information from historical data, hindcasting model and the evidence produced in the movable model.

2 Model Characteristics

The movable bed model was constructed at the Coastal and Oceanographic Engineering Laboratory, University of Florida, for the purpose testing the littoral and ebbshoal sand drift processes at the Sebastian Inlet due to different alternative structural configurations.

2.1 Modeling Laws and Model Scales

The movable bed modeling laws utilized here were developed by Wang et.al. [6,7]. The basic hypotheses are that the similarities of both wave form and suspended sediment trajectories are preserved between the model and prototype. Based upon this hypothesis, the following modeling laws were derived:

$$\delta = W^{2/5}\lambda^{4/5} \tag{1}$$

$$N_T = \lambda/\sqrt{\delta} \tag{2}$$

$$N_t = \sqrt{\delta} \tag{3}$$

where λ is the horizontal length scale, δ is the vertical length scale, W is the fall velocity scale, N_T is the fluid motion time scale, and N_t is the morphological time scale. All the scales are defined as the ratios of prototype to model.

Since the modeling laws are based on suspended sediment mode, they seem to be more applicable to storm conditions as opposed to mild wave environment. In the model, natural fine sand with D_{50}=0.17mm was used as the bed material whereas the beach sand in Sebastian Inlet has a D_{50}=0.35mm. The corresponding fall velocities to the two grain sizes at 10°C or 50°F are 0.6inch/sec and 1.8inch/sec, respectively. Thus, W=3 in Eq.(1). A horizontal length scale of $\lambda = 60$ was

selected, which permits to model the desired prototype range without encountering significant scale effect. The proper vertical length scale was then calculated from Eq.(1), which yielded $\delta = 41$. This vertical scale was rounded off to 40 in the model. That is, the movable bed model constructed is, accordingly, scaled with a horizontal to vertical distortion of 3:2.

The fluid motion time scale and the morphological time scale were computed from Eqs.(2) and (3), which gave $N_T = 9.5$ and $N_t = 6.324$. Thus, for examples, a one-second wave in the model is equivalent to a 9.5-second wave in the prototype, and the amount of sediment transport in a duration of one hour in the model is equivalent to a duration of 6.324 hours in the prototype.

2.2 Model Construction

The movable bed model was conducted in the three dimensional wave basin at the Coastal and Oceanographic Engineering Laboratory, University of Florida. It models the study area approximately 2,000 ft of shoreline on either side of the inlet entrance, landward of the 30 ft offshore depth contour to the A1A bridge (Figure 3). The model was constructed by placing a layer of natural fine sand, D_{50}=0.17mm., over the existing fixed-bed physical model. The sand layer is generally thick, at least 2 inches in thickness to insure movable bed characteristics, in the beach and ebbshoal area, and becomes thinner in the offshore region. The bed was then molded by sections using templates to the scaled-down prototype topography of 1989 survey (provided by Coastal Tech. Corp.). Since the Inlet bottom is bed rocks; it was simulated with small pebbles to attain the proper roughness. The model bathymetries were leveled in with reference to 1929 N.G.V.D. The model setup is shown in Figure 3.

The general north-to-south transport of sediment is also simulated in the model where a sufficiently large amount of source sand was placed just inside the north beach boundary before an experiment. Therefore, the original shoreline in model is seen curving toward the sea near the north boundary.

3 Experiments

The existing inlet configuration and eight structure alternatives were tested in the movable-bed model experiment. In each case, a combination of current/wave conditions was tested. The survey program was also established in the experiment to monitor the sediment drift in the model from different structure alternatives.

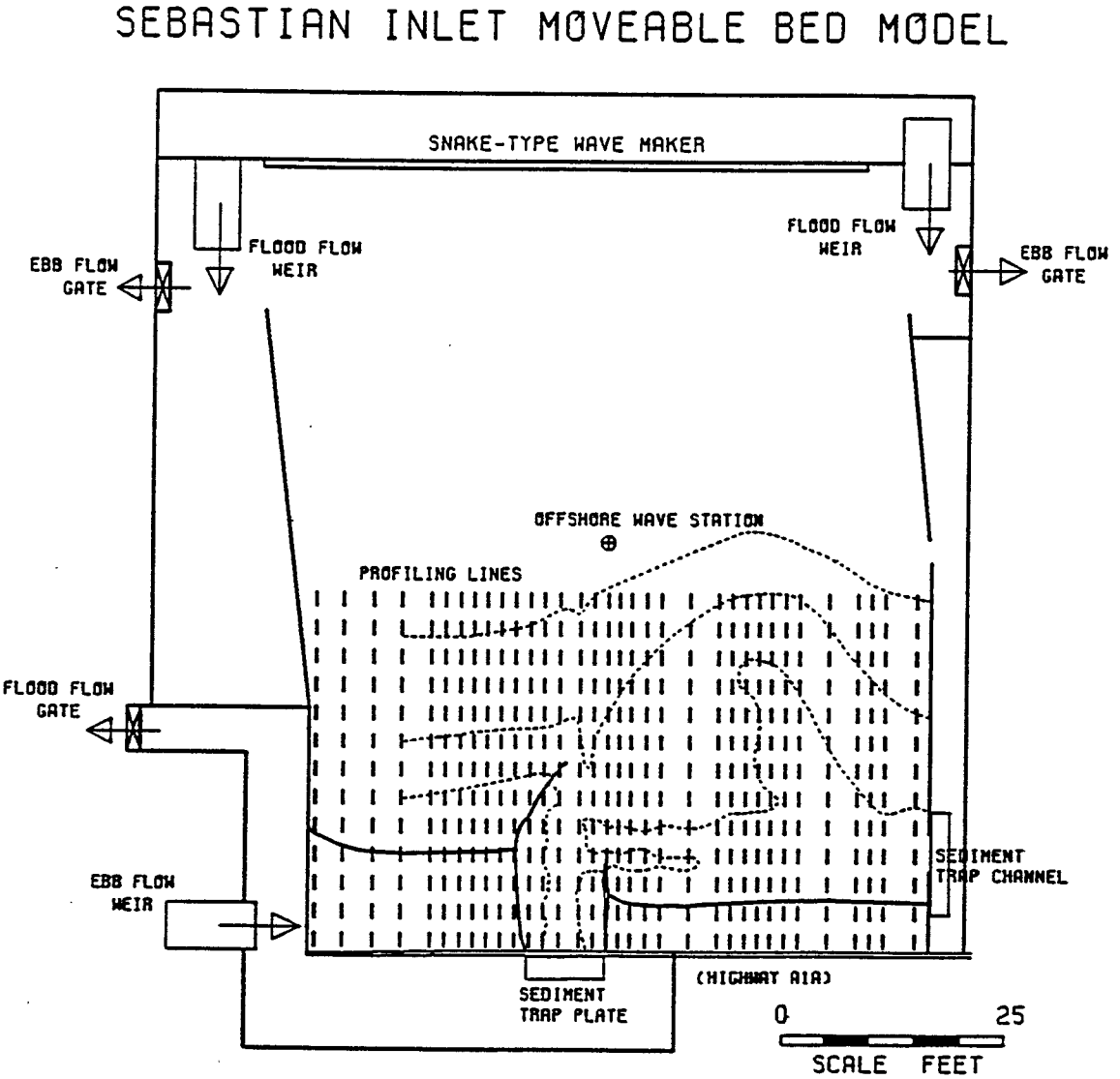

Figure 3: A sketch of the movable bed model; short-dashed lines showing locations for monitoring the bottom profiles.

3.1 Test Program

The test program is designed to examine the following:

- The effects of jetty alternations on shoreline and nearshore topography.
- The effects of ebb tidal shoal removal (partial and total) on shoreline and nearshore topography.
- The effects of beach nourishment to nearshore environment.

The existing jetty configuration and eight other structure alternatives are selected for the movable-bed model experiment. They are identified as S0, S1, S2, $\cdots$ to S8 structures. with the existing jetty configuration designated as S0 These nine structural configurations, one existing and eight alternatives, are described as follows:

A brief summary of these structures are given below:

S0 – Existing jetty configuration.

S1 – The S0 configuration with the north jetty extended 250 ft southeastward with a radius of approximately 900 ft.

S2 – The S1 configuration with a hooked south jetty extension of 150 ft.

S3 – S0 configuration plus 150 ft south jetty extension but with no north jetty extension.

S4 – S0 configuration with nearly 50% ebb shoal removal in the order of 500,000 yd^3, herein referred as total or full removal.

S5 – S0 with about 25% ebb shoal removal in the amount of 230,000 yd^3, herein referred to as partial removal.

S6 – S4 with both north and south jetties removed.

S7 – S0 with a 250,000 yd^3 nourishment on the south beach. The width of the beach is increased by approximately 150 ft.

S8 – S7 with south jetty extended by 500 ft from the existing jetty configuration.

These nine configurations are shown in Figure 4.

The test wave conditions include storm waves, moderate normal waves, and swell-dominated waves. The wave directions are from NE (10^o left to shoreline

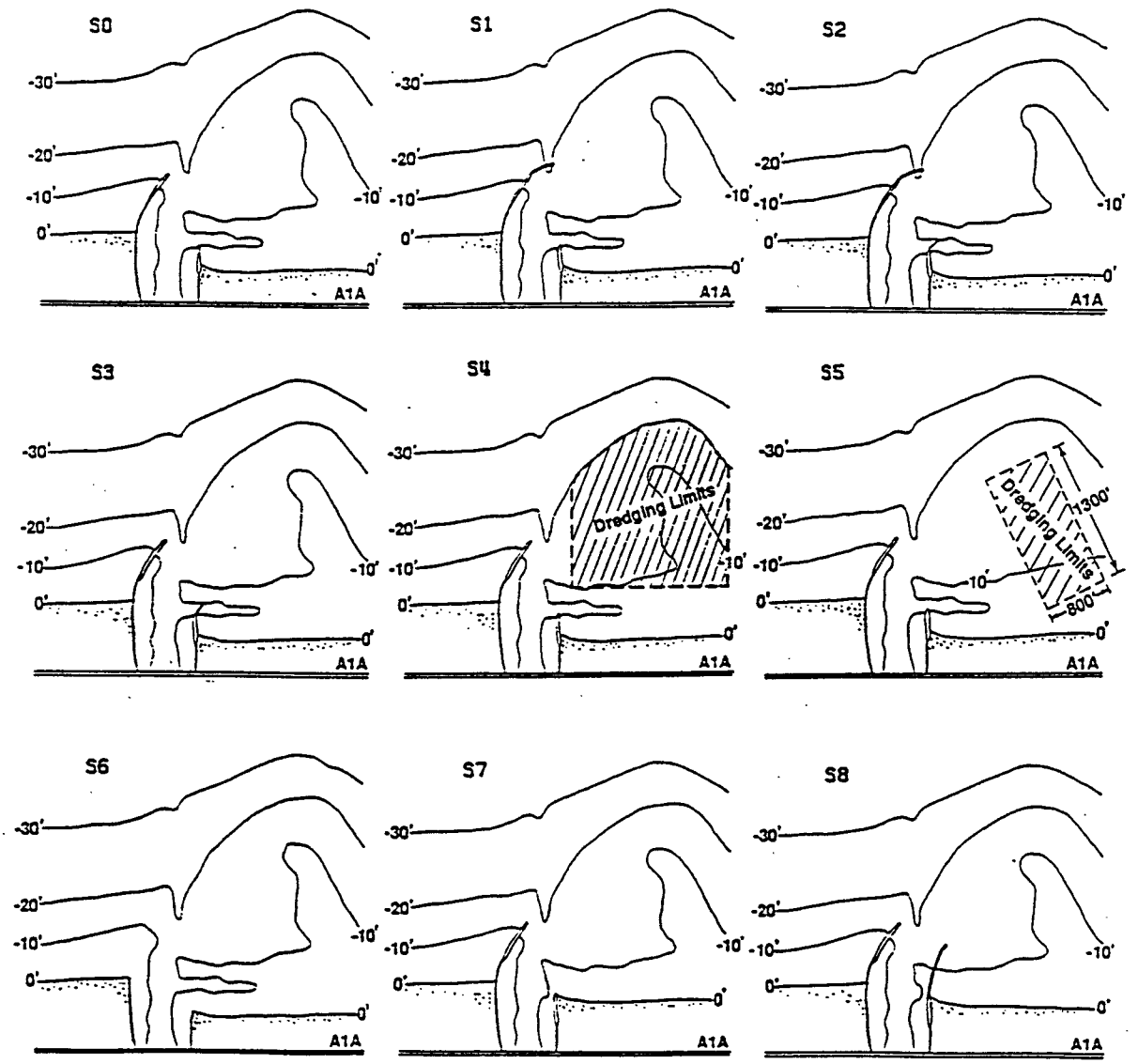

Figure 4: Nine tested structural configurations.

Table 1: The input wave conditions.

Tested Case	Wave Height	Wave Period
6 Days NE Storm Waves	6 ft	8 sec
8 Days E Swells	2 ft	16 sec
20 Days NE Normal Waves	2 ft	6 sec
6 Days SE Storm Waves	6 ft	8 sec

normal), E (shoreline normal) and SE (10° right to shoreline normal). These conditions are given in Table 1.

The test durations vary from 6 to 8 days prototype equivalent depending upon whether the test is for storm erosion (6 days) or moderate erosion (8 days) or swell-dominated recovery process (8 days). Within each test period, the maximum flood and ebb currents for semi-diurnal tides (approximately two high, two low tides in a day) are generated alternately based on the scaled time durations. The corresponding current strength is 6.6 ft/sec for flood and 5.0 ft/sec for ebb. These current strengths are determined from field measurements reported in the fixed bed model study [3].

The survey program of the model experiment includes monitoring 34 bottom profiles – six profiles are located at the inlet – with the spacings and ranges shown in Figure 3. Along each line, the survey intervals are 3 inches (15 ft prototype equivalent) from shoreline to the 10 ft contour line and one foot (60 ft prototype equivalent) beyond the 10 ft contour line.

The bottom profiles were surveyed regularly before and after an experiment. Due to rapid topographic changes in the case of storm erosion, the prototype equivalent 2-day storm profiles were generally surveyed for all tested cases. Several more intermediate surveys for the storm erosion case were also conducted for the S0 and S1 configurations; for the S0 configuration these additional surveys were at intervals of 1/4, 1/2, 1, and 2-day prototype-equivalent and for the S1 configuration they were at 1/4, 1/2, 1, 2, 3, and 4-day prototype-equivalent.

Table 2 summarizes the test program described above.

Table 2: Testing program and experimental conditions.

Wave Condition structure*	6-day NE† Storm wave ht:6' period: 8s	8-day E Recovery 2' 16s	8-day NE Normal 2' 6s	6-day SE Storm 6' 8s
(S0) Existing configuration	6-day run+ 3 surveys	6-day run+ 1 survey	8-day run+ 1 survey	6-day run+ 2 surveys
(S1) Extension of N jetty	same	same	—	—
(S2) Extension of N/S jetties	same	same	same	—
(S3) Extension of S jetty	same	same	—	same
(S4) Total ebb shoal removal	same	same	same	—
(S5) Partial ebb shoal removal	same	same	—	same
(S6) Removal of N/S jetties	same	same	same	—
(S7) South beach nourishment	same	—	—	—
(S8) Jetty extension and beach fill	same#	—	—	—

† Wave directions (from).

* North jetty is extended by 250 ft in S1 and S2, and south jetty by 150 ft in S2 and S3; Ebb shoal is dredged in S4 and S5; South beach is nourished in S7 and S8.

Also tested for the case when inlet is closed by a gate.

3.2 Test Procedures

The experimental procedures are:

- Preparation of initial bathymetry.
- Survey of initial profiles.
- Establishment of the specified current and water level conditions following the same procedures as the fixed-bed model experiments.
- Generation of waves in model to start the experiment for the scaled duration. For instance, a 6-day storm wave test is equivalent to a total 22.8 hours run time in the model consisting of 12 complete semi-diurnal tidal cycles (one complete tidal cycle consists of one high and one low tides).
- Survey of bottom profiles at designated tidal cycles, say, at 1, 2, 4 or other integer number of tidal cycles and the post-experiment profiles.
- collections of sand transported to the inlet and those to the downdrift boundary.
- Reshape of the bottom to the initial bathymetry for the next experiment. For recovery tests, the initial condition is the post-storm condition. And for normal erosion tests, the initial condition is the post-recovery condition.

4 Experimental Results

The existing jetty configuration (S0) and eight structural alternatives (S1 to S8) were tested subject to NE storm waves for a duration equivalent to six days in prototype. For the S0 to S6 configurations the tests were continued with E swells intended for beach recovery for eight days prototype-equivalent. The S0, S2, S4, and S6 structures were also tested with the NE normal waves; the test duration was 20 days prototype-equivalent for S0 and eight days for the rest. For the SE storm wave condition, only S0, S3, and S5 were tested for a 6-day prototype-equivalent since the SE storms of this duration are rare events in this area.

The state of erosive or accretive beach against the tested wave conditions is determined by the established criterion delineated in Figure 5 using the wave steepness, $2\pi H/gT^2$ (where H and T stand for wave height and period, respectively), and the non-dimensional sediment fall velocity, $\pi W/gT$ (where W stands for the fall velocity) as the parameters. If the plotting position of the test condition falls in the region above the diagonal line, the condition should be accretional (or normal

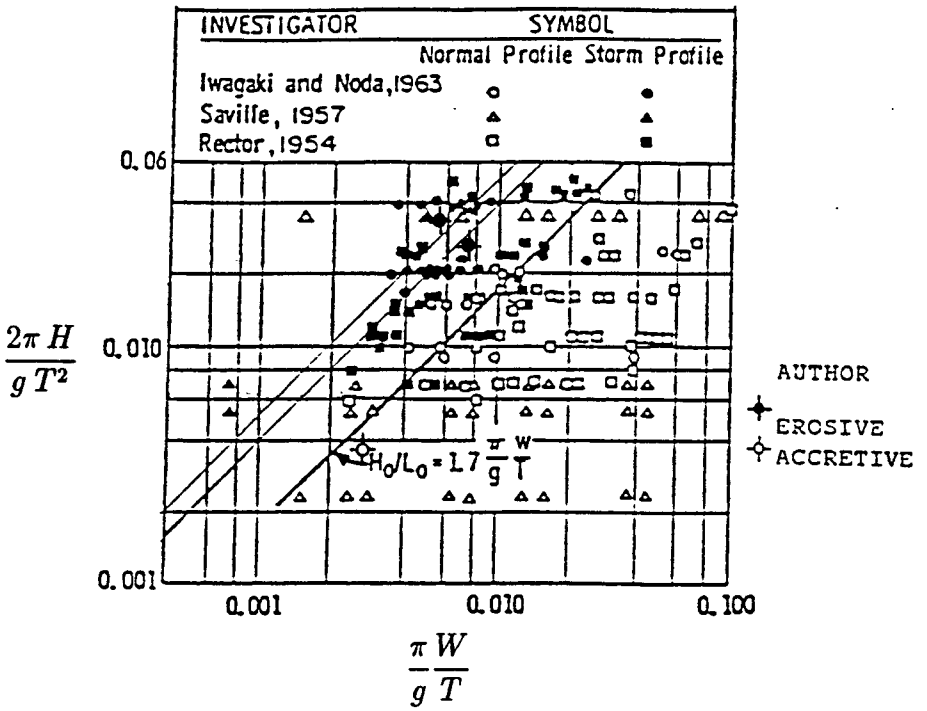

Figure 5: Criterion of normal and storm profiles.

profile); if the plotting position falls below the line it is erosional (or storm profile). It is seen that the tested storm condition falls inside the zone of erosive profile and the recovery condition falls in the zone of normal profile.

4.1 General Observations

Surveys were generally performed for the tested structure along the 34 profile lines as shown in Figure 6. They were numbered from the north boundary at JA (in the present case the updrift boundary) to the south boundary at J30 (the downdrift boundary). The spacing between any two adjacent profiles ranged from 1.5 ft to 3.5 ft. The surveys for the S1 and S2 structural configurations, however, included only 26 (J3 to J27) and 30 (JA to J27) profiles, respectively, as they were selected in the earlier stage of the experiment. More survey lines were added in the latter experiments to provide better spatial resolutions. The northernmost four profiles (JA to J2) and the southernmost four profiles (J28 to J30) were judged to be in the regions influenced by the model boundaries. Therefore, they were excluded in most of the analyses. Along each profile, bottom was surveyed at a regular intervals of 1 ft in the offshore region and 1/4 ft in the nearshore region.

The north jetty was located in the model at J6 and the south jetty was at J12. The shoreline south of the inlet was about twice as long as the shoreline north of the inlet in the model. The initial profile lines surveyed for the S0 structural configuration is shown in Figure 7. Ideally, these initial profiles should be the same for all other configurations. In practice, they varied somewhat because of the remolding process after each test configuration. All the surveyed data collected

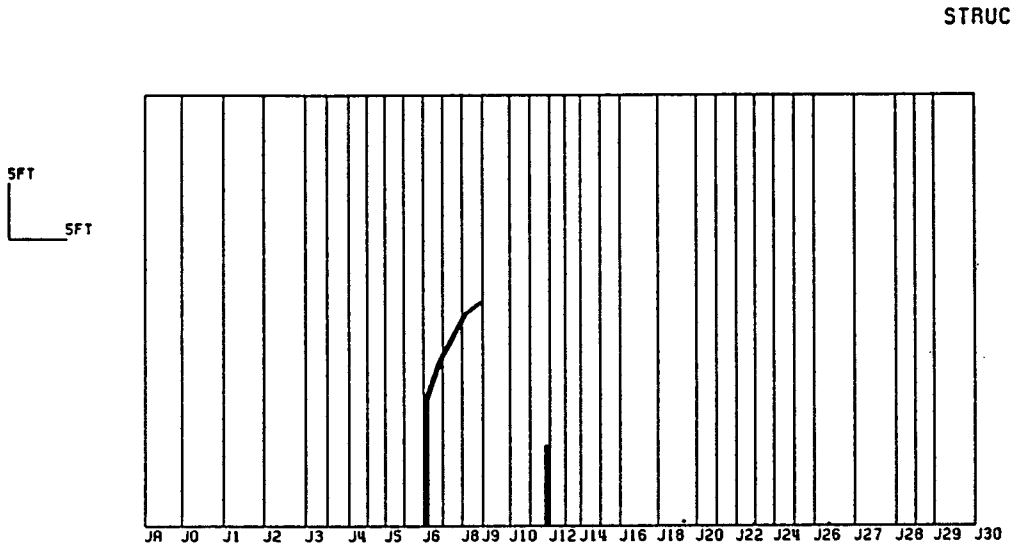

Figure 6: Locations and labels of bottom profiles surveyed in the model.

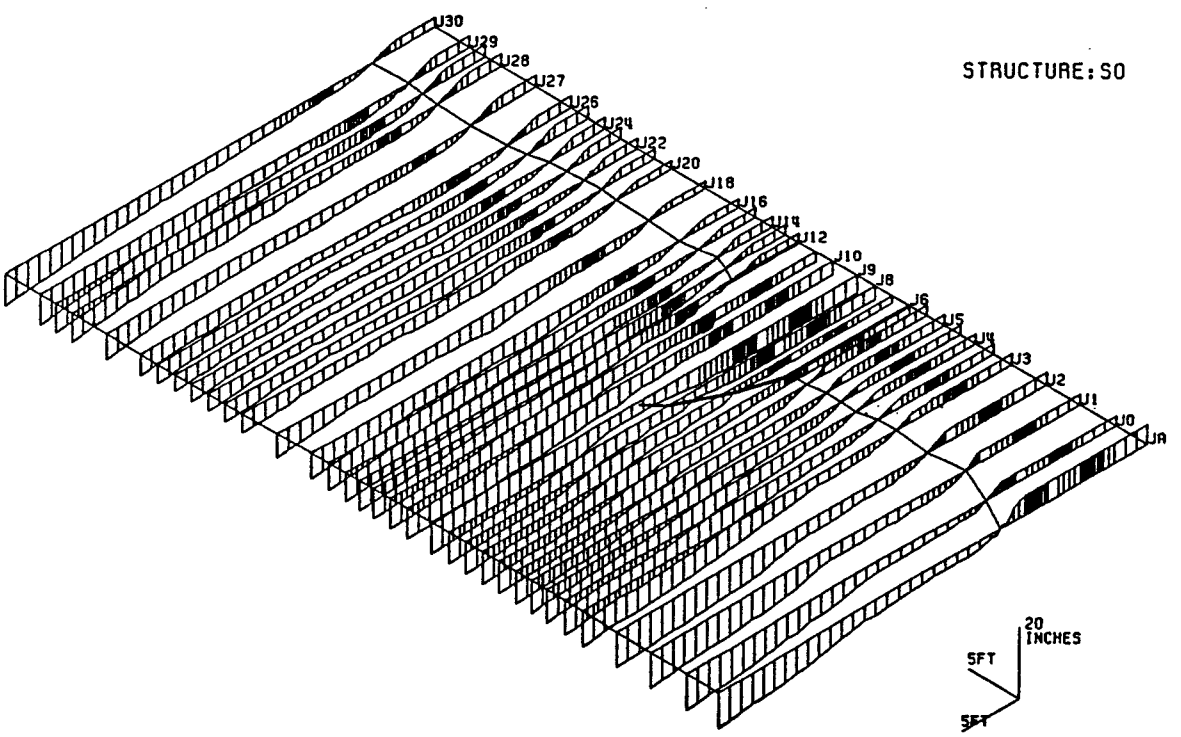

Figure 7: Initial profiles prepared in the model.

are digitized and stored in the VAX-8350 computer and the reduced data are available in 3.5" floppy diskettes at the Department of Coastal and Oceanographic Engineering, University of Florida.

Based upon the results of the profile survey, the shoreline and topographic changes were determined as the differences between the survey and the initial profiles. Figure 8 shows an example of the profile changes and shoreline positions for the S0 configuration under 6-day NE and SE storm waves; Figure 9 shows the results corresponding to a 8-day swell-like waves from the east and to a 20-day moderate waves from NE simulating normal wave conditions in this region. In here, the positive values of elevation change correspond to accretion and negative values indicate erosion. The shoreline in the model is defined as corresponding to the 2 ft NGVD elevation in the prototype. These figures provide a visual display of the erosional and accretional patterns.

The same data can be used to construct the contour maps of bathymetric changes between surveys. Examples of the contour maps of bathymetric changes for the S0 configuration corresponding to the cases shown in Figures 8 and 9 are given in Figures 10 and 11. The quantities of net sediment loss or gain in any designated area can be determined from these maps by integrating the volume differences within the area. The complete set of contour maps of the bathymetric changes for all the tested configurations are given in Appendices I, II, III, and IV.

The general sediment transport patterns for all the tested configurations under various wave conditions were similar to those for S0 shown in Figures 10 and 11. Beach erosion and nearshore sand losses were always noticeable on both sides of the inlet near the jetties. Under NE storm waves, the overall sand transport direction was from north to south. Under SE storm waves, the overall sand transport direction was then seen from south to north. Under E swell-like recovery waves and NE moderate waves, sand transport in the longshore direction was negligible on either side of the jetties except for S6 configuration where both jetties were removed. Under this configuration, the inlet behaved like a sink drawing large quantity of sand from both sides.

Under the NE storm wave condition, the sediment transport on the north side near the inlet followed a path from nearshore to offshore and then to south – with most of the sand transported seaward of the north jetty, bypassing the inlet, to the downdrift south side beach through the ebb shoal; a much smaller amount of sediment was carried directly into the inlet following the flood currents in the main channel. The southward sand bypassing was, however, weaker in S1 and S2 in which the north jetty was extended which tends to block the passage of the sediment. Nevertheless, this weaker southward transport could be a transient phenomenon. As the bathymetry becomes gradually adjusted to the new jetty configuration, the southward transport could also be gradually restored to the existing condition.

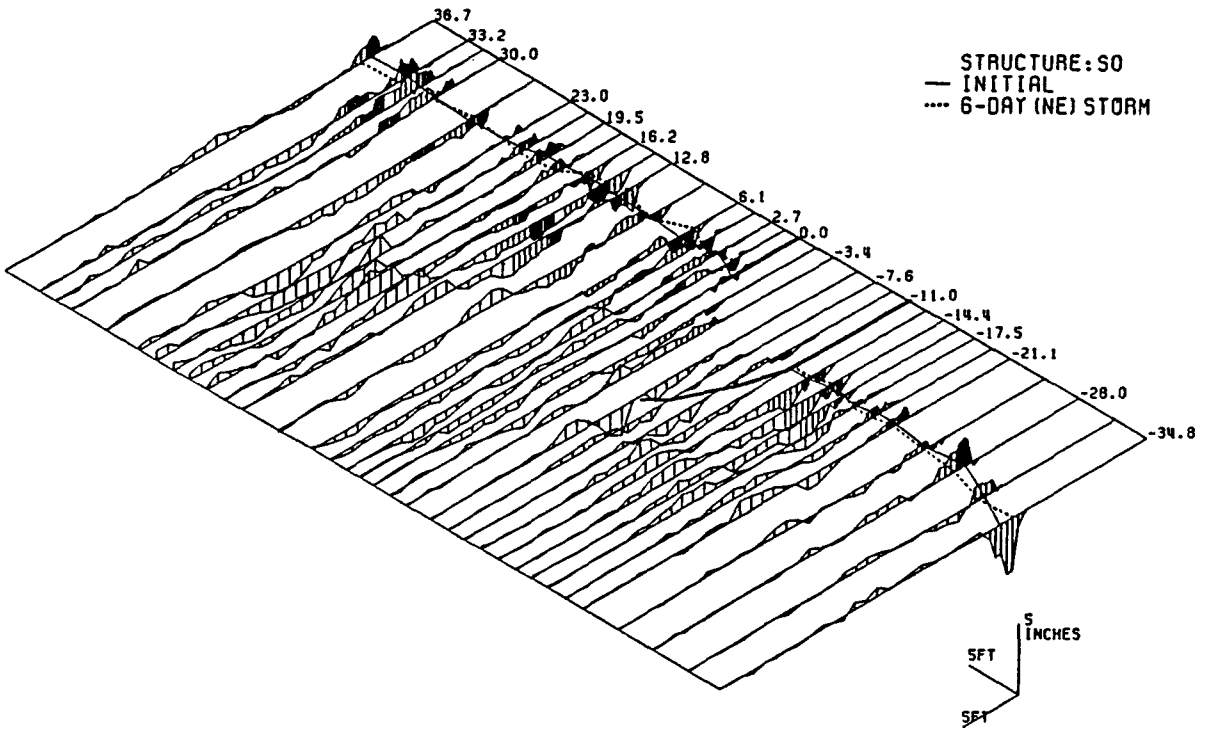

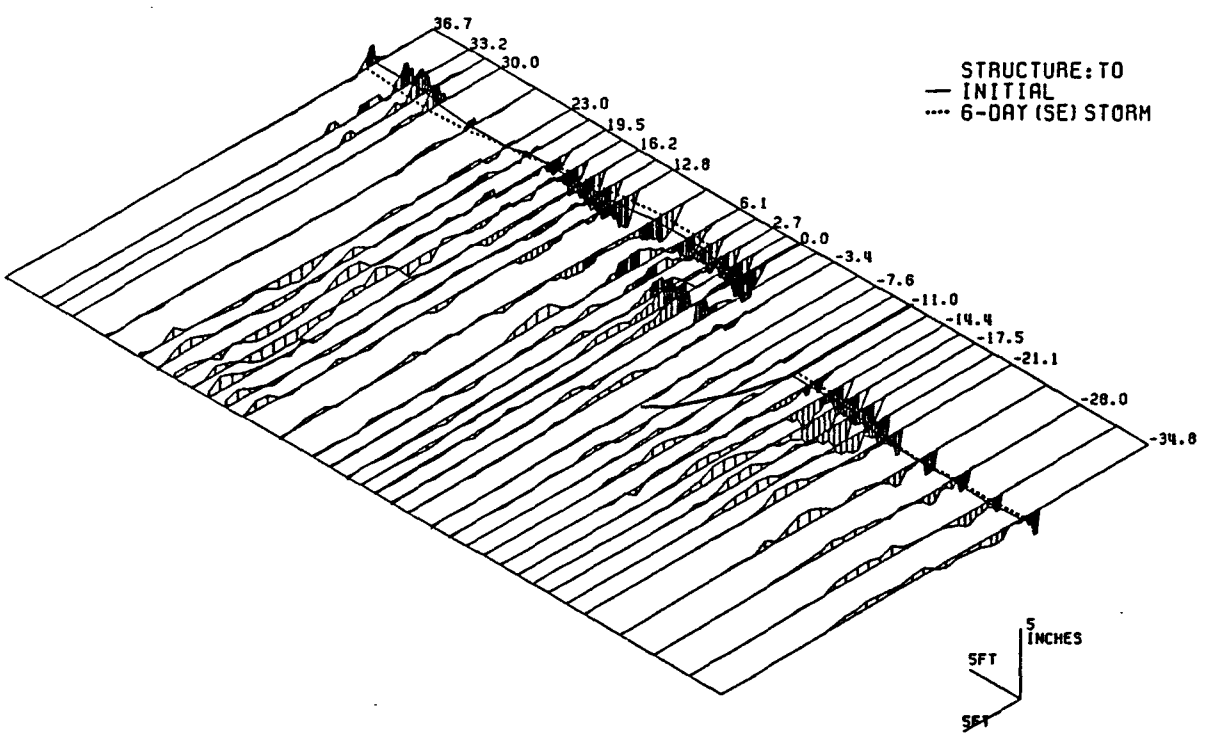

Figure 8: Profile changes for S0 under 6-day NE and SE storm processes.

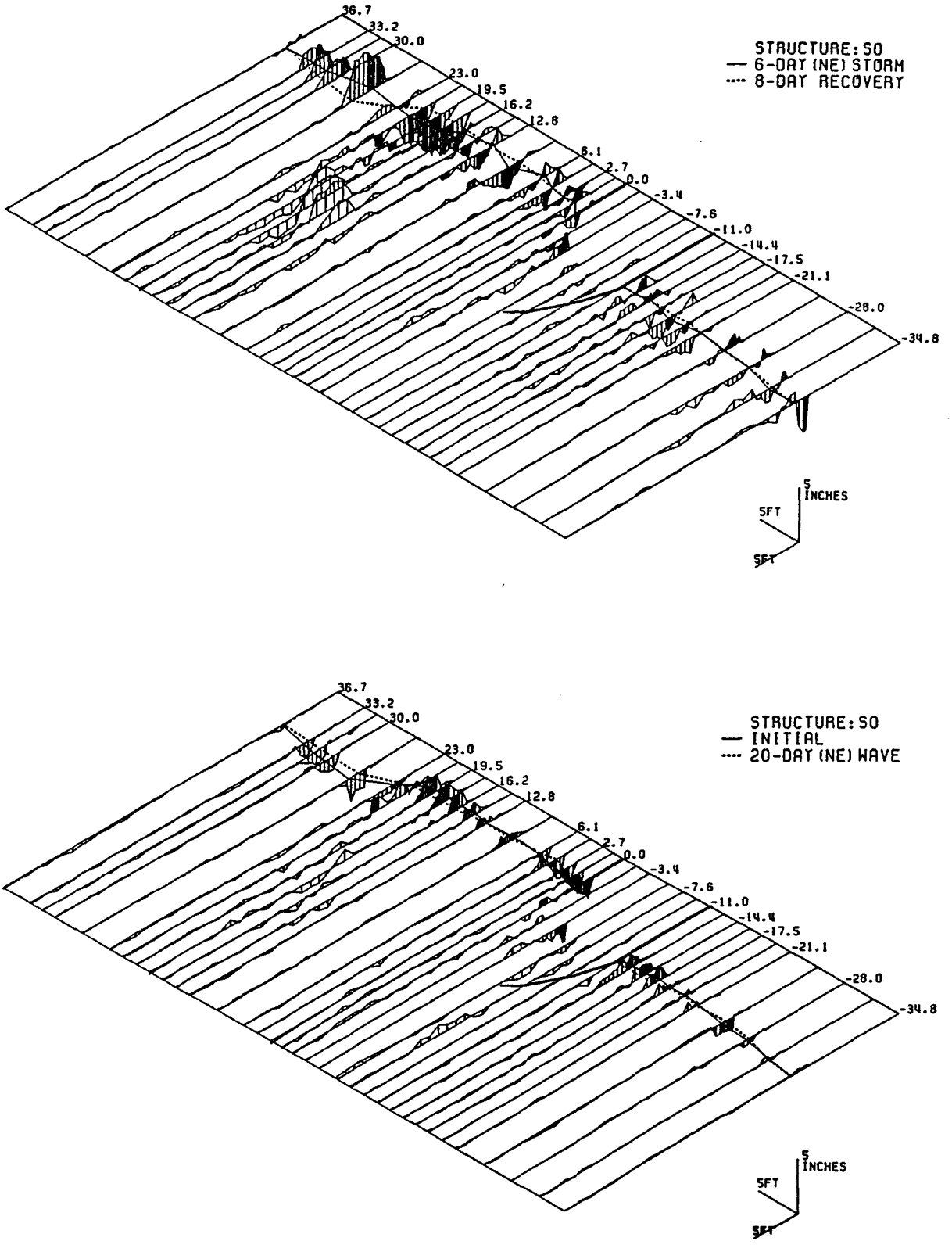

Figure 9: Profile changes for S0 in recovery and moderate wave processes.

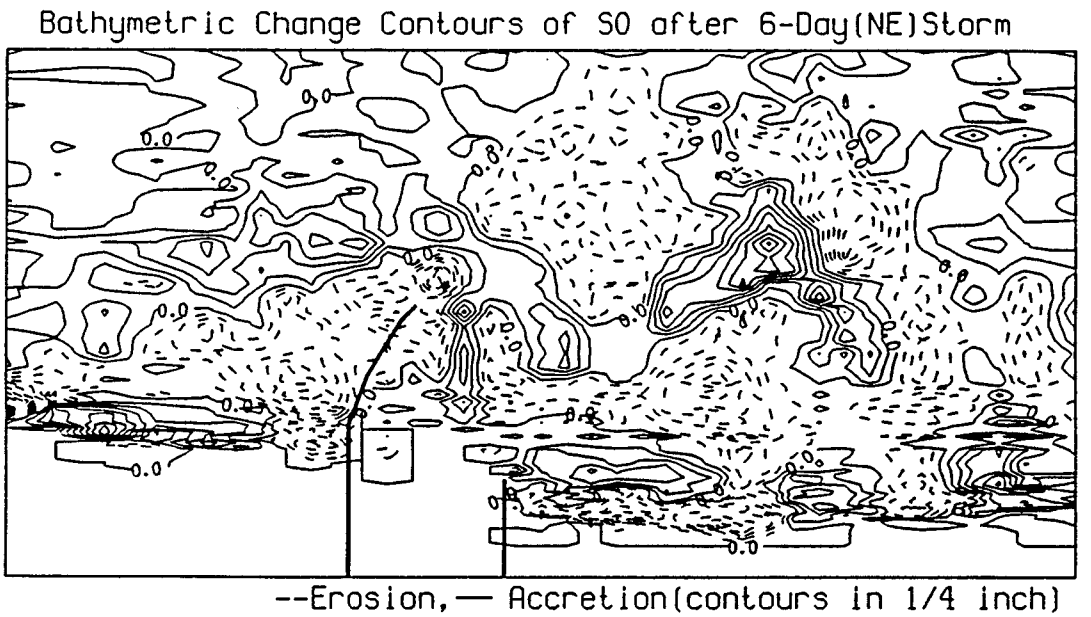

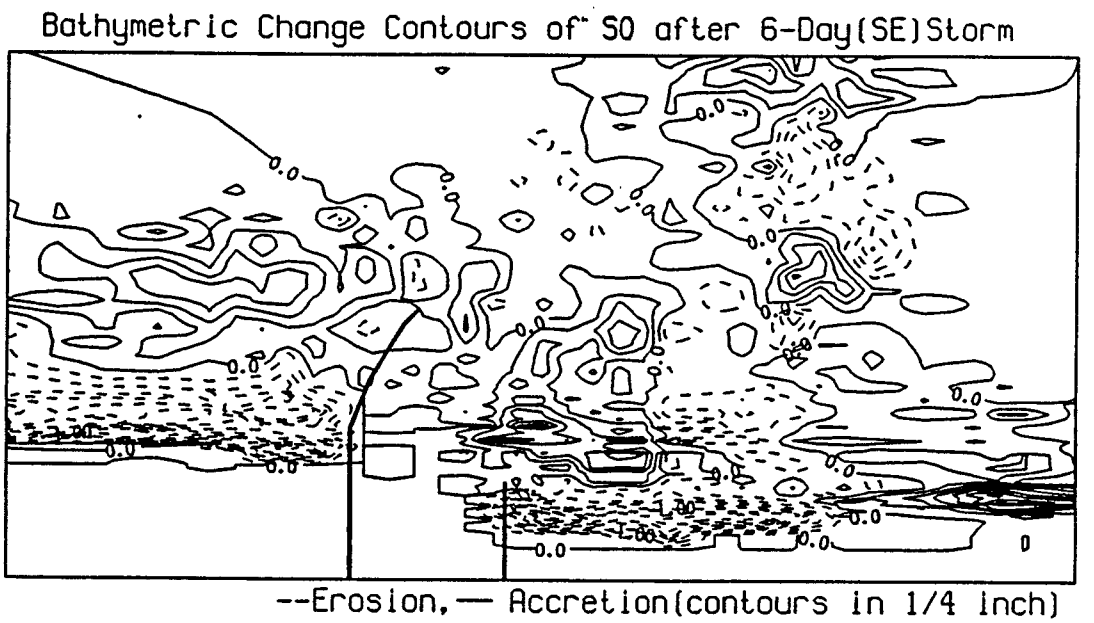

Figure 10: Bathymetric changes for S0 under 6-day NE and SE storm process.

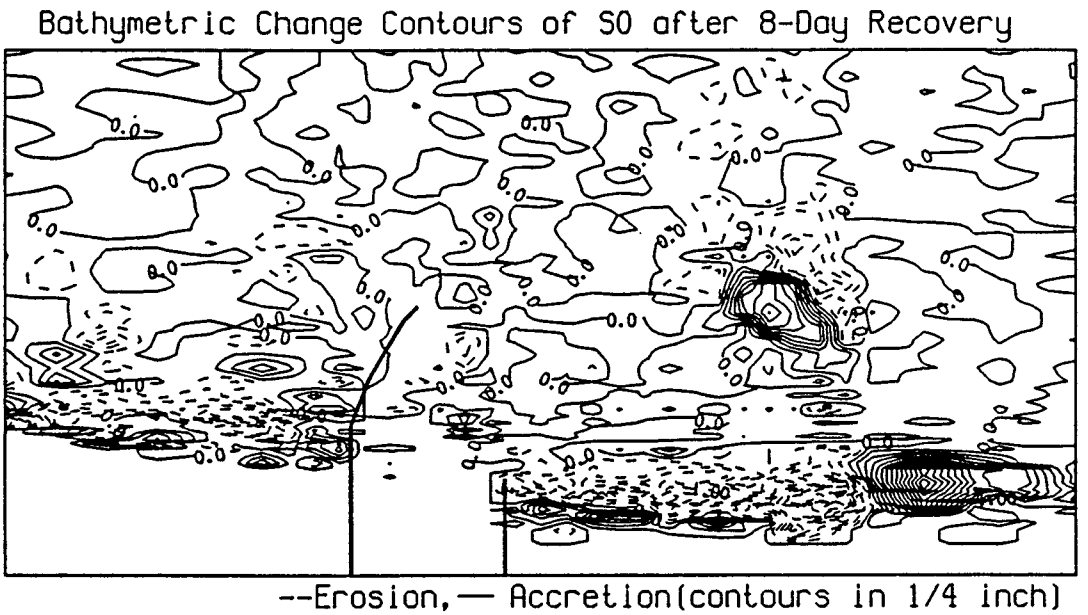

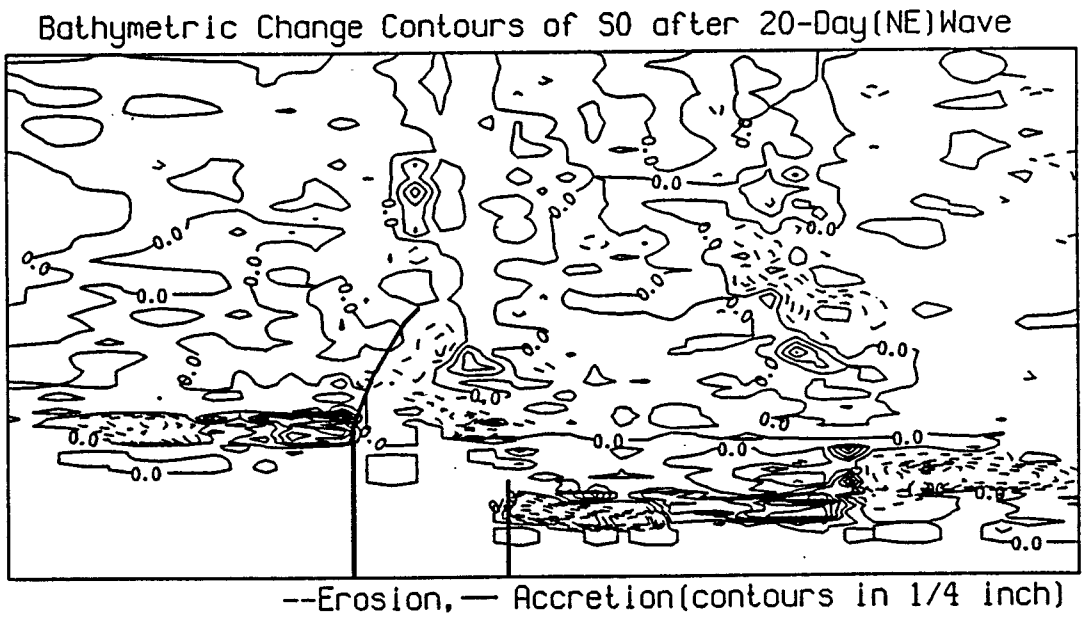

Figure 11: Bathymetric changes for S0 in recovery and moderate wave processes.

Under the SE storm wave condition, the sediment transport pattern was similar to that of the NE storm condition but with the reversed transport direction. Sand was seen to move from the nearshore region south of the inlet towards the inlet and then accumulated near the tip of the south jetty. A small amount of sand was also observed to bypass the inlet to the offshore bars on the north side of the inlet.

Sediment came into the inlet in all tested wave conditions. It was apparent that the majority of the sediment transport into the inlet was from south side around south jetty. This was the case for all the tested configurations to the wave directions. Consequently, the S2, S3 and S8 configurations with the extended south jetty resulted in the smallest sand loss to the inlet.

The sediment movement in the ebbshoal region was found only active in the upper layer. Visually, the ebbshoal appeared to be slowly moving towards south under NE storm conditions. The pattern of ebbshoal change, however, was not all that clear and not all consistent from run to run.

As far as the inlet channel change is concerned, it varied from case to case in response to the different configurations. In all cases, accretion was visible inside the jetties, particularly near the inlet entrance. Under the storm condition, erosion in the main channel was also noticeable due to the often shoaling or accumulation of sand near the south jetty. This was particularly the case for the S4 and S5 configurations where the ebb tidal shoal was fully or partially removed.

4.2 Shoreline Response

From the experiments, the northshore was rather stable for all tested cases except the for case when the jetty was removed (S6). On the other hand, changes along southshore were rather pronounced for all the test conditions. Therefore, shoreline response was examined here mainly for the southshore.

The test configurations can be roughly grouped into 4 categories depending upon the nature of the modifications in relation to the existing structures:

- Category 1: Jetty structure modification only – S1, S2 and S3.
- Category 2: Ebb shoal removal – S4 and S5.
- Category 3: Removal of both jetties – S6.
- Category 4: Southside nourishment with or without jetty modification – S7 and S8.

Shoreline changes are then examined in each of the four categories.

Figure 12(a) shows the net southside shoreline changes after the 6-day NE storm experiment for Category 1 and that for the S0 structure. The shoreline is again defined as corresponding to an elevation of 2' NGVD in prototype. It is seen that the experimental results were spatially irregular; however, the nature of the changes as well as the magnitude of the changes were clearly similar for all the structure configurations in this Category. Therefore, for the three structure modifications, S1, S2 and S3. their effects on shoreline changes are most likely limited to some local perturbation. Based on the faired-in mean curve (thick line) shown in Figure 12(a), the magnitude of the shoreline retreat immediate to the south jetty is in the order of 70 ft ($\pm$50 ft) in prototype for an extended storm. This magnitude decreases towards downdrift and becomes negligible around 2,000 ft from the south jetty. Within the 2,000 ft distance, S2 and S3 appeared to cause slightly more shoreline retreat than S0 and S1. This is the consequence of south jetty extension which retards the downdrift northerly circulation that carries sand towards the south jetty.

Figure 12(b) compares the net shoreline changes for Categories 2 and 3 configurations for the 6-day NE storm case. Here, S4 is with full ebb shoal removal, S5 is with partial ebb shoal removal, and S6 is similar to S4 but with removal of both jetties, which is close to the situation when inlet is originally opened. The solid line represents the mean curve shown in Figure 12(a). It appears that the full removal of ebb tidal shoal causes a slight increase of shoreline retreat both in magnitude and the extent. Partial removal of ebb tidal has negligible added effect on downdrift shoreline changes other than local perturbation. The removal of both jetties as in Category 3 (S6) configuration results in shoreline retreat on both sides of the inlets and inlet becomes rapidly filled in.

In Category 4 structural configurations, the initial shoreline position was advanced approximately 2.5 ft in the model (150 ft prototype equivalent) due to beach nourishment. The net shoreline changes for the 6-day NE storm case are shown in Figure 13(a) together with the mean curve defined earlier. To obtain the true position of the shoreline with respect to the existing (unnourished) shoreline one simply add 150 ft to the ordinate such as shown in Figure 13(b). From this Figure, one can see that downdrift beach nourishment without extending the south jetty (S7) has lost significant amount of the added material in the vicinity of the jetty. In fact, the shoreline near the jetty was retreated to the position close to Category 1 configurations. For the case with jetty extension (S8) the overall net shoreline change was similar to Category 1 structures but the shoreline retreat was larger than the mean curve in Category 1 structures in the vicinity of the jetty.

From the above results it appears that under the NE storm condition the ultimate shoreline position on the downdrift side is somewhat dictated by the downdrift jetty configuration; too short a jetty will result in an unacceptably recessed

(a) Category 1 configuration:

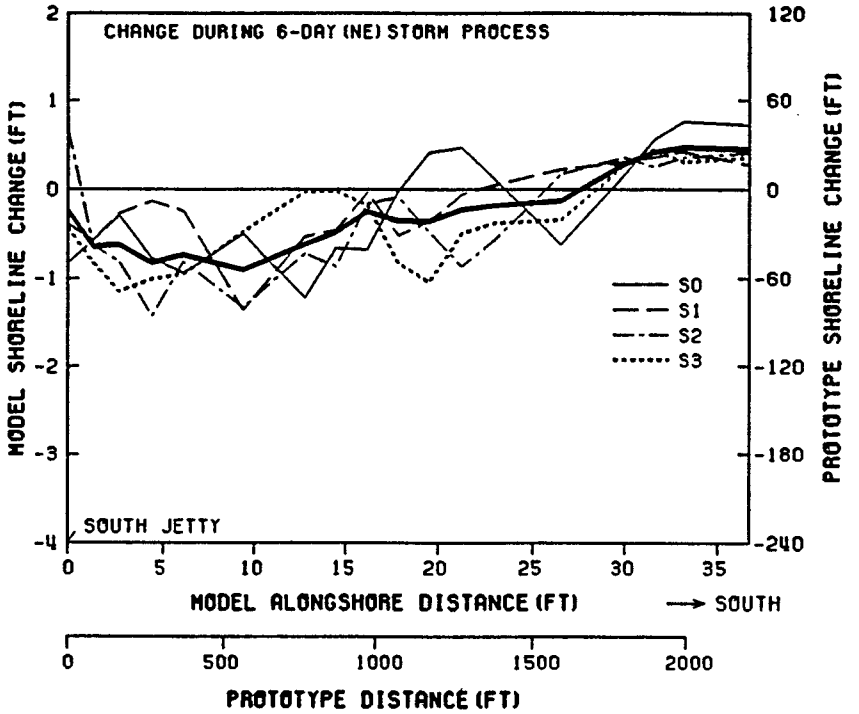

(b) Categories 2 and 3 configurations:

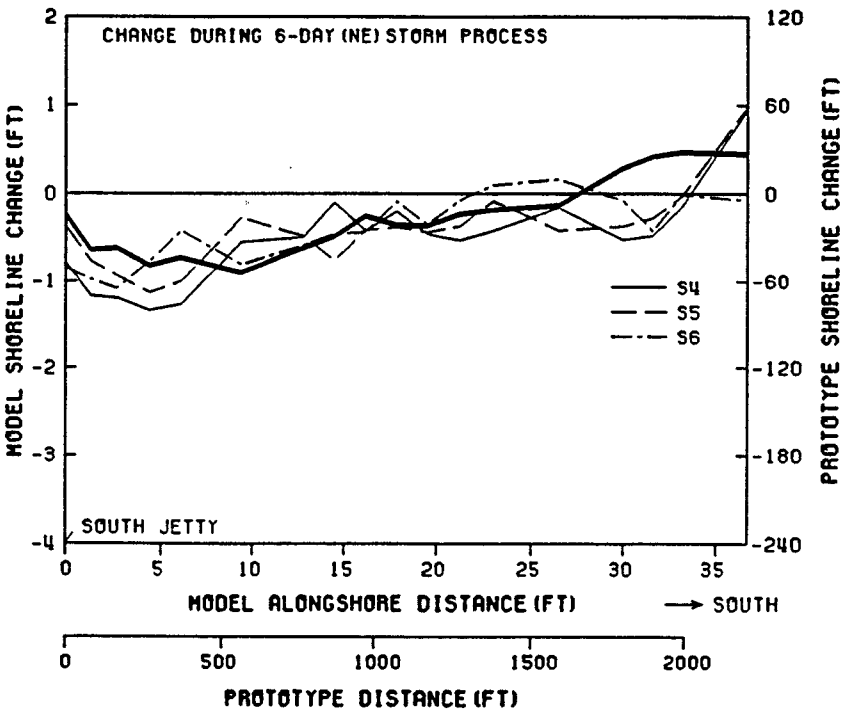

Figure 12: Shoreline changes in 6-day NE storm for Category 1,2,3 structures.

(a) Net Shoreline changes:

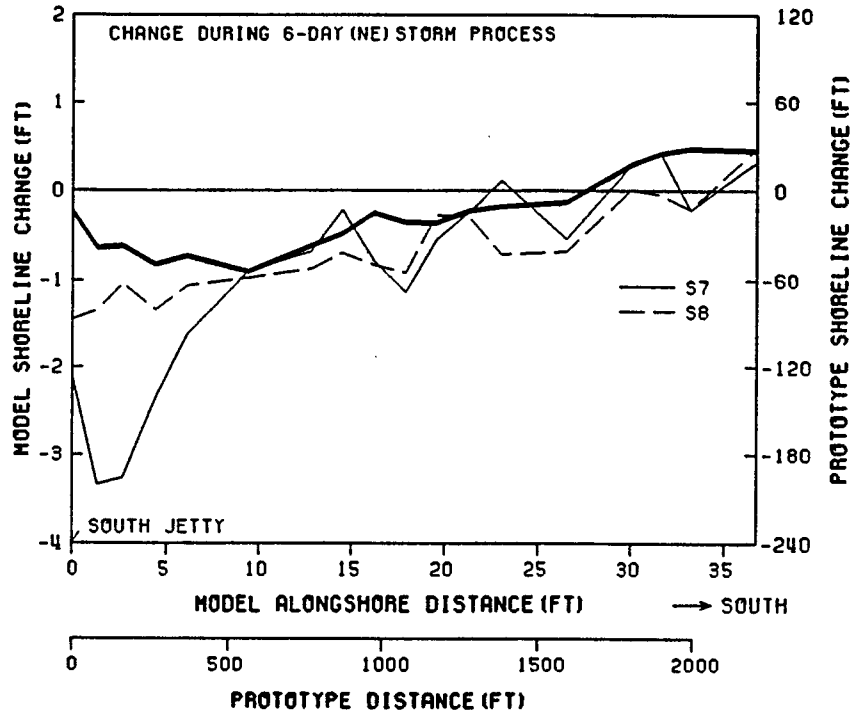

(b) Changes relative to existing shoreline:

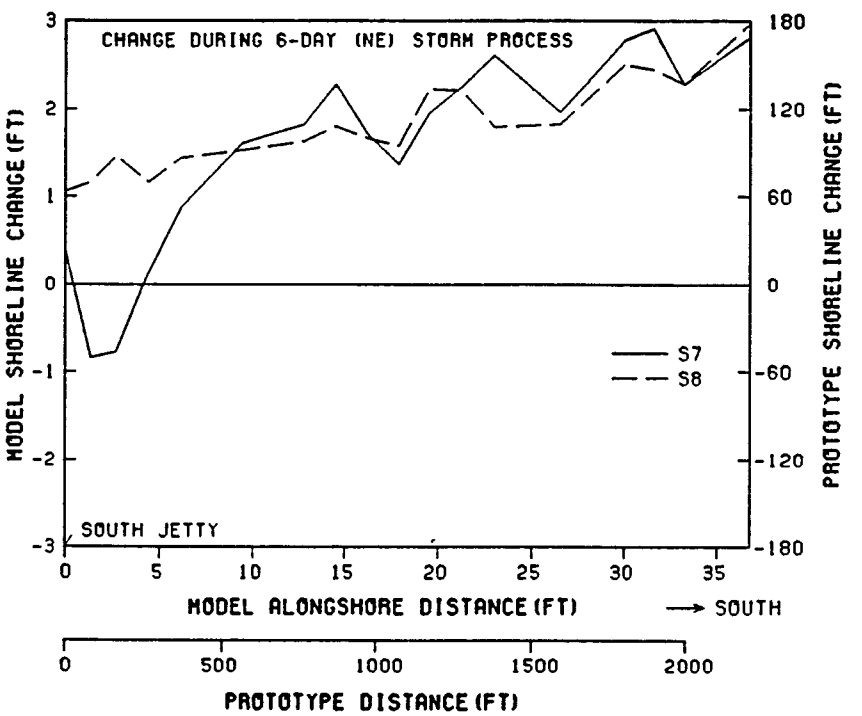

Figure 13: Shoreline changes in 6-day NE storm for Category 4 structures.

shoreline while too long a jetty may promote local erosion in its immediate vicinity. Ebb shoal removals do not seem to have a significant effect on the ultimate position of shoreline under storm events.

Also shown in Figures 12 and 13 is a general accretion of shoreline located between 30 and 40 ft in model (1800 and 2400 ft prototype equivalent) south of the south jetty. This shoreline accretion is, however, small, with the rate of accretion less than 1 ft/day in model (10 ft/day in prototype) for all test configurations.

Figure 14 shows the southside shoreline position relative to the existing shoreline from the 8-day E swell-dominated recovery waves for S0 configuration and for Categories 1, 2 and 3 configurations (Category 4 was not tested). It is seen that the shoreline was generally in the status of recovery for all the tested configurations. The recovery was seen to be spatially uneven but the mean position appeared to be near complete recovery. The recovery patterns were similar for S0 and S3 due to the small differences in jetty configuration. The recovery patterns of the other configurations were spacially different. The foreshore beach face of the recovered shoreline was considerably steeper than the pre-test condition. In the previous report (7), the shoreline is defined from a level of ± 0 NGVD instead of +2 ft NGVD which is used in this report. The results showed that the 0 NGVD line kept receding in most of the configurations. This beach steepening phenomenon will be reflected in the results of the nearshore volumetric changes presented in latter section.

Figures 15 and 16 show the shoreline changes relative to the existing shoreline from the 8-day NE moderate wave and 6-day SE storm wave processes, respectively. Only four configurations (S0, S2, S4 and S6) were tested for the 8-day NE moderate wave condition and three (S0, S3 and S5) for the 6-day SE storm waves. From the 8-day NE moderate wave experiments, all four tested structures sustained mild shoreline recession, smaller than the recession rate in the 6-day NE storm process. In the 6-day SE storm experiments, the three tested configurations showed shoreline change patterns similar to the 6-day NE storm case in that shoreline receded in the immediate vicinity of the south jetty but was progressional further south. The point where shoreline progression began appeared to be closer to the south jetty in the SE storm case. Apparently, sediment was transported towards the inlet from the south but was sucked into the inlet.

Based on the surveyed profile data, averaged net shoreline changes with respect to the initial shoreline were computed. The results for the 6-day NE storm, 8-day E recovery, 8-day NE moderate waves, and 6-day SE storm process, are presented in Tables 3, 4, 5 and 6, respectively.

These results showed that under storm condition, on the average the downdrift shoreline receded up to J27 (or about 1,600 ft prototype distance southward from the south jetty) under all tested configurations. Beyond J27, the shoreline actually

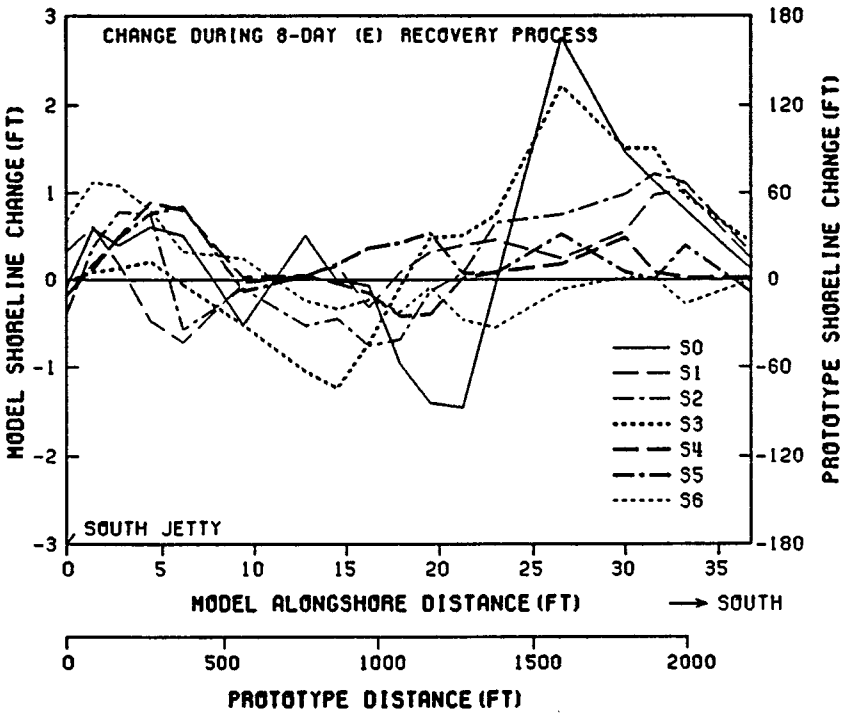

Figure 14: Shoreline changes in 8-day recovery condition.

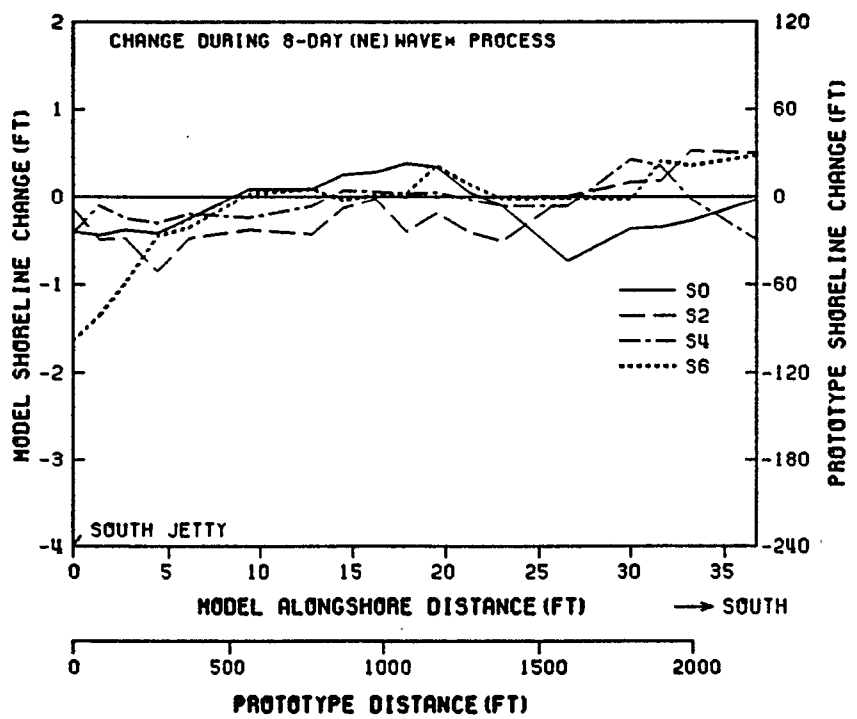

Figure 15: Shoreline changes in 8-day NE moderate wave process.

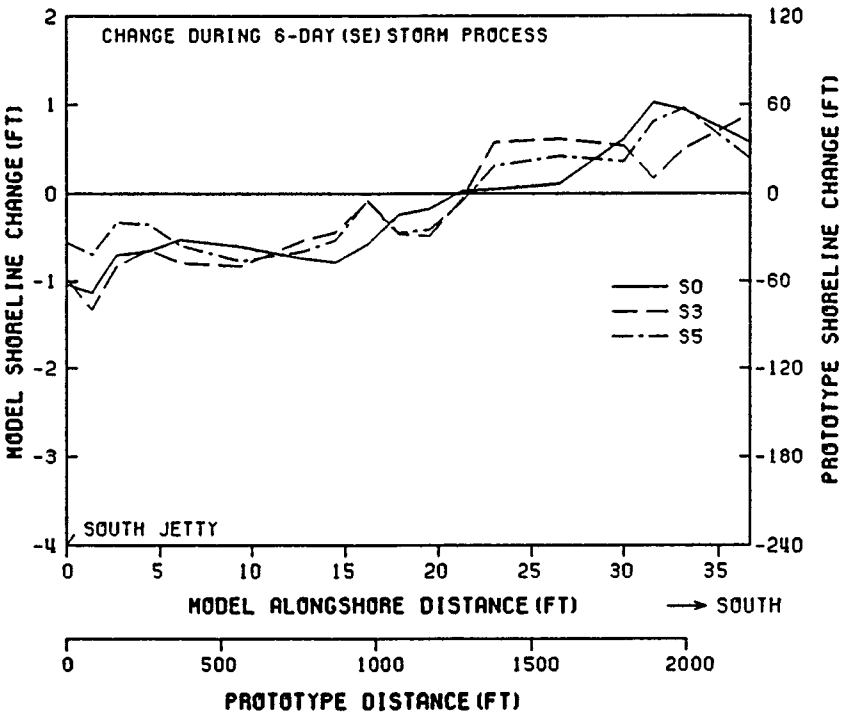

Figure 16: Shoreline changes in 6-day SE storm process.

Table 3: Averaged shoreline changes(ft) in 6-day NE storm process.

Structure	Segment (range) Included in Computation*						
	J12-21 (14.5')	J12-22 (16.2')	J12-23 (17.8')	J12-24 (19.5')	J12-25 (21.2')	J12-26 (23.0')	J12-27 (26.5')
S0	-0.67	-0.67	-0.60	-0.51	-0.43	-0.39	-0.41
S1	-0.55	-0.49	-0.49	-0.48	-0.45	-0.41	-0.36
S2	-0.74	-0.68	-0.62	-0.60	-0.63	-0.62	-0.56
S3	-0.61	-0.56	-0.59	-0.63	-0.62	-0.60	-0.58
S4	-0.86	-0.81	-0.75	-0.72	-0.71	-0.69	-0.65
S5	-0.72	-0.68	-0.65	-0.63	-0.61	-0.57	-0.56
S6	-0.74	-0.71	-0.64	-0.62	-0.57	-0.52	-0.47
S7	0.69	0.80	0.86	0.96	1.07	1.18	1.24
S8	1.40	1.43	1.45	1.52	1.58	1.59	1.61

* Shoreline changes are relative to the existing shoreline; negative values indicate shoreline recession.

Table 4: Averaged shoreline changes(ft) in 8-day E recovery wave process.

Structure	Segment (range) Included in Computation*						
	J12-21 (14.5')	J12-22 (16.2')	J12-23 (17.8')	J12-24 (19.5')	J12-25 (21.2')	J12-26 (23.0')	J12-27 (26.5')
S0	0.25	0.21	0.10	-0.04	-0.16	-0.15	0.06
S1	0.01	-0.02	-0.01	0.02	0.05	0.08	0.09
S2	-0.02	-0.10	-0.16	-0.16	-0.14	-0.08	-0.02
S3	-0.31	-0.36	-0.33	-0.25	-0.19	-0.12	0.05
S4	0.27	0.22	0.16	0.11	0.10	0.10	0.10
S5	0.27	0.28	0.30	0.32	0.30	0.28	0.30
S6	0.46	0.38	0.31	0.27	0.21	0.15	0.13

* Shoreline changes are relative to the existing shoreline; negative values indicate shoreline recession.

Table 5: Averaged shoreline changes(ft) in 8-day NE normal wave process.

Structure	Segment (range) Included in Computation*						
	J12-21 (14.5')	J12-22 (16.2')	J12-23 (17.8')	J12-24 (19.5')	J12-25 (21.2')	J12-26 (23.0')	J12-27 (26.5')
S0	-0.18	-0.13	-0.08	-0.04	-0.03	-0.04	-0.09
S2	-0.42	-0.38	-0.38	-0.36	-0.37	-0.38	-0.35
S4	-0.19	-0.17	-0.15	-0.13	-0.12	-0.12	-0.12
S6	-0.59	-0.52	-0.46	-0.39	-0.35	-0.32	-0.30

* Shoreline changes are relative to the existing shoreline; negative values indicate shoreline recession.

Table 6: Averaged shoreline changes(ft) in 6-day SE storm process.

Structure	Segment (range) Included in Computation*						
	J12-21 (14.5')	J12-22 (16.2')	J12-23 (17.8')	J12-24 (19.5')	J12-25 (21.2')	J12-26 (23.0')	J12-27 (26.5')
S0	-0.77	-0.75	-0.70	-0.65	-0.59	-0.54	-0.50
S3	-0.79	-0.72	-0.69	-0.67	-0.62	-0.53	-0.45
S5	-0.56	-0.50	-0.50	-0.49	-0.45	-0.39	-0.34

* Shoreline changes are relative to the existing shoreline; negative values indicate shoreline recession.

experienced mild advances in most cases. The extension of north jetty (S1 and S2 structure) appeared to have only minor effect on the southside shoreline response as compared with the existing condition. As discussed earlier, lengthening the south jetty increased shoreline recession in the immediate vicinity of the south jetty. The absolute magnitude of the shoreline retreats were found to be quite modest comparing with some of the open coast erosions experienced along the Florida coast under comparable storm strength. For instance, the most severe shoreline recession which occurred immediately south of the south jetty and was in the order of 1.5 ft in six days (or less than 100 ft prototype). This modest shoreline recession is due to the combined shielding effects provided by the jetties and the ebb tidal shoal as well as due to the drift reversal which continuously feeds sand to this region.

Under recovery wave condition, all configurations responded in shoreline recovery. However, foreshore beach face was considerably steeper than the pre-tested condition.

The shoreline response to storm waves from SE was found to have similar pattern as that from NE.

4.3 Bathymetric Changes and Erosional Patterns

Under storm condition, the most visible bathymetric changes occurred in the nearshore zone on the south side of the inlet including the region near the tip of the south jetty. In the early stage of the storm, beach face was being eroded by wave action and sand was being carried out towards offshore forming offshore bars. Meanwhile, the ebb tidal shoal region also experienced vigorous sediment motion due to wave breaking and sediment was carried both into the nearshore zone and to the downdrift offshore area by wave induced currents. During flood cycle, a portion of the ebb shoal material was carried directly into the inlet.

In the nearshore zone south of the inlet, it received material from both beach face and ebb tidal shoal. During flood cycle, the sediment accumulated in the nearshore zone was transported towards and into the inlet by the tidal currents through marginal flood channels and around the tip of the south jetty creating strong erosion zone in the vicinity of the inlet. During ebb tide, the sand in the nearshore zone south of the inlet was also being carried towards the inlet and then back to the ebb tidal shoal region following an ebb-current induced clockwise gyro on the downdrift side. Figures 17 and 18 show the regions of accretion and erosion with patterns of sediment motion based on sand tracer study during a single flood and ebb cycles, respectively. These patterns of sediment motion were in close agreement with the current patterns measured in the fixed-bed model.

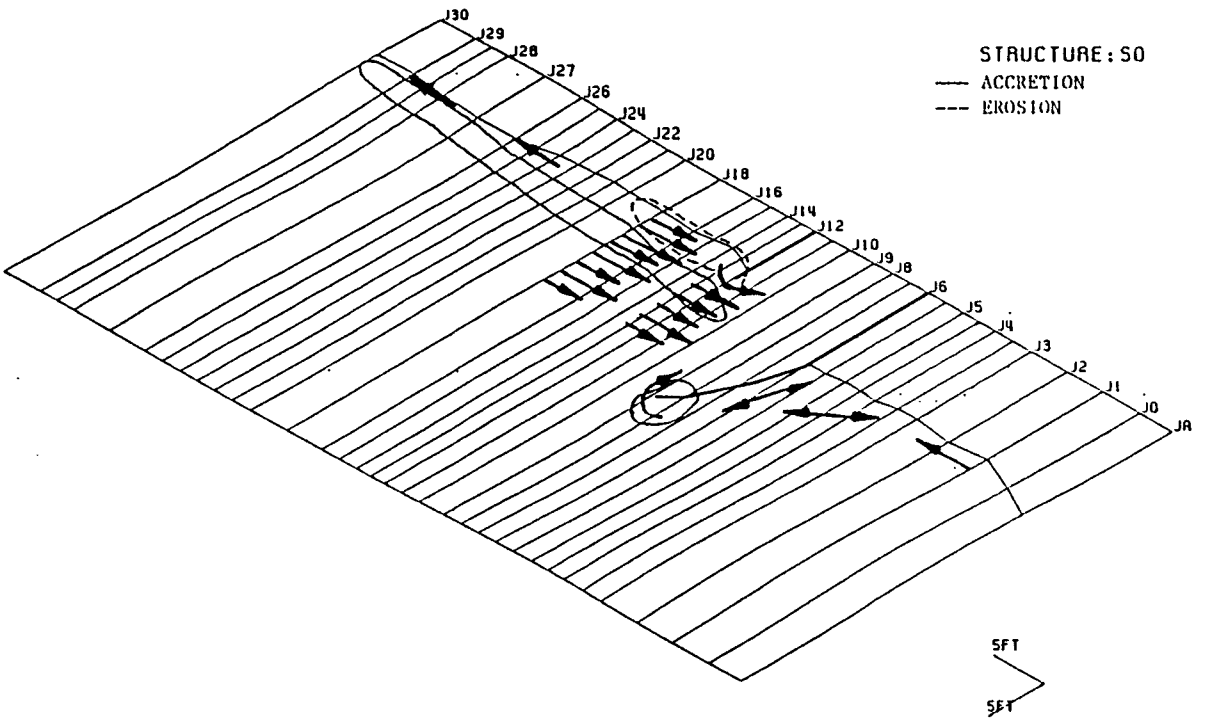

Figure 17: Sediment accretion and erosion pattern during flood.

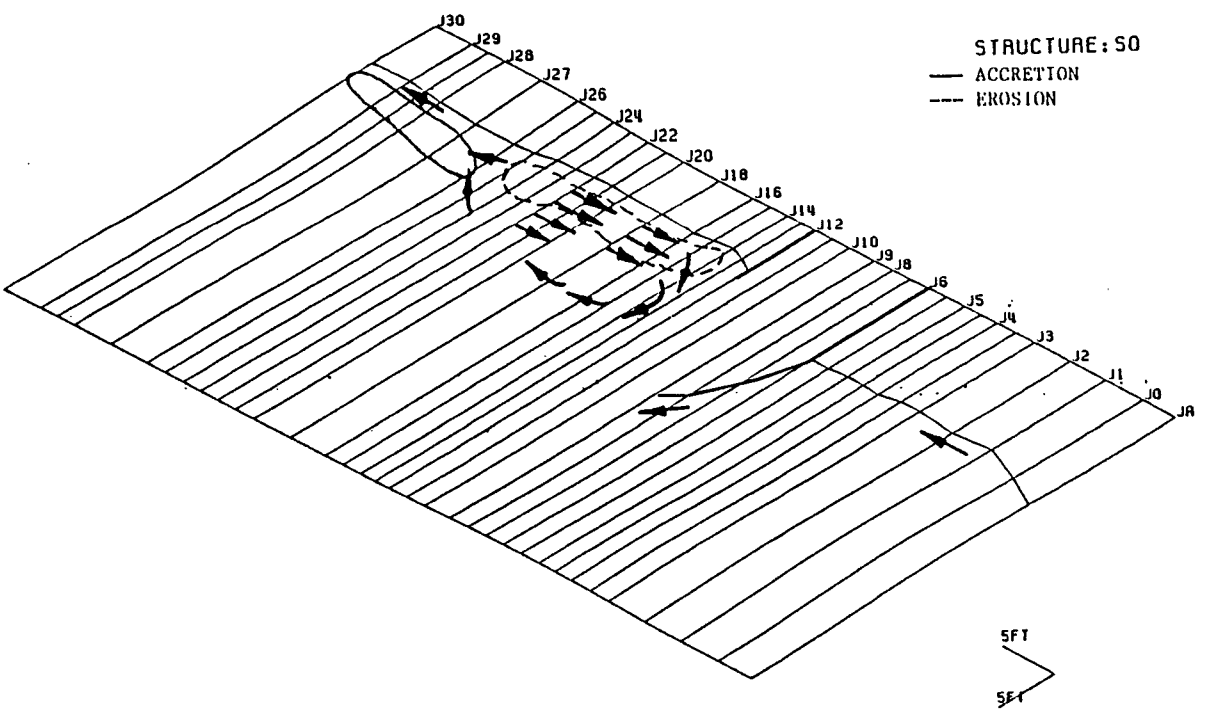

Figure 18: Sediment accretion and erosion pattern during ebb.

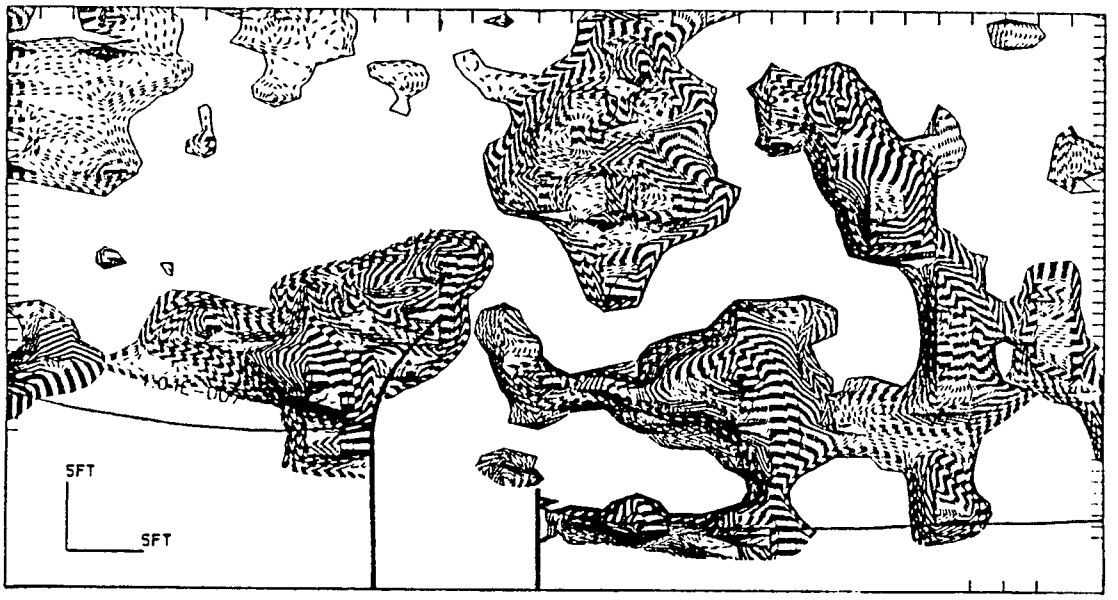

Figure 19: Erosion pattern after 6-day storm for S0.

The cumulative effect of bathymetric changes over a number of tidal cycles is patched erosional and accretional patterns such as shown in Figure 19 for S0. These patterns vary in detail for different configurations but in general agreement with the current patterns.

For recovery runs, no bottom survey was made after a single flood or ebb. The integrated effects appeared to be that the offshore bar created by storm waves gradually diminished and moved towards the shore. However, the strong currents in the vicinity of the south jetty appeared to prevent the offshore bar material from reaching the nearshore zone to rebuild the beach. The shoreline recovery addressed earlier appeared to be at the expense of the foreshore material causing beach face to steepen. Since the onshore movement of the offshore bar material was interrupted by the nearshore current and the foreshore material was moved onshore to rebuild the shoreline, the nearshore zone continued to lose material even under rebuilding cycle. The quantity of loss will be addressed in Section 4.5.

To examine the erosional and accretional patterns in further detail, the profile lines surveyed at different time stages are plotted against each others. Figures 20 and 21, for instance, show the comparisons of the 12 profile lines located south of the inlet for S0. Here, at each location 3 profiles representing the initial, the 6-day post storm and the subsequent 8-day post-recovery profiles are given. Also plotted in these Figures is the quasi-equilibrium profile (thick line), which represents the beach in an equilibrium form away from the inlet. Similar plots for other

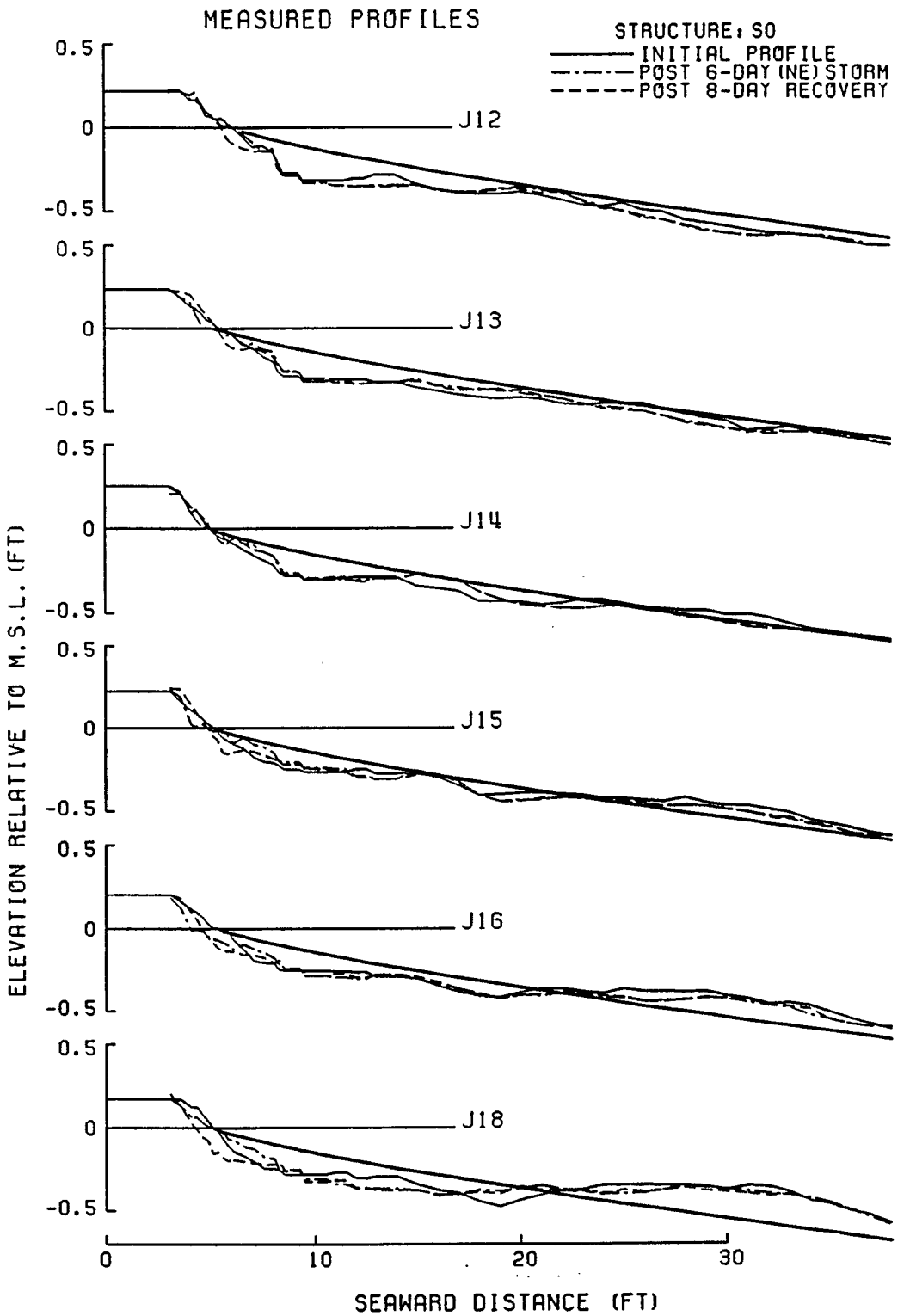

Figure 20: Comparisons of surveyed profiles from J12 to J18 for S0

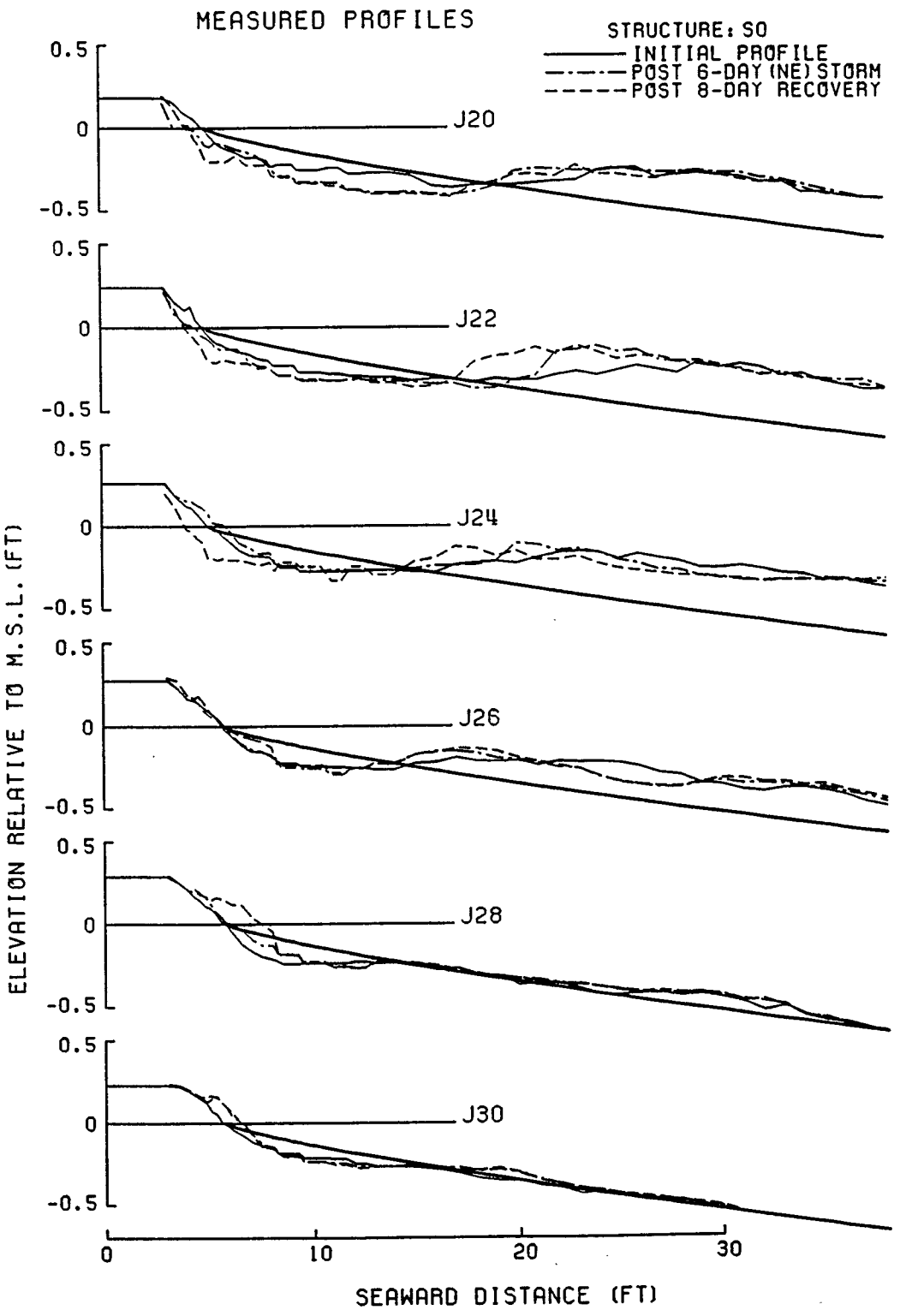

Figure 21: Comparisons of surveyed profiles from J20 to J30 for S0.

configurations are presented in Appendix V.

4.4 Ebb Shoal Movement

The ebb tidal shoal was overall stable under both storm and recovery waves for all the configurations. The sediment movement in the ebb shoal region was found active mainly in the upper layer. Under NE storm condition, the ebb shoal as a whole appeared to be slowly moving towards south in cases with jetty structures and the existing ebb shoal configuration. In S4 and S5 where ebb shoal was either partially or fully removed, the ebb shoal grew back fairly rapidly under both storm and recovery conditions. The pattern of ebb shoal change, however, was not all that clear and was not necessarily consistent from run to run.

4.5 Sediment Balance Computations

A scheme of sediment balance analysis was developed to quantify performance evaluation for alternative configurations. The test region is divided into five zones – Zone 1 to Zone 5 (see Figure 22). Zone 1 is defined as updrift zone which covers the area north from the tip of the north jetty. Zone 2 is the inlet zone which covers area inside the line connecting the tip of north jetty to the tip of south jetty. Zone 3 is the south nearshore zone which covers the area within the 6 ft prototype contour line on the south side of the south jetty to the downdrift border. Zone 4 is the ebb tidal shoal zone which is the area south of Zones 1 and 2 and east of zone 3. Zone 5 is a small area south of the last surveyed profile (J30) where the downdrift transport is estimated. The sediment balance analysis were then accomplished by comparing volumes in each respective zone before and after the tests.

Figure 23 shows the results of the sediment balance computations in five regional zones for the 6-day NE storm experiments. The values given are the rate of volume change in the model scale in ft^3/day; the values in the parentheses are the equivalent prototype rate in $10^3 yd^3$/day. The results are also summarized in Table 7. Since S0, S3, S4, S5, S7 and S8 all have the same updrift boundary condition, i.e., the north jetty configuration is the same, a same updrift response is normally expected. In the actual tests, however, this updrift response varied slightly from one experiment to the other. This is not desirable for comparison purposes. To facilitate comparisons with the same reference, the averaged updrift (Zone 1) volume change from these 6 configurations is used as the base value. The values in zone 1 of these 6 configurations are all adjusted to this same base value. The adjustment was also made to S1 and S2 configurations which have the same north jetty configuration. The adjusting factors for these configurations are given in Table 8.

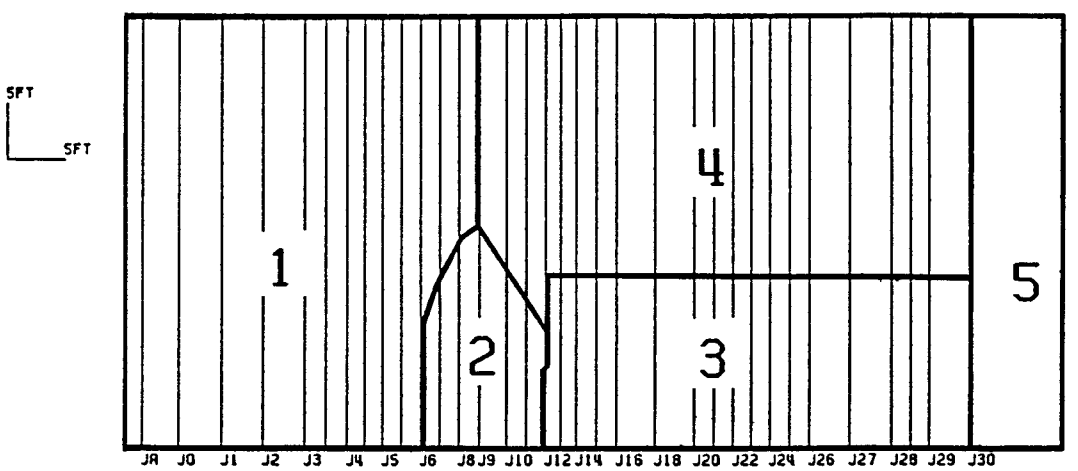

Figure 22: Five regional zones for sediment balance computations.

The above results can also be presented with reference to those of S0 configuration for comparison of the individual structural performance. This is given in Table 9, where the data of volume changes over the ebb shoal (Zone 4) are not shown since the extent of the ebb shoal is difficult to define. Results of sediment balance computations for other test wave conditions are shown in Figures 24 to 26 and in Tables 10 to 12.

Based upon these results and the results of shoreline change presented earlier, the performance of various tested configurations are then evaluated.

A summary of sand budget in south shore erosion, downdrift transport, and the loss to the inlet, in terms of histogram presentation from the tests is given in Appendix VI.

The experimental results of shoreline change and sediment balance presented here are used in the next Section as the bases for evaluating the performance of the different alternative configurations.

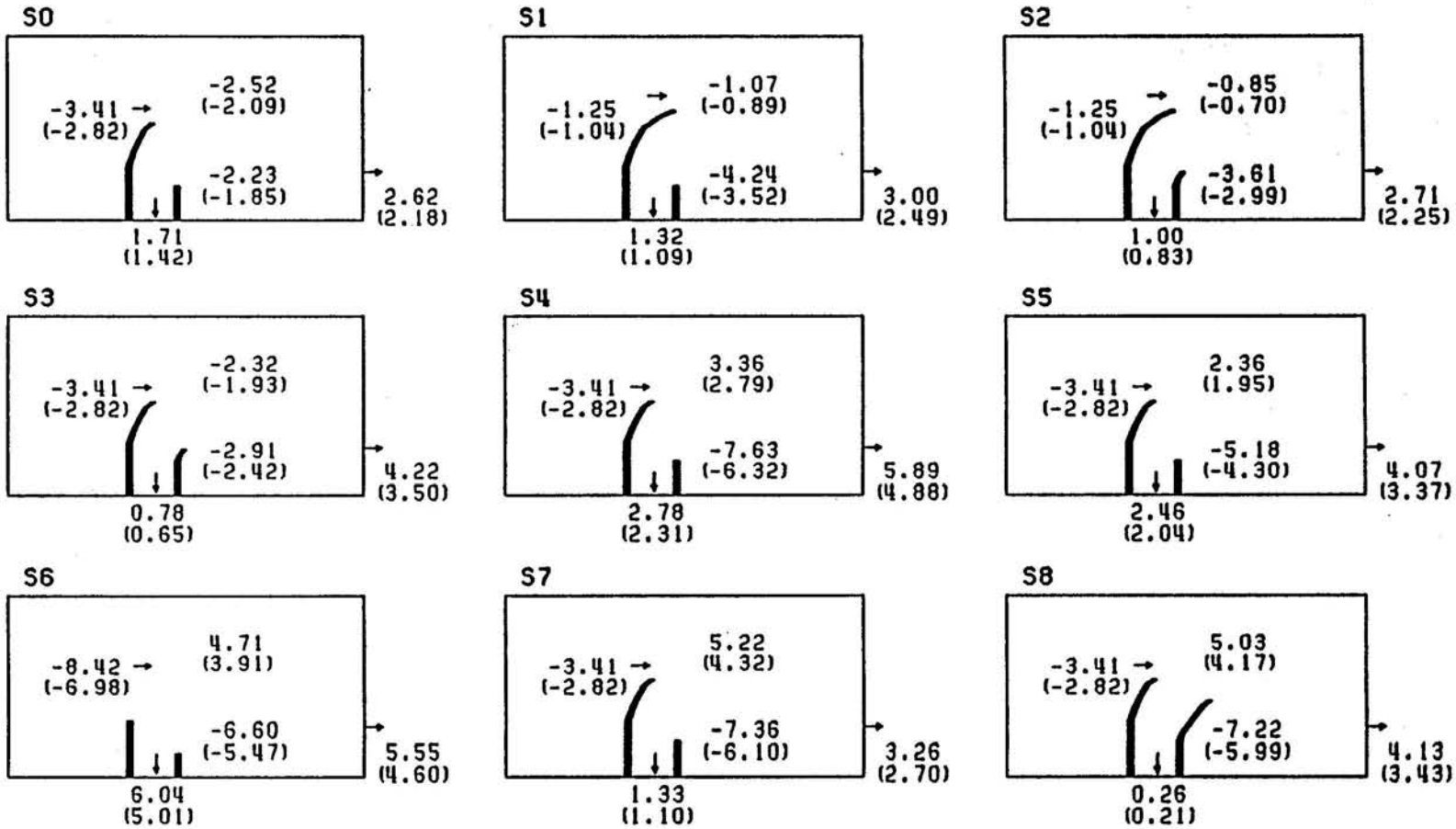

Figure 23: Sand budget in ft^3/day ($10^3 yd^3$/day in prototype) from 6-day NE storm experiment.

Table 7: Rate of volumetric change ($10^3 yd^3$/day) in 6-day NE storm process.

Structure	Rate of Volumetric Change*($10^3 yd^3$/day)				
	Inlet North Region	Ebb Shoal Region	Inlet South Shore	Downdrift Transport	Loss to Inlet
S0	-2.82	-2.09	-1.85	2.18	1.42
S1	-1.04	-0.89	-3.52	2.49	1.09
S2	-1.04	-0.70	-2.99	2.25	0.83
S3	-2.82	-1.93	-2.42	3.50	0.65
S4	-2.82	2.79	-6.32	4.88	2.31
S5	-2.82	1.95	-4.30	3.37	2.04
S6	-6.98	3.91	-5.47	4.60	5.01
S7	-2.82	4.32	-6.10	2.70	1.10
S8	-2.82	4.17	-5.99	3.43	0.21

* Shown in prototype scale; negative values indicating the sand volume loss.

Table 8: Adjusting factors for updrift volume changes in NE storm test.

Structure	S0	S1	S2	S3	S4	S5	S7	S8
Factor	0.93	0.98	1.02	1.03	1.01	0.98	0.86	1.19

Table 9: Comparison of volume change rates in 6-day NE storm process.

Structure	Rate of volumetric change relative to S0 ($10^3 yd^3$/day)			
	Updrift Impoundment	Southside Volume	Downdrift Transport	Loss to Inlet
S1	1.78	-1.67	0.31	-0.33
S2	1.78	-1.14	0.07	-0.59
S3	0.00	-0.57	1.32	-0.77
S4	0.00	-4.47	2.70	0.89
S5	0.00	-2.45	1.19	0.62
S6	-4.16	-3.62	2.42	3.59
S7	0.00	-4.25	0.52	-0.32
S8	0.00	-4.14	1.25	-1.25

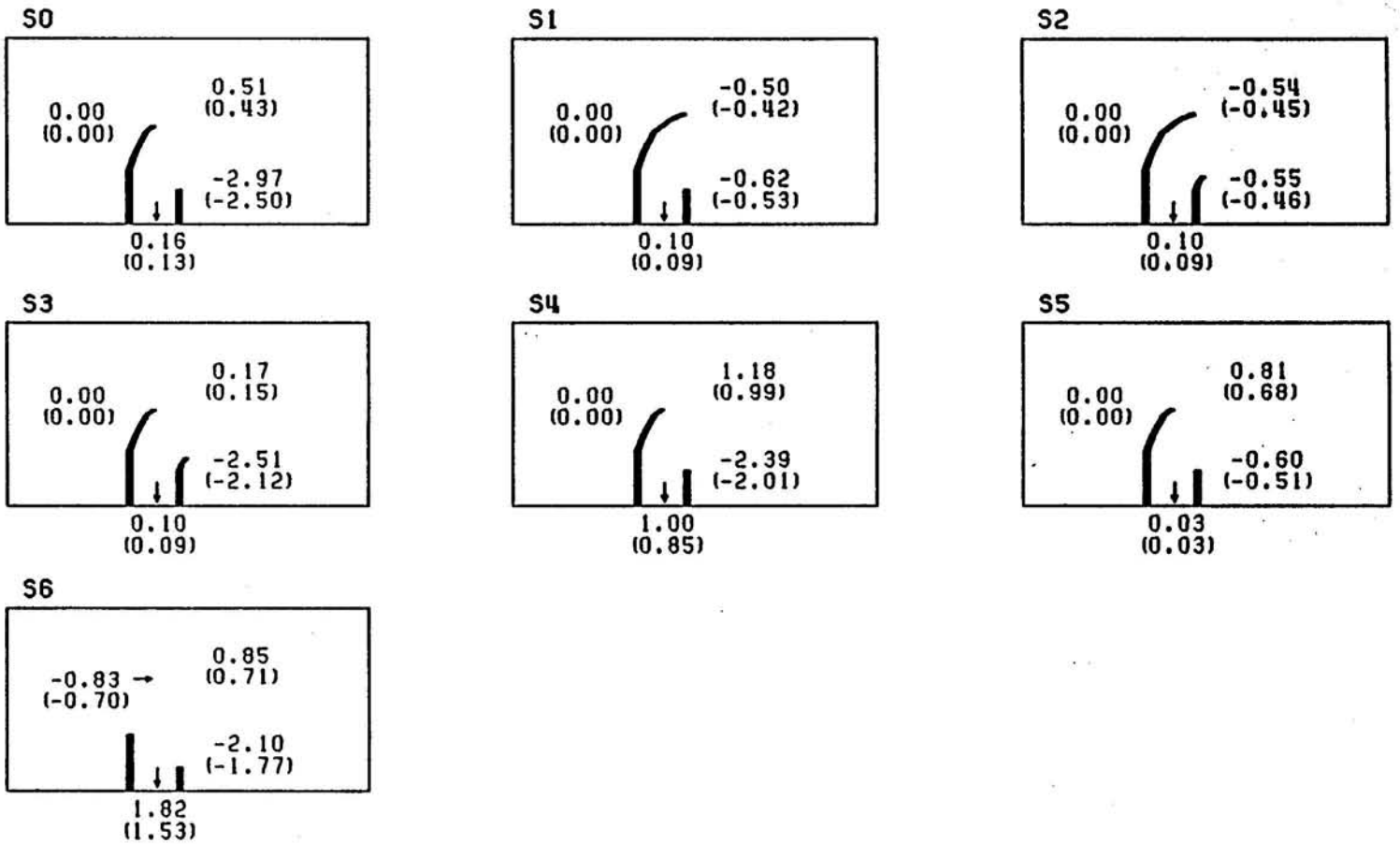

Figure 24: Sand budget in ft^3/day ($10^3 yd^3$/day in prototype) from 8-day E recovery experiment.

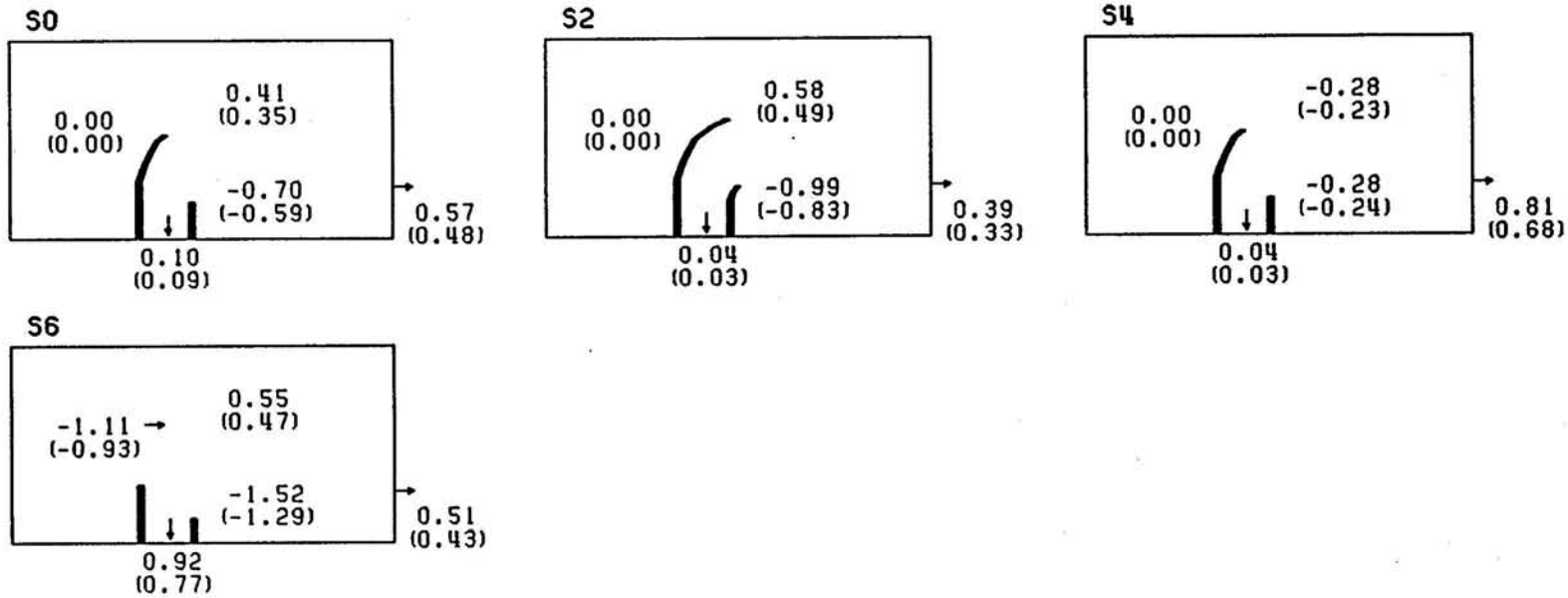

Figure 25: Sand budget in ft^3/day ($10^3 yd^3$/day in prototype) from 8-day NE normal wave experiment.

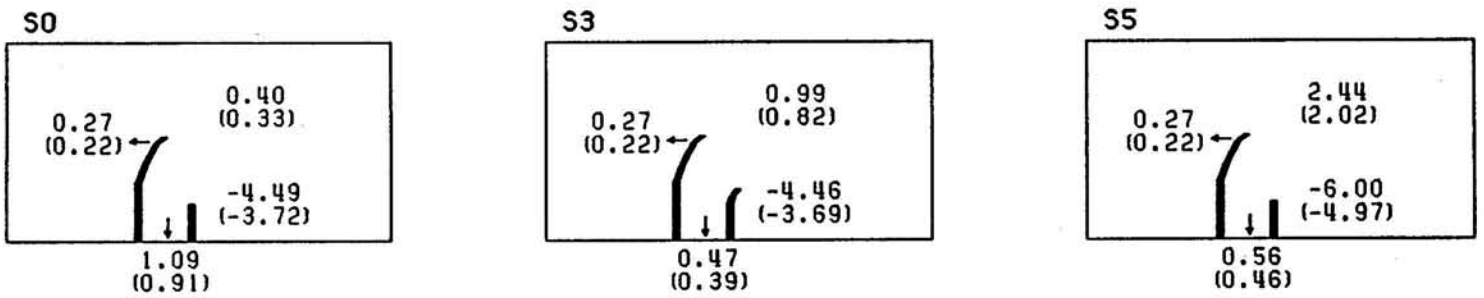

Figure 26: Sand budget in ft^3/day ($10^3 yd^3$/day in prototype) from 6-day SE storm experiment.

Table 10: Volume change rate ($10^3 yd^3$/day) in 8-day E recovery wave process.

Structure	Rate of Volumetric Change*($10^3 yd^3$/day)			
	Inlet North Region	Ebb Shoal Region	Inlet South Shore	Loss to Inlet
S0	0.00	0.43	-2.50	0.13
S1	0.00	-0.42	-0.53	0.09
S2	0.00	-0.45	-0.46	0.09
S3	0.00	0.15	-2.12	0.09
S4	0.00	0.99	-2.01	0.85
S5	0.00	0.68	-0.51	0.03
S6	-0.70	0.71	-1.77	1.53

* Shown in prototype scale; negative values indicating the sand volume loss.

Table 11: Volume change rate ($10^3 yd^3$/day) in 8-day NE normal wave process.

Structure	Rate of Volumetric Change*($10^3 yd^3$/day)				
	Inlet North Region	Ebb Shoal Region	Inlet South Shore	Downdrift Transport	Loss to Inlet
S0	0.00	0.35	-0.59	0.48	0.09
S2	0.00	0.49	-0.83	0.33	0.03
S4	0.00	-0.23	-0.24	0.68	0.03
S6	-0.93	0.47	-1.29	0.43	0.77

* Shown in prototype scale; negative values indicating the sand volume loss.

Table 12: Volume change rate ($10^3 yd^3$/day) in 6-day SE storm process.

Structure	Rate of Volumetric Change*($10^3 yd^3$/day)			
	Inlet North Region	Ebb Shoal Region	Inlet South Shore	Loss to Inlet
S0	0.22	0.33	-3.72	0.91
S3	0.22	0.82	-3.69	0.39
S5	0.22	2.02	-4.97	0.46

* Shown in prototype scale; negative values indicating the sand volume loss.

5 Performance Evaluations of Structural Alternatives

Five criteria are used to compare the performance of structural alternatives. They are:

- Sand losses to the inlet.
- Downdrift transport.
- Volume changes in southside nearshore zone.
- Ebb shoal volume changes.
- Updrift volume changes.

5.1 Channel Shoaling and Sand Losses to the Inlet

The experiments showed that inlet channel shoaling and net transport into the inlet was dominated by storm events. For the existing S0 configuration, the net transport into the inlet during storm period was found to be about 1,400 yd^3/day for NE storm and about 910 yd^3/day for SE storm. Under normal wave conditions (2 ft height) this transport magnitude was found to be only about one tenth of the above values. Of the eight alternative configurations five (S1, S2, S3, S7, and S8 configurations) showed improvement of channel shoaling and sand losses to the inlet and three (S4, S5 and S6) worsened the condition. Evidently, major improvement was always associated with south jetty extension. This was particularly the case for the S8 configuration, when the jetty is extended beyond the existing marginal flood channels; here the net transport into the inlet was cut down to 210 yd^3/day under NE storm, or 15% of the existing condition. The next best one was the S3 configuration of which the transport rate was found to be about 46% of the existing condition.

Extending north jetty (S1) also cut down sediment transport into the inlet but to a lesser extent (about 77% of the existing condition). Removal of ebb tidal shoal, whether partially or fully, increased the channel shoaling rate by 40 to 60% under storm condition. Removal of both jetties (S6) would drastically increase the inlet transport. Under storm condition, the rate was found to be about 5,000 yd^3/day, or about 3.5 times the existing rate of transport. At this rate, the inlet likely will become impassable. This results demonstrated the necessity of the jetty structures.

5.2 Downdrift Transport

Downdrift transport is defined here as the material passing through the test region onto the south side, 2,500 ft beyond the south jetty. The test results showed that removal of ebb shoal promotes downdrift transport by an increase of 50 to 100% initially. This was mainly due to fact that waves diffraction around the ebb shoal was either eliminated or reduced. In either case, the littoral zone was re-established to a normal condition of plane beach south of the jetty. Therefore, as the ebb shoal rebuilds one expects the downdrift transport to reduce rapidly.

The removal of both jetties also increased the downdrift transport significantly. The mechanism, however, is different from the ebb shoal removal situation. This increase in downdrift transport was mainly due to the increase of sand supply from the updrift as the northshore rapidly adjusted back to a plane beach form.

For cases with beach nourishment, S7 and S8, downdrift transport was also increased. This increase was likely aided by the diffusion of sand to the two ends of the nourished area.

For configurations with jetty modifications only(S1, S2 and S3), lengthening north jetty has little effect on the downdrift transport away from the shadow zone of the jetty. Extension of south jetty, on the other hand, improved downdrift transport by reducing losses to the inlet. This is seen by comparing the downdrift transport rates of S0 with S3 and of S7 with S8 in Table 7.

5.3 Volume Changes in Southside Nearshore Zone

As discussed earlier, the bulk of the downdrift erosion took place within 2,000 ft from the south jetty. The results of volume change computation under storm condition (see Table 7) indicated that all tested alternatives induced more south-side erosion than the existing S0 configuration. However, under recovery condition the trend seemed to be reversed (Table 10). One explanation is that S0 is the closest to an equilibrium state under the current natural condition than the others. Therefore, under storm condition the profile adjustment in S0 was not as pronounced as the others, hence the volume loss to offshore was also less. On the other hand, during recovery, the test results showed the amount of sand returning to the nearshore zone was also less than the other configurations. This can further be shown in the time history plot of downdrift erosion (Figure 27). Here, at the end of the storm period S0 had the smallest total volume loss. However, at the end of the recovery period, volume loss in S0 was no longer the smallest. For cases with beach nourishment, S7 and S8, this profile adjustment was considerably larger under storm condition and more sand was being transported offshore. This

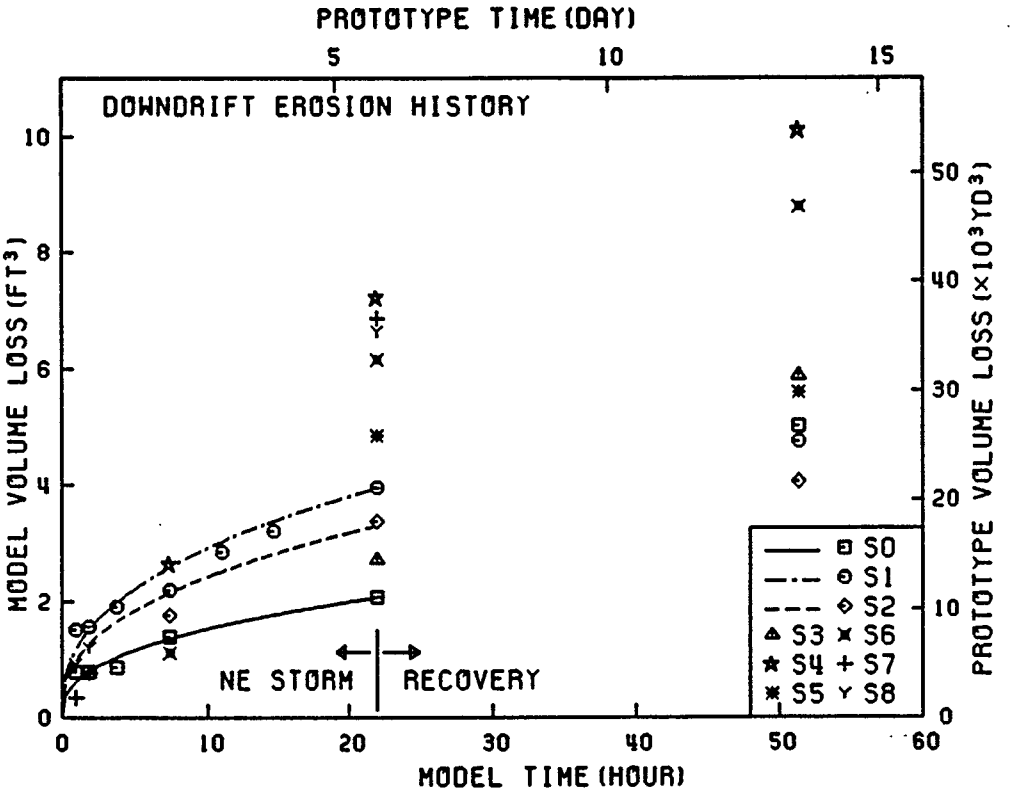

Figure 27: Downdrift erosion history from storm and recovery processes.

is revealed in Table 7 as the ebb shoal volume grew considerably in both cases. Unfortunately, recovery test was not carried out for S7 and S8 to determine the extent of beach recovery.

In the case of ebb shoal removal, complete shoal removal caused significantly increase in the nearshore volumetric erosion whereas partial removal seemed to promote both erosion during storm period and recovery during recovery period. Again, the ebb shoal gained material under both wave conditions.

Finally, for the case with both jetties removed, the south shore volume loss was large under storm condition owing to the increased transport into the inlet.

5.4 Ebb Shoal Volume Changes

The entire ebb tidal shoal volume is quite substantial in the order of 1.3 million yd^3. It is a difficult task to measure the change in short-duration tests as any small inaccuracy in survey will lead to large error in volumetric computation. Therefore, the shoal volume computations are restricted in an area in the immediate vicinity of the inlet. Even in such restricted condition one should be cautious in interpreting the results.

Under NE storm condition, the sediment motion is very active in the ebb shoal region owing to wave breaking over the shoal. The material was then transported by currents induced by tides and waves. The tidal current carries the ebb shoal material into the inlet during flood and re-circulates the material following a clockwise circulation in the vicinity of the south jetty during ebb. The wave induced current transport part of the material into the nearshore zone towards the downdrift direction. However, significant portion of the material simply moves in the offshore region towards south. Therefore, under NE storms, ebb tidal shoal lost material in the immediate vicinity of the inlet entrance but fed material into the inlet and the downdrift nearshore zone; on the same time, the entire ebb shoal appeared to shift to the south due to transport in the offshore region. This same pattern held for S1, S2 and S3 where only jetty structures were modified.

From the fact that shoal volume changes were similar between S0 and S3 (no N jetty extension), and between S1 and S2(with N jetty extension), the volume change in this region was mainly influenced by the north jetty configuration. Apparently, the north jetty extension reduced the downdrift bypassing thus reduced the volume change in this region.

For cases with ebb tidal shoal removal, the region gained instead of lost material as part of the ebb shoal re-generating process. This was also the case for S6 with the removal of the jetties, since the initial configuration in S6 has no ebb tidal shoal; the material gaining was a normal ebb tidal shoal generating process in the presence of an inlet. The patterns of ebb shoal growth were similar for the three configurations of S4, 5 and 6 with material being accumulated near the inlet entrance and gradually spreading towards downdrift.

For the two configurations with beach nourishment, the ebb tidal shoal region also gained material. Since ebb tidal shoal was present in the initial condition the pattern of growth of was somewhat different from the situation while the ebb shoal was removed. Here, most of the gain was just outside the nearshore zone in the form of an offshore bar, mainly as a consequence of profile adjustment. It is unclear whether this material will become a permanent part of the ebb tidal shoal or will be brought back to the beach during normal and/or recovery wave conditions as no test were conducted under those conditions.

5.5 Updrift Volume Changes

Updrift volume changes were mainly associated with the change of north jetty configuration. Extending the north jetty as in S1 and S2 resulted in additional impoundment of sand at a rate of about 1,000 yd^3/day during the extended storm tests. This additional impoundment is very minor. Furthermore, this quantity is expected to diminish as the north shore gradually adjusts to the new jetty

configuration. Removal of north jetty caused significant updrift volume loss as expected. This loss is likely a transient phenomenon and probably will diminish rapidly as the updrift profile adjusted to normal.

5.6 Summary of Performance Evaluation

Performance of different structural alternatives was evaluated from the point of view of sediment budget. The main components in the eight alternative configurations tested in the laboratory consisted of extension of north jetty, extension of south jetty, ebb tidal shoal removal and utilization, beach nourishment and the combination of the above.

- The extension of north jetty reduces the rate of inlet shoaling slightly but also increases downdrift erosion slightly. Additional sand is initially impounded on the north side of the north jetty but the rate of impoundment is likely to slow down and eventually becomes negligible as the updrift shoreline adjusted to a new equilibrium configuration. For the configuration tested the amount of the additional impoundment should be small. The ebb shoal volume is to grow modestly owing to the reduction of ebb shoal bypassing.
- The extension of south jetty has the major benefit of reducing inlet shoaling and loss of material to the inlet, as well as promoting more downdrift transport. However, Erosion in the immediate vicinity of the south jetty also increases; the degree of severity will depend upon the length and shape of the extension. For the configurations tested (150 ft and 500 ft extensions), the added erosions are modest. The final stable shoreline position will be largely governed by the south jetty configuration. The current prevailing shoreline recessed by a mount of 60 - 75 ft roughly corresponds to the mean final position under extended NE storms. Under the present south jetty configuration, a stable shoreline seaward of the current prevailing shoreline position can not be maintained within reasonable cost and means. The effect on ebb tidal shoal depends upon the extent of the jetty extension and it relationship to the north jetty; for the configurations tested, the effect will be modest as the south jetty still remains in the shadow zone of the north jetty under prevailing northeasters. The south jetty extension shows little or no effect on the updrift region.
- Removal of both jetties is not a viable alternative as the inlet will become innavigable.
- Ebb tidal shoal removals cause increased channel shoaling and downdrift erosion in the immediate vicinity of the inlet; the effect of the latter is likely to be local. Downdrift transport increases initially but is likely to diminish as the shoal re-generates. Ebb shoal re-generates at a fairly rapid pace.

- Beach nourishment increases downdrift transport at the expense of the nourished material. Under storm conditions a significant portion of the material(larger than the portion transported downdrift) is transported offshore to form a bar. This bar is located beyond the tip of the existing south jetty and extends northward into the channel. This is likely to impair inlet navigation. The problem can be contained with the south jetty extension.

6 Sediment Budget Analysis

Sediment budget is defined here as the annual net transport rate with reference to a control area shown in Figure 28. To attempt a sediment budget analysis for this control area one needs to establish six transport quantities:

- Q_1: net transport across updrift boundary.
- Q_2: net transport across downdrift boundary.
- Q_3: net gain (loss) from updrift shoreline erosion (accretion).
- Q_4: net gain (loss) from downdrift shoreline erosion (accretion).
- Q_5: net loss to the inlet.
- ΔV: net ebb tidal shoal volumetric change.

It is not an easy task to establish these quantities with our current level of knowledge on inlets. Information from different sources are pieced together here to facilitate the best estimations. Unfortunately, as will be seen later, many of these sources have very low reliability. The problem is further compounded by the fact that these sources all have different spatial and temporal resolutions and some of them have large annual variations. Therefore, the results are, at best, an educated guesstimate and should be used with extreme discretion.

A detailed analysis was performed here for the existing condition (S0).

6.1 Historical Shoreline Changes

The quantities Q_3 and Q_4 which are associated with the long term gain(loss) due to shoreline erosion (accretion) can be estimated by examining historical shoreline changes in this region.

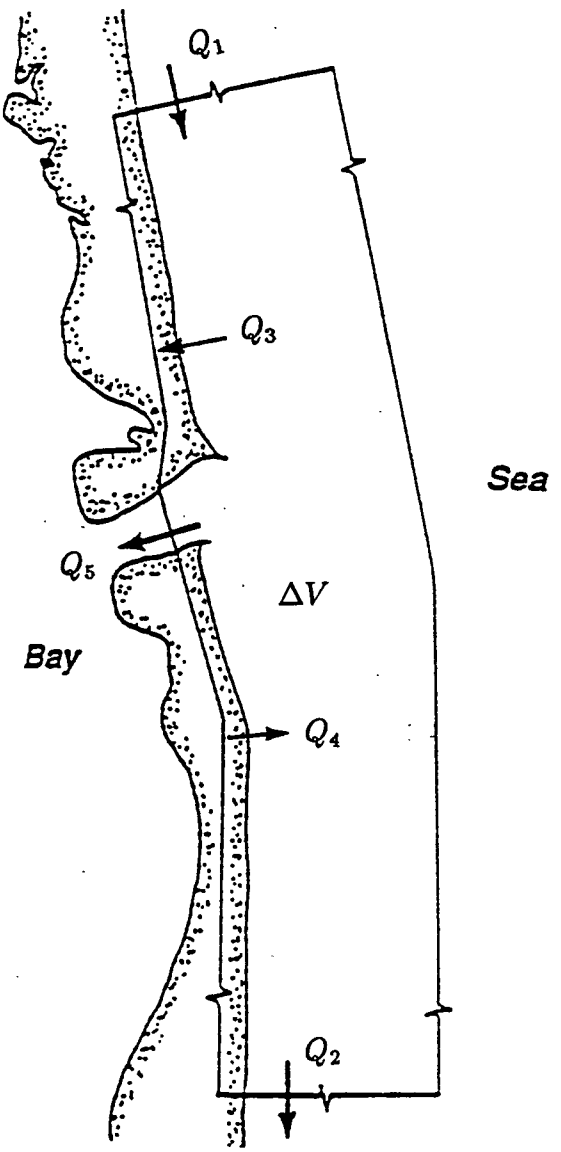

Figure 28: A sketch of sand budget control box near inlet.

The history of Sebastian Inlet can be divided into three stages. During the first stage of 1886–1924, many unsuccessful attempts were made to open the inlet. These attempts failed because the work was at a level that was too small in scale, and consequently the minimum flow cross-section required for a stable inlet was not met. During the second stage, 1924–1942, the inlet remained open but not stable. This was due to insufficient flow cross-sections and insufficient jetty protection from wave induced littoral drift. The third phase of the inlet begins with the reopening of the inlet in 1948. A series of dredging operations and jetty improvements have widened the flow area and reduced littoral drift so that the inlet has been stable since then. However, this inlet stabilization also caused drastic shoreline changes.

Based upon historical maps, aerial photos and actual field surveys the shoreline changes in the vicinity of the inlet were analyzed by Ahn et.al.[8]. Odd-even analysis and Fourier analysis were used to separate the background erosion and the effects of inlet. These two analysis practically yielded identical results. The shoreline changes can be roughly divided into three stages. Prior to the inlet stabilization in 1946, the shoreline in this region was relatively stable and mildly accretional. After the stabilization, the shoreline apparently underwent significant changes in the first 20 years. The rate of change reduced afterward as the inlet matured. Figure 29 shows the rates of shoreline change during these three periods. From 1929–1947, the shoreline was stable and mildly accretional. From 1947–1970, the change showed extensive downdrift erosion and appreciable updrift accretion. It appeared that the shorelines have been affected for approximately 5 miles on either side of the inlet with the most significant changes occurring within 2 to 3 miles from the inlet. The net north and south shoreline offset, at present, is close to 400 ft. The average downdrift shoreline retreat over the 5 miles distance was about 120 ft., or an average rate of approximately 5 ft per year. The updrift shoreline has accreted on the average of approximately 70 ft over 5 miles, or a rate of 3 ft per year. During the period from 1970 to 1986, the rate of erosion decreased to 1.5 ft per year and the rate of accretion also decreased.

In terms of annual volumetric rate of changes, the following values are obtained by assuming equilibrium profile to -6 ft. contour:

- Updrift: +1,300 yd^3 per year from center of inlet to 7,000 ft updrift.
- downdrift: -2,300 yd^3 per year from center of inlet to 15,000 ft downdrift; 4,500 yd^3 per year from center of inlet to 25,000 ft downdrift, and 6,800 yd^3 per year from center of inlet to 40,000 ft downdrift.

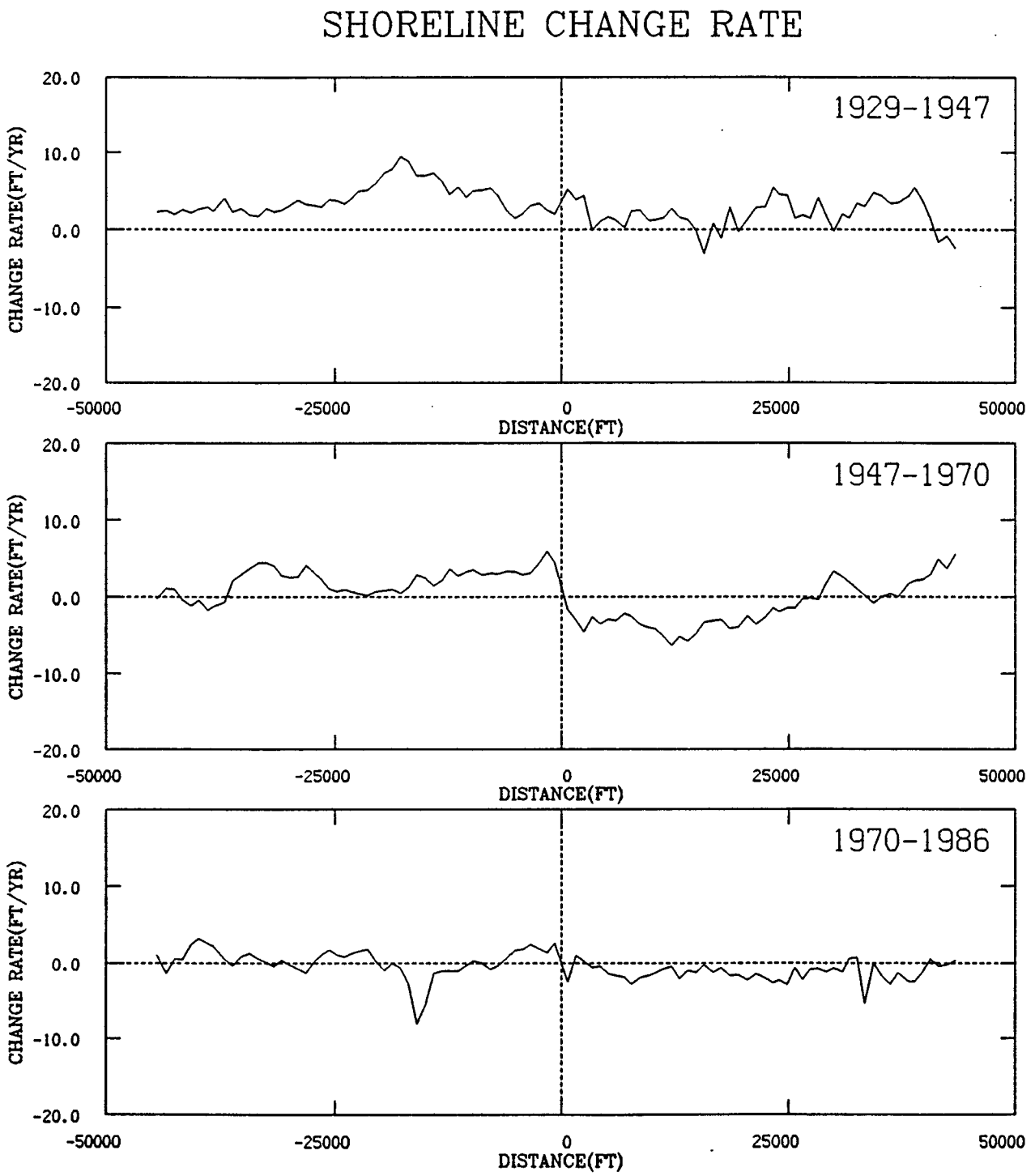

Figure 29: Shoreline change rates from 1929 to 1986.

6.2 Background Littoral Drift Environment

The sediment transport at the updrift boundary, Q_1, can be treated as the background littoral drift in the absence of the inlet. This quantity has been estimated by a number of previous investigations:

- 300,000 cubic yard per year (Southward–USAE)
- 160,000 cubic yard per year (Southward–Walton)
- 157,000 cubic yard per year (Southward–Coastal Tech.)

An attempt was made here to estimate the littoral transport rate based on wave hindcast data.

The Army Corps of Engineers Wave Information Study (WIS) contains 20 years (1956–1975) of hindcast wave data for the east US coast including Sebastian Inlet area. In addition, approximately 5 years (1986–1990) of real wave data for Vero Beach (located about 15 miles south of the Sebastian Inlet) was available from the Coastal Data Network (CDN), Coastal and Oceanographic Engineering Department at the University of Florida.

The WIS data was generated by using numerical hindcast models and offshore meteorological records to calculate wave growth and wave transformation from deep to shallow water. This data does not include the effects of tropical storms or hurricanes. The wave height, period, and angle of approach were calculated for the sea and swell conditions separately and then combined. The combined sea and swell conditions were used for this study. The data was collected at 3-hour intervals and the calculations performed for a shallow water depth of 10 m. For this study, the WIS data was rearranged to twelve data sets of monthly statistics.

The CDN data which is real wave data was collected at 6-hour intervals (with the exception of equipment downtime) at a depth of approximately 10 m off Vero Beach CDN. As reported in the Part I Report the measured waves at Sebastian Inlet were almost the same as that at the Vero Beach. Thus the CDN data could serve the purpose of adjusting the hindcast data.

The CDN and WIS data compare relatively well, however, the WIS data shows slightly larger wave heights and smaller wave periods. To account for this, the WIS data was adjusted by first dividing the mean monthly CDN wave heights and periods by those from the WIS data to obtain correction coefficients. These monthly correction coefficients were applied to the WIS data set. Table 13 compares the CDN and WIS results and the tabulates the correction coefficients. The adjusted WIS data was used as input for longshore sediment transport rate calculations.

Table 13: Comparison of CDN and WIS wave data.

Month	Mean H_{CDN} (m)	Mean H_{WIS} (m)	Coef.	Mean T_{CDN} (sec)	Mean T_{WIS} (sec)	Coef.
Jan	0.80	0.95	0.84	8.57	6.22	1.33
Feb	0.74	0.93	0.80	8.36	6.41	1.23
Mar	0.77	0.88	0.88	8.26	6.40	1.29
Apr	0.39	0.94	0.42	9.61	7.07	1.36
May	0.56	0.72	0.77	8.51	5.36	1.59
Jun	0.44	0.60	0.74	7.85	5.51	1.42
Jul	0.37	0.47	0.78	7.73	4.90	1.58
Aug	0.42	0.51	0.82	8.31	5.05	1.65
Sep	0.62	0.93	0.67	9.42	6.29	1.50
Oct	0.83	1.25	0.66	8.38	7.16	1.17
Nov	0.83	1.11	0.74	8.14	6.66	1.22
Dec	0.82	1.05	0.78	9.17	6.79	1.35

The volumetric longshore transport rate is computed here by [9]

$$Q = \frac{K\, H_b^2\, C_{gb}\, \cos\alpha\, \sin\alpha}{8\,(s-1)(1-p)} \tag{4}$$

where H_b is the breaking wave height, C_{gb} is the wave group velocity at wave breaking depth, and α is the angle between the wave ray and the shore perpendicular line, p is the porosity of sediment and s is the specific gravity of sediment. The coefficient K is empirically determined.

If the bathymetry is assumed as parallel to the shoreline and the energy losses from deep water are neglected, Eq.(4) can be expressed in terms of deep water conditions as follows:

$$Q = \frac{K\, H_o^{2.4}\, T^{0.2}\, \cos\alpha_o \sin\alpha_o}{8\,(s-1)(1-p)2^{1.4}\pi^{0.2}\kappa^{0.4}\cos^{0.2}\alpha_b} \tag{5}$$

Necessary assumptions for the derivation of Eq.(5) are the shallow water asymptotes, $C_{gb} = \sqrt{gh_b}$, $H_b = \kappa h_b$, with the deep water asymptote, $L_o = gT^2/2\pi$, the conservation of energy, and Snell's law.

For estimating the longshore sediment transport at Sebastian Inlet the following values were used: $\cos^{0.2}\alpha_b \approx 1$, g=32.2 ft/sec^2, s=2.65, p=0.4, κ=0.78. Then, the longshore sediment transport rate, Q, in ft^3/sec was estimated as

$$Q = 0.3374\, K\, H_o^{2.4}\, T^{0.2} \cos^{1.2}\alpha \sin\alpha \tag{6}$$

where K is a function of sediment size, among other factors. A value of K=0.77 was often recommended [9] in Eq.(6) as using the root-mean-square wave height for H_o. Harris [10] suggested the value of 0.77 to be too high when he applied the equation to Jupiter Inlet and adjusted the value downward to about 0.28. In the present study, it was found that calculated littoral drift rate varied greatly from year to year. Selecting K=0.28 would yield a 20-year averaged transport rate in the same range as those estimated by previous investigators.

The root-mean-square wave height is related to the significant wave height by the following equation assuming a Rayleigh distribution of wave heights:

$$H_s \approx \sqrt{2} H_{r.m.s.} \approx 1.6 H_m \tag{7}$$

where H_s denotes the significant wave height, $H_{r.m.s.}$ denotes the root-mean-square wave height, and H_m denotes the average wave height.

The longshore sediment transport rate was then computed at 3 hour intervals for the 20 years period from 1956 to 1975. The statistics are then complied. Table 14 shows the computed longshore transport values the percentage of drift

Table 14: Estimated longshore transport (yd^3/year) from 1956 to 1975.

year	Q_{south}	Q_{north}	Q_{net}	Q_{gross}	Percentage of Drift	
					% south	% north
1956	467,487	106,523	360,964	574,010	81.4	18.6
1957	304,377	196,522	107,855	500,900	60.8	39.2
1958	343,140	196,576	146,564	539,716	63.6	36.4
1959	508,983	248,095	260,888	757,077	67.2	32.8
1960	427,207	200,425	226,782	627,631	68.1	31.9
1961	389,891	190,606	199,285	580,497	67.2	32.8
1962	591,284	103,221	488,063	694,505	85.1	14.9
1963	496,666	130,036	366,630	626,701	79.3	20.7
1964	414,068	190,440	223,628	604,508	68.5	31.5
1965	318,070	195,616	122,454	513,685	61.9	38.1
1966	395,820	246,691	149,130	642,511	61.6	38.4
1967	483,036	94,026	389,009	577,061	83.7	16.3
1968	192,039	76,195	115,843	268,234	71.6	28.4
1969	400,836	198,553	202,283	599,389	66.9	33.1
1970	315,070	225,263	89,808	540,333	58.3	41.7
1971	342,872	139,837	203,035	482,708	71.0	29.0
1972	406,650	175,286	231,364	581,936	69.9	30.1
1973	655,430	100,284	555,146	755,715	86.7	13.3
1974	227,433	73,887	153,546	301,320	75.5	24.5
1975	207,392	105,227	102,165	312,619	66.3	33.7
Ave.	394,384	159,665	234,722	554,053	70.7	29.3

to the south and to the north for the 20 year period. By convention, positive transport denotes southward and negative transport denotes northward. The net drift Q_{net}, is the difference between the positive and negative components, while the gross drift, Q_{gross}, is the sum of the drift magnitudes.

The average value of annual net transport rate of 234,722 yd^3 per year falls in between those estimated by previous investigations. This value may be on the high side as wave attenuation is neglected in the wave transformation from deep to shallow water.

Table 15 shows the monthly littoral drift statistics based on daily longshore transport values for the 20-year period from 1956 to 1975. Table 16 shows the statistical parameters including the mean, μ and the standard deviation, σ, of the daily transport rate, and also the mean and standard deviation of the daily log-transport rate, μ_{log} and σ_{log}, respectively, for the same 20-year period.

The overall seasonal trend of the longshore transport is similar from the 20-year data. During winter (from October to February), the net transport is southward

Table 15: Monthly percentage of longshore transport direction from 1956 to 1975.

Month	Jan	Feb	Mar	Apr	May	Jun	Jul	Aug	Sep	Oct	Nov	Dec
%South	65.7	65.6	61.0	61.8	44.2	40.5	26.3	36.3	57.3	76.9	70.0	70.0
%North	34.2	34.2	39.0	37.7	54.8	58.7	71.6	62.1	42.2	22.9	30.0	29.8
% Zero	0.1	0.2	0.0	0.5	1.0	0.8	2.1	1.6	0.5	0.2	0.0	0.2

Table 16: Statistics of longshore transport rate (yd^3/day) from 1956 to 1975.

Month	μ	σ	μ_{log}	σ_{log}
Jan (South)	3,318	5,190	3.013	0.804
(North)	1,477	2,211	2.671	0.808
Feb (South)	2,673	4,148	2.936	0.777
(North)	1,631	2.520	2.728	0.795
Mar (South)	2,476	3,708	2.951	0.728
(North)	1,741	2,927	2.744	0.752
Apr (South)	352	510	2.212	0.598
(North)	412	472	2.185	0.845
May (South)	1,136	2.236	2.546	0.827
(North)	1,111	1,599	2.505	0.886
Jun (South)	532	1,145	2.132	0.814
(North)	755	1,492	2.302	0.841
Jul (South)	351	453	1.992	0.867
(North)	503	857	2.199	0.831
Aug (South)	718	1,740	2.257	0.838
(North)	533	861	2.259	0.739
Sep (South)	1,407	2,701	2.626	0.706
(North)	961	1,891	2.473	0.787
Oct (South)	2,068	3,260	2.882	0.661
(North)	1,232	1,864	2.653	0.692
Nov (South)	2,767	3,981	2.974	0.744
(North)	1,452	1,890	2.741	0.753
Dec (South)	2,733	3,999	3.045	0.676
(North)	1,615	2,483	2.726	0.781

characterized by episodic large transport rate associated with Northeast Storm events. During summer (May to August), the transport rate is much smaller and the duration of northward transport becomes longer. Late spring and early fall form the shoulder seasons with less predictable trend. Clearly, the bulk of the annual cumulative transport rate is due to episodic events. Since episodic events vary greatly from year to year, it helps to explain the large variance of the annual transport rate as calculated from WIS wave data.

6.3 Ebb Shoal Volume

In the presence of an inlet, sediments which would have been transported to the downdrift beach are instead being carried into the inlet by flood current as well as being pushed offshore by ebb tidal currents. Therefore, the shoal formed in the offshore region is known as the ebb tidal shoal. The rate of accumulation of sediment in the ebb shoal thereby causes a depletion of sand at the downdrift side of the inlet and needs to be accounted for in sediment budget analysis. From the field experience, this quantity could be very large. Unfortunately, it is also very difficult to estimate this volume and it is even more difficult to estimate the annual volume change for lack of adequate long term data. Earlier estimates of the ebb tidal shoal volume varied widely from 50,000 to 1,5000,000 yd^3.

The ebb shoal volume is estimated here from 1987, 1988, and 1989 topographic survey data using a quasi-equilibrium profile as the reference. Determining the equilibrium profile that would exist in the absence of the inlet requires some judgement and experience. It was determined that the northernmost profile for each year was the best representation of the equilibrium profile and was used as the basis for calculating the ebb shoal volume. The volume was first calculated by using the Trapezoidal Rule as an estimate and then by Simpson's Rule with 100 ft interval to obtain more accurate result. The ebb shoal was considered to extend from the north jetty to the southernmost edge of the available survey data, and offshore to an estimated closure depth of 36 ft(see Figure 30). The southern offshore limits of the survey data fell slightly short of the full extent of the ebb shoal. To account for the offshore portion of the ebb shoal, extrapolation from the existing survey data was used to estimate the additional volume (about 5% addition of volume was estimated). However, any additional volume to the south of the survey boundaries was neglected due to the inaccuracy of extrapolating data in this region. The ebb shoal volumes are shown in Table 17. Figure 31, for instance, shows contours of the elevation differences for the 1989 survey. Three-dimensional images of the ebb shoal were generated and shown in Figure 32 from two viewing angles. Figure 32 reveal two very interesting aspects. First, the shape of the ebbshoal with respect to the reference plane appears to be very symmetrical even though it is crescent-shaped in the prototype. Second, the sand deficit in the downdrift nearshore zone and the ditch effect as discussed before are clearly demonstrated.

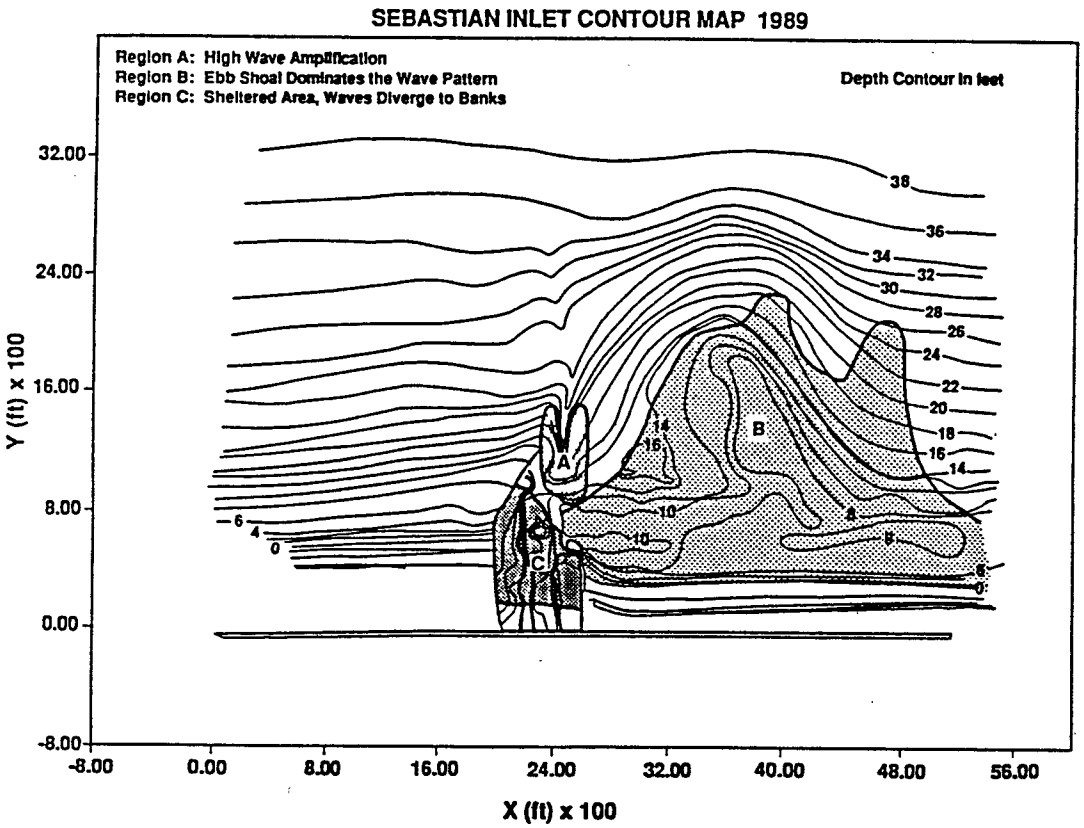

Figure 30: Bathymetric Survey map for 1989.

Table 17: Ebb shore volume computed for 1987 to 1989.

Year	Volume From Survey Data (yd^3)	Extrapolated Volume (yd^3)	Total Estimated Ebb Shoal Volume (yd^3)
1987	1,320,000	90,000	1,410,000
1988	1,390,000	90,000	1,480,000
1989	1,220,000	60,000	1,280,000

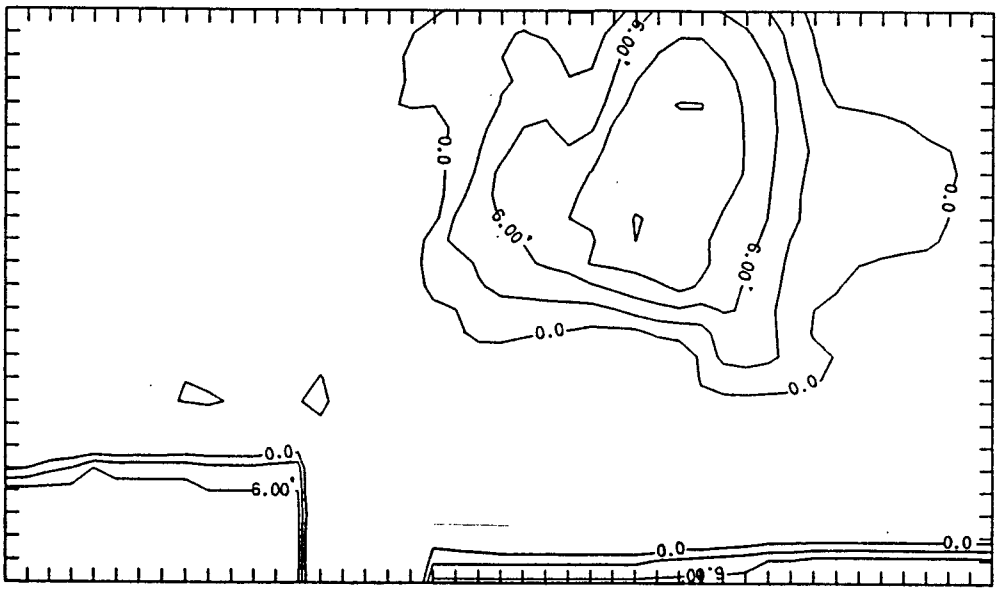

Figure 31: Contours of ebbshoal volume computed from 1989 survey.

From these values, it appears that the ebb tidal shoal is rather stable in recent years. Unfortunately, these values are usually large that even a small annual change here could dominate other quantities in the sediment budget. For instance, the volume difference between 1988 and 1987 is 70,000 yd^3 which represented only 5% change. However, this 70,000 yd^3 is about one third of the estimated annual background transport rate. The difference between 1989 and 1988 is 200,000 yd^3 which would certainly overshadow other transport quantities. Since computations are carried out based on survey data over a large area, small survey inaccuracy will also result in substantial error. Again, one must approach this value with extreme caution.

6.4 Interpretation from Laboratory Results

The laboratory results suffer two drawbacks. First, they are for short term extreme events and can not be easily extrapolated to long term sediment budget application. Second, the updrift condition is significantly influenced by the boundary effects. Therefore, one can not rely on the data to establish updrift transport rate. The results are believed to be reliable for downdrift boundary longshore transport, downdrift shoreline erosion, ebb tidal shoal changes and transport to inlet as given in Section 4.5. These results do confirm the fact that sediment transport and hydrographic changes are dominated by storm events.

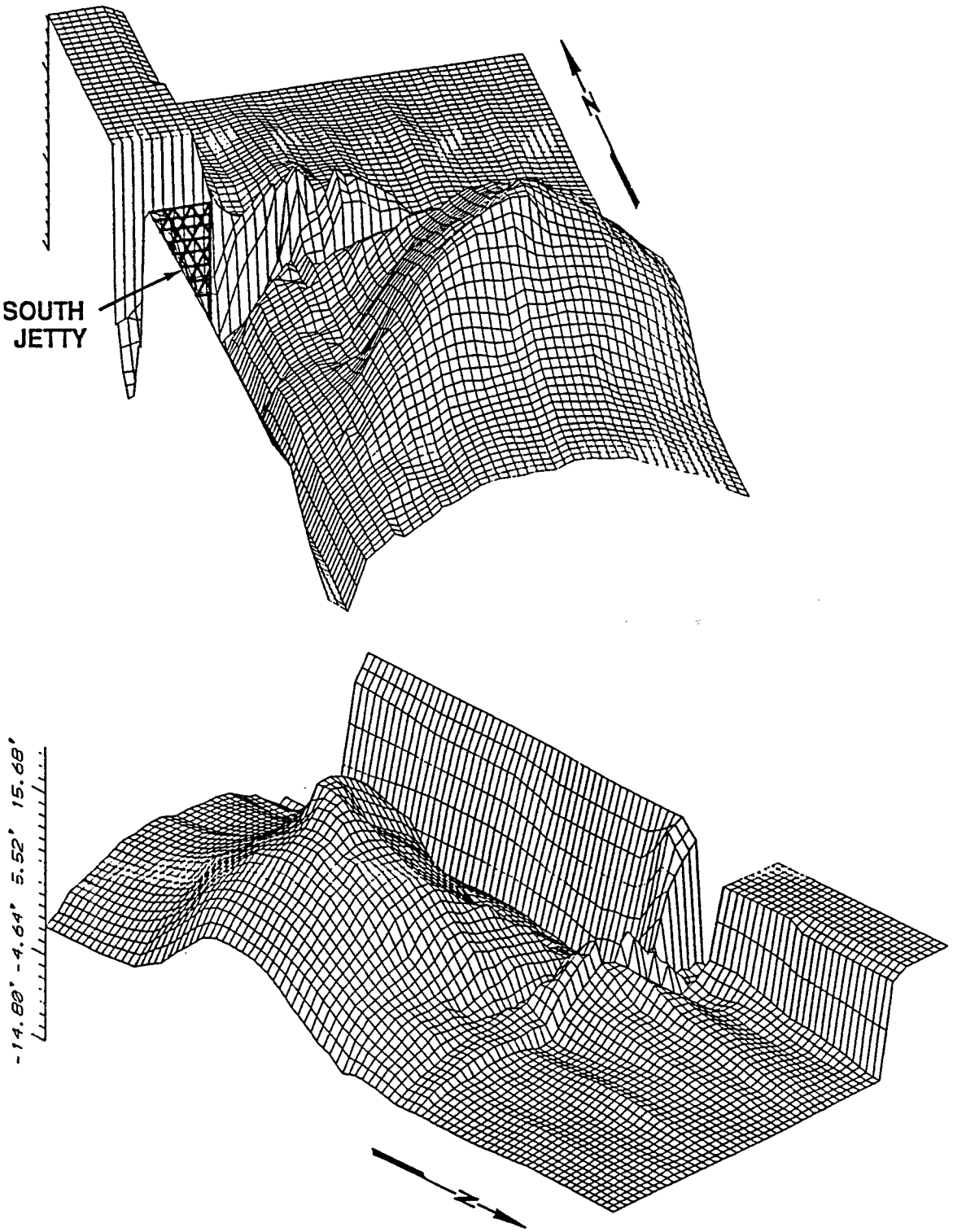

Figure 32: Orthographic plots of ebb shoal volume from 1989 survey.

The results from the S0 structure configuration showed that a 6-day NE storm of 6 ft wave produced about 2,200 yd^3/day average transport rate on the downdrift boundary whereas a moderate NE wave of 2 ft produced only 480 yd^3/day average downdrift transport. This is also true for net sediment losses into the inlet. For storm waves this net loss amounted to 1,400 yd^3/day and it reduced to less than 100 yd^3/day for the moderate normal wave condition. The ebb tidal shoal behaved differently under storm and normal wave conditions. During NE storm, the ebb tidal shoal immediately downdrift of the inlet lost material to the downdrift and offshore directions. Under moderate NE waves, the ebb tidal shoal region immediately south of the inlet gained material. Therefore, as discussed earlier that during extreme events the ebb tidal shoal expanded towards downdrift and offshore at the expense of drawing sediment from the existing shoal. Also part of the ebb tidal shoal material was fed into the downdrift littoral zone which eventually ended in the downdrift beach. On the other hand, during moderate NE waves, the material lost in the existing shoal was being replenished by the updrift material.

For waves from east, the net littoral transport was nil. Material, however, was continuously lost to the inlet mainly at the expense of downdrift shore erosion. For the SE waves, the quality of data was not as good. The general pattern shows continued loss of sediment into the inlet, erosion at the south side and modest growth of ebb tidal shoal.

6.5 Sediment Deficit Estimation

Sediment deficit estimation is always an extremely difficult task for a number of reasons. First of all, the annual longshore transport rate varies greatly from year to year. Secondly, the change of ebb shoal volume is a dominant factor but current information is insufficient to make a reasonable estimate. Finally and foremostly there is simply a lack of long-term reliable field information to facilitate such an estimate.

The sediment deficit estimation made here is extremely simplified. It is assumed here that the northshore is stable, the ebb shoal is in a state of equilibrium so that the net deficit is approximately equal to net loss of sand into the inlet. Furthermore, it is assumed that the laboratory results obtained under storm events can be extrapolated to annual application based upon the idea of equivalent storm days.

The equivalent deepwater wave conditions for the storm waves used in the laboratory can be established by the following equation:

$$H_o = \frac{H}{K_s K_r} \tag{8}$$

where K_s and K_r are the shoaling and refraction coefficients, respectively. The laboratory water conditions are H=6 ft. T=6s, $\theta = \pm 10°$ and h = 30 ft. The corresponding deepwater wave conditions are $H_o = 6.5ft$ and $\theta_0 = 14°$. Substituting these values into Eq.(6) using K=0.28, the longshore transport rate is calculated to be 9,500 yd^3/day. Based upon Table 14 the average annual southward transport is about 394,000 yd^3 and the average northward transport is 160,000 yd^3. The equivalent storm days are:

- Equivalent storm days causing southward transport=394,000/9,500=42 days
- Equivalent storm days causing northward transport=160,000/9,500=17 days

Since both southward transport and northward transport contribute to sediment loss to the inlet, the total annual loss is obtained by:

$$Q_d = Q_{ln}\, D_n + Q_{ls}\, D_s \tag{9}$$

where Q_d is the annual sediment deficit; Q_{ln} is the net inlet loss per day due to NE storm; Q_{ls} is the net inlet loss per day due to SE storm; D_n is the equivalent transport days due to NE storm and D_s is the equivalent transport days due to SE storm.

From Figure 33, Q_{ln}=1,420 yd^3/day and Q_{ls}=910 yd^3/day. Therefore, the average Q_d based on Eq.(9) is

$$Q_d = 1,420 \times 42 + 910 \times 13 = 75,110$$

or about 75,000 yd^3 a year. Since the littoral transport rate varies greatly from year to year, the annual deficit is also expected to vary greatly. Once again, the value calculated here only represents the net sediment loss to the inlet.

6.6 Sediment Budget

Based upon analysis give above the annual sediment budget can be constructed. Figure 33 shows the balance for the control area given. This balance is based on the average values presented earlier in Table 14. As one can see, the balance is a mix of large and small quantities. Various quantities are obtained by various means at various time scales. For instance, the beach erosion rate is based on the average value of 23 years from field evidence during which time, numerous sand transfer has been carried out; the background transport is based on empirical equation using 20 years hindcast data; the net sand transport into the inlet, on the other hand, is based on laboratory data. Perhaps the weakest link of the entire balance act is the assumption that the ebb shoal is in a state of equilibrium. As explained earlier,

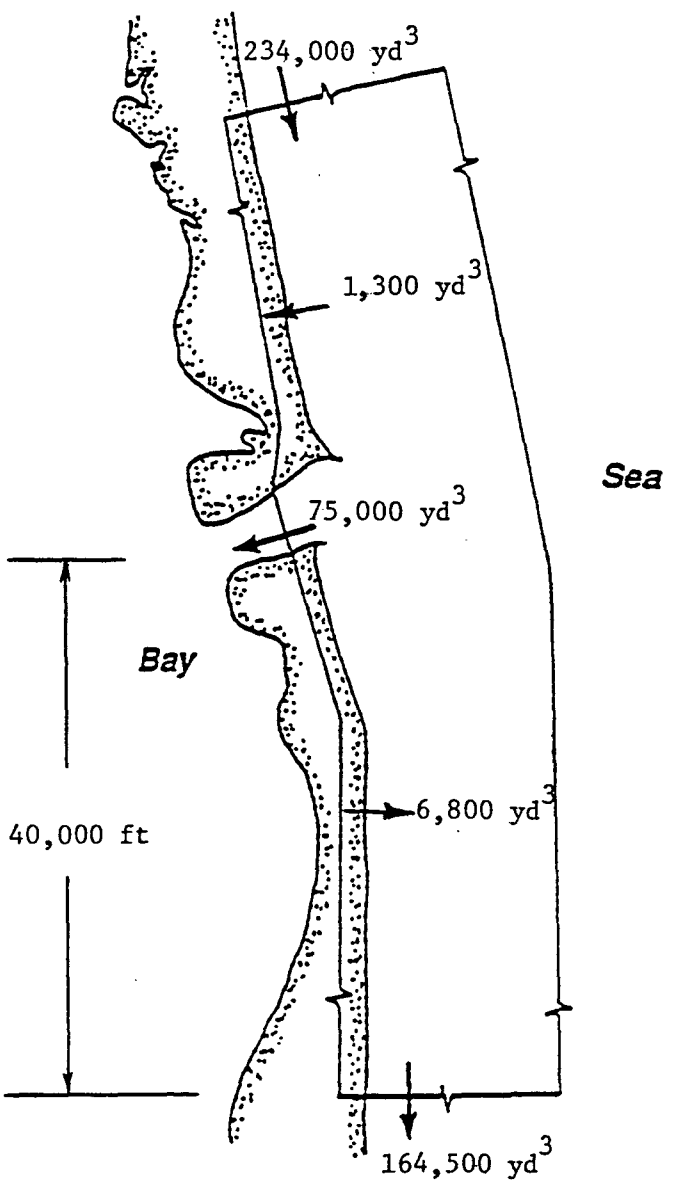

Figure 33: An estimate of annual sediment budget.

the ebb shoal quantity is large, any fluctuation in this quantity may have a large effect on the sediment budget. Unfortunately, the laboratory evidence shows that although the entire ebb shoal remains reasonably stable visible changes will occur under storm events, particularly in the top layer. Since the frequency of storm events varies greatly from year to year as can be witnessed from the 20 years wave hindcast data the annual ebb shoal volumetric fluctuation is also expected to be large.

7 Summary and Recommendations

Movable bed experiments were carried out for Sebastian Inlet to assess the sediment transport process. The main objective of the study is to explore various structural alternatives aimed at improving inlet navigation as well as beach preservation in the vicinity and, particularly, downdrift of the inlet. A total of nine configurations were tested. These nine configurations constitute various combinations of jetty structure modification, ebb shoal material removal, and beach nourishment. The test conditions consisted of 6-day (prototype equivalent) storm waves from NE and SE; 8-day recovery waves from E and 8-day normal waves from NE direction.

In addition, a sediment budget analysis for the study region was performed aimed at determining the annual sediment deficit.

7.1 Summary

The findings from this study are summarized here:

- The updrift zone north of the north jetty is relatively stable for all structural configurations under all test wave conditions except for the case where both jetties were removed. Under storm conditions, material in the nearshore zone moves to offshore to form a bar as one expects. Extension of north jetty induces sediment impoundment on the northside. The magnitude of this impoundment is found to be modest. The location of the impoundment is mainly in the offshore region, near the tip of the north jetty extension and further updrift, and the area is rather diffused. Under normal NE waves, the beach recovers by smoothing out offshore bar. Waves from east is less effective in this updrift zone recovery.
- The downdrift shoreline immediately south of south jetty (to approximately 2,000 ft south) suffers recession for all structural configurations under storm wave conditions from NE and SE. It also suffers mild recession under normal

NE wave condition. Most the shoreline recession is confined within 2,000 to 2,500 ft from the south jetty. The shoreline recession is the smallest for the existing structural configuration (S0). Extension of north jetty increases downdrift shoreline recession. This is also true for the short south jetty extension (150 ft). The magnitude of recession is estimated to be around 70 ft $\pm$ 50 ft for the 6-day NE storm. Of this magnitude, 50% or more takes place within the first 24 hours. The rate of recession decreases almost exponentially as the storm progresses. Also, the magnitude of recession decreases downdrift and becomes negligible beyond 2,000 ft.

Full removal of ebb shoal causes further increase of shoreline recession but partial removal has negligible added effect. Beach nourishment without corresponding extension of south jetty causes drastic shoreline recession with respect to the nourished shoreline position. This large recession can be largely eliminated by extending the south jetty beyond the nourished shoreline position.

Under east swell-like wave condition, the shoreline (+2 ft NGVD) recovers but the foreshore slope steepens considerably resulting net loss of sand in the nearshore zone.

- The ultimate shoreline position that can be maintained in the vicinity of the south jetty appears to be dictated by the length and configuration of the south jetty. Under the existing condition, the current shoreline appears to be in a stable position.

- The most visible bathymetric changes occur in the nearshore zone on the south side of the jetty, where sediment transport is active due to strong nearshore current. This is also seen as a zone of sediment deficit which attracts sand from both beach face and ebb shoal. Because of the strong nearshore currents, post-storm recovery in this region appears to be difficult.

- For most of the structural alternatives (except S6 and S7), both shoreline recession and nearshore erosion are modest, certainly no worse than open coast erosion under storms of similar strength. Unlike plane beach on open coast, recovery is difficult in the vicinity of the south jetty.

- There are two more regions where sediment movement is active, one in the outer region around the north jetty and the other over the ebb shoal. In the former region, it is erosional under storm condition on both side of the jetty and accretional under recovery condition on the north side, mainly in the offshore area outside the jetty. However, the rate of accretion or erosion does not appear sufficient as a potential permanent bypassing site. The sediment movement in the ebb shoal is active under storm condition. Sediment in this region is diverted into the channel, fed into the downdrift littoral zone and transported southward in the offshore zone. It appears that the offshore zone transport is substantial.

- The ebb shoal has a total volume of about 1.3 million yd^3. It is overall a stable shoal with most of the sediment movement occurring in the top layer which moves southward.

- The region between the jetties is, overall, accretional and the inlet behaves like a sediment sink under all tested conditions. Sediment converges into the inlet from three sources: updrift around the north jetty, downdrift from the ebb shoal and nearshore material around the south jetty with the last one being the major contributor. Consequently, shoaling mainly occurs near the tip of south jetty. This shoal, from time to time, will spill into the navigation channel. The navigation channel, however, is not threatened, due to strong current. Adequate extension of south jetty could cut sand loss into the inlet significantly. The test result, for instance, shows that for a 500 ft south jetty extension sediment transported into the inlet was reduced to about one-fourth of that of existing configuration under a 6-day storm.

- Ebb shoal removal, extension of south jetty and beach nourishment all induce increased rate of downdrift transport. The rate increase from the first two sources may be at the expense of the accelerated shore erosion if no adequate sediment supply is provided. Extension of north jetty retards downdrift transport slightly as more sediment being diverted offshore.

- Based upon historical shoreline survey information the influence of inlet is estimated to be around five miles on each side of the inlet. The averaged annual shoreline change and the associated erosion as well as accretion are modest. The analysis, however, did not consider the numerous sand transfer activities that took place in the past.

- The average background littoral transport rate is around 394,000 yd^3/year southward and 160,000 yd^3/year northward. This yields a net southward transport of 234,000 yd^3/year. These values may be on the high side owing to the simplified assumption employed in computing the deepwater wave height. The results clearly demonstrates that the sediment transport is dominated by episodic events. Consequently, the variations of annual rates are large.

- Sediment budget analysis was performed. The average sediment deficit is estimated to be in the order of 75,000 yd^3 a year. In this computation, the ebb shoal is assumed to be stable with no net annual gain or loss. The actual deficit will have large variations from year to year.

7.2 Recommendations

The recommendations made here are based on the experimental results from both fixed bed model and movable bed model with the weighted considerations of improving navigation as well as mitigating downdrift erosion. The recommendations

provide a general frame of improvement scheme and are given in order of preference. A plan to reach the final design configuration is also presented.

Structural Modifications

It is recommended here that the south jetty be extended. The length of the extension is estimated to be in between 300 to 500 ft. The shape of the south jetty extension should follow the north jetty contour such that the extension remains in the shadow zone of the north jetty and that the cross-sectional area of the inlet channel is maintained at the existing condition. This extension is expected to significantly reduce the net drain of sand into the inlet, reduce the shoaling rate in the inlet region and promote downdrift transport. Again, a 500 ft extension such as tested in the movable bed experiment is seen to cut the loss of sand into the inlet over 75% under 6-day storm condition. In concurrence with the jetty modification considerations should be given to nourish the beach in the immediate downdrift of the south jetty to soften the impact of the sudden structural change. This nourishment if deemed desirable is expected to be rather modest. One may also wish to consider dredging the shoaling zones within the jetty so as to ease the strong current-wave interaction near the entrance.

It is also recommended here to consider north jetty modification. There are two viable options. The first one is to sand tight the existing jetty and monitor its performance for a number of years. The second one is to extend the north jetty in the order of 200 to 250 ft. The first one will likely to further cut down shoaling inside the inlet. The cost is likely to be modest but the extent of benefit is not clear. The second option improves the wave condition in the navigation channel. For the 250 ft extension tested in the laboratory, the wave height reduction under NE storm condition is found to be in the order of 25–50% under ebb current and of 18–45% under flood current. The extension of north jetty will, however, reduce downdrift sand transport initially. This reduction might be transient. A longer test period is required to establish the real long term impact. The ebb shoal is also expected to grow slightly under this jetty modification.

Finally, no jetty modification remains an option, though not a desirable one. In this case, sandtrap dredgings, at least, at the current frequency need to be maintained and downdrift shoreline is likely to experience oscillations when compared with the alternative of south jetty extension.

Sand Transfer Plans

Sand trapping in the inlet still appears to be the most efficient means. It is estimated here that the average annual sand drain into the inlet is in the order of 75,000 yd^3. The actual annual quantity, however, is expected to vary owing to the fact that the transport is storm dominated. With the south jetty extension, this quantity is expected to reduce significantly. It is recommended here to develop a

sand bypassing scheme based on inlet sand trapping to soften the impact of the predicted large annual variations in sand deficit.

The sand storage in the ebb tidal shoal is substantial comparing with the demand of sand deficit in the downdrift. The re-generating process after removal is shown to be rather rapid but the area is diffused. It remains a viable option as sand source for nourishment and renourishment. However, further studies are required to establish the impact, the optimum utilization, and the economic viability.

The test results show that the accumulation of sand on the northside is at most moderate and the area of accumulation is rather diffused and in the offshore zone. Therefore, permanent sand bypassing plant on the northside is not recommended at this stage.

Recommended Follow-up Actions

This study provides specific information on the current and wave conditions in the inlet region, the process, deficit and budget of sediment transport, and the effects of structural modifications. Also, to the extent possible the cause and effect relationships are identified. The desirable follow-up actions are listed below:

Immediate Plan

- Determine specific design configuration for structural modification. This entails the determination on the optimum length and configuration of the south jetty extension based on extended test period to determine the long term benefit of channel dredging reduction and downdrift transport improvement. The desirability and/or the extent of initial beach nourishment after jetty extension as well as the benefit and/or the effect of initial dredging of shoaling zones in the inlet should also be determined. With the south jetty modification determined the incremental beneficial effect of north jetty extension could be tested if deemed desirable.
- Design and evaluate sand transfer scheme/schedule based upon inlet trapping as the primary means of sand collection. This design should take into consideration the anticipated annual variations and its effect on the downdrift.

Long Term Plan

- Explore the option of ebb shoal sand utilization in the long term planning of inlet management.
- Extend the study area downdrift 3-5 miles which is judged to be the limit of influence zone by the Sebastian Inlet.

References

[1] Law of Florida, Chapter 12259.

[2] Mehta, A.J., Wm.D. Adams, and C.P. Jones, 1976. "Sebastian Inlet Glossary of Inlets, Report #3," Coastal and Oceanographic Engineering Laboratory, University of Florida. UFL/COEL-76-011.

[3] Wang, H., L. Lin, H. Zhong, and G. Miao, 1991. "Sebastian Inlet Physical Model Studies: Part I – Fixed Bed Model," Coastal and Oceanographic Engineering Department, University of Florida. UFL/COEL-91-001.

[4] Engineering and Industrial Experiment Station, 1965. "Coastal Engineering Hydraulic Model Study of Sebastian Inlet, Florida," Coastal and Oceanographic Engineering Laboratory, University of Florida. UFL/COEL-65-006.

[5] Coastal Technology Corporation, Florida, 1988. "Sebastian Inlet District Comprehensive Management Plan".

[6] Wang, H., T. Toue, and H.H. Dette, 1990. "Movable Bed Modeling Criteria for Beach Profile Response," Proc. 22nd Coastal Engineering Conf., Deft, The Netherlands, pp.2566-2579.

[7] Wang, H., L. Lin, H. Zhong, and G. Miao, 1991. "Sebastian Inlet Physical Model Studies: Part II – Movable Bed Model, Interim Report" Coastal and Oceanographic Engineering Department, University of Florida. UFL/COEL-91-014.

[8] Ahn, K., A. Assaly, L. Wicker, M. Wrock, S. Samuel, T. Oh, and T. Kim, 1991. "Downdrift Erosion Prevention Project at Sebastian Inlet, Florida," Coastal and Oceanographic Engineering Department, University of Florida.

[9] Shore Protection Manual, 1983. Coastal Engineering Research Center, Corps of Engineers, U.S. Army. Vicksburg, Mississippi.

[10] Harris, P., 1991. "The Influence of Seasonal Variation in Longshore Sediment Transport with Applications to the Erosion of the Downdrift Beach at Jupiter Inlet, FL." Coastal and Oceanographic Engineering Department, University of Florida. UFL/COEL-91-015.

APPENDIX I:
Summary of Bathymetric Change Figures for S1 to S8 in 6-Day NE Storm Process.

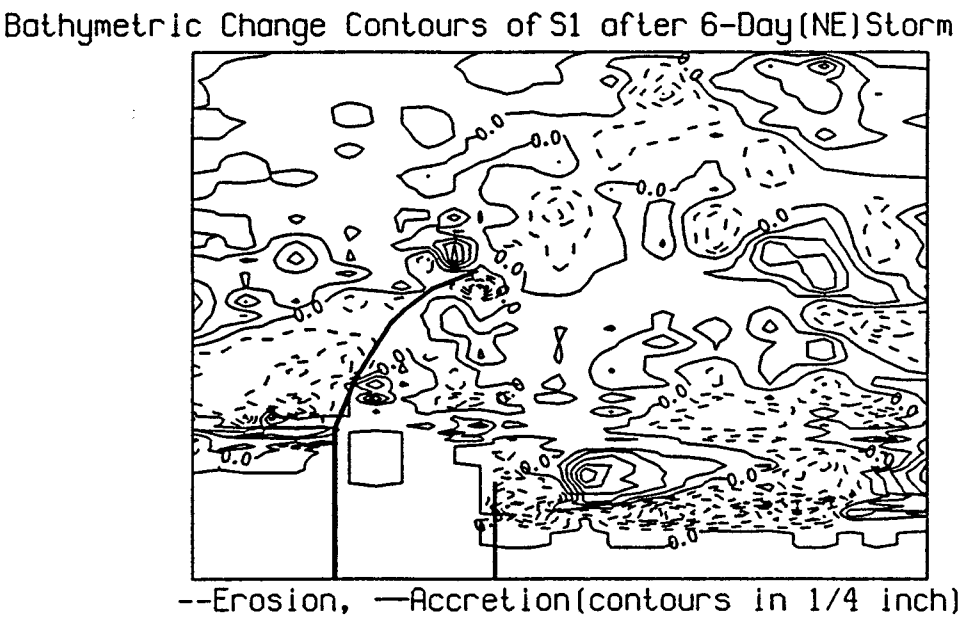

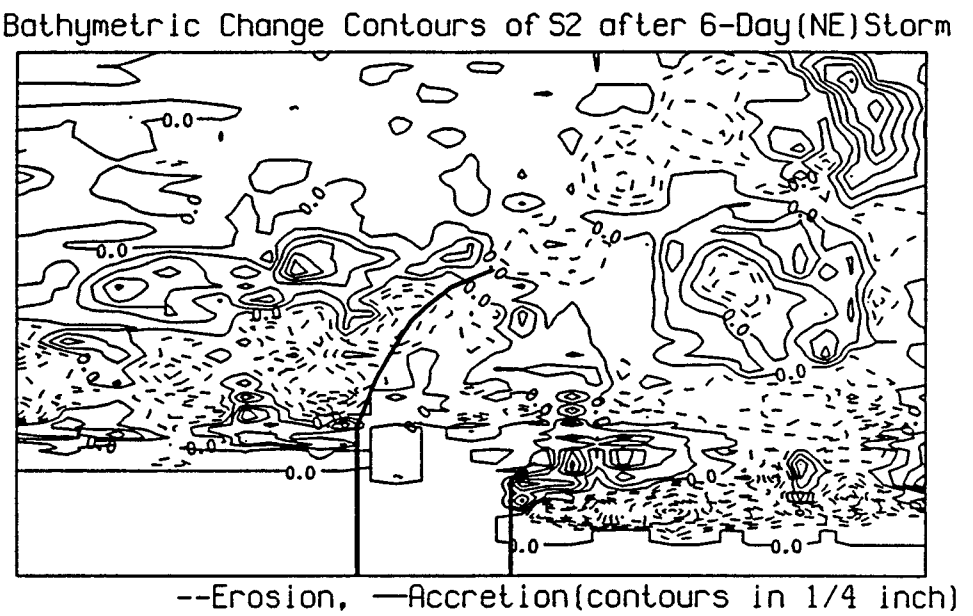

Figure I.1: Bathymetric changes for S1 and S2 in NE storm.

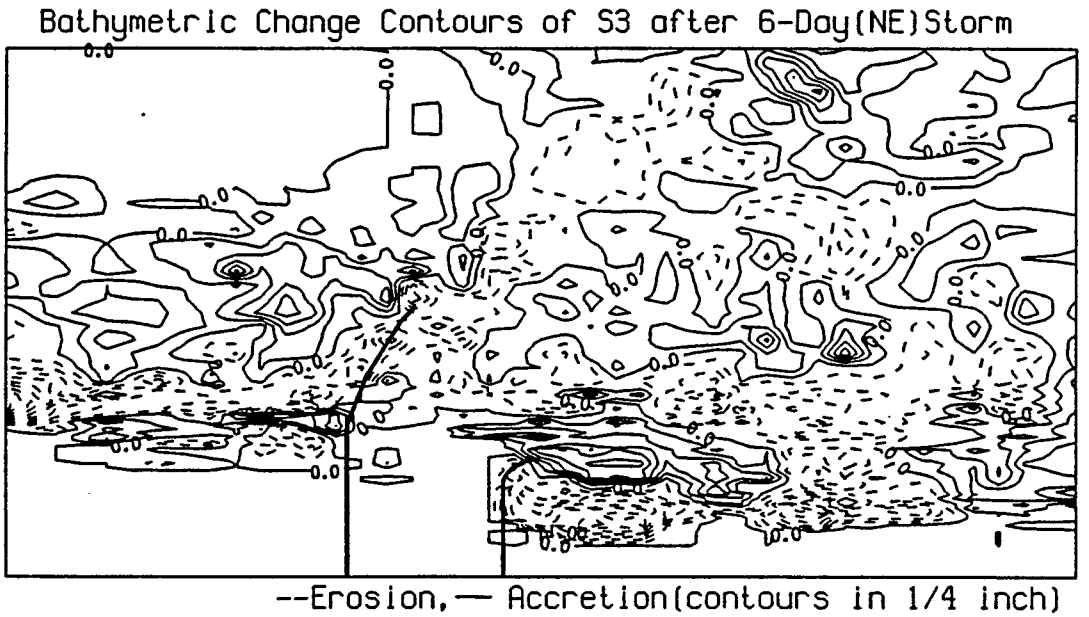

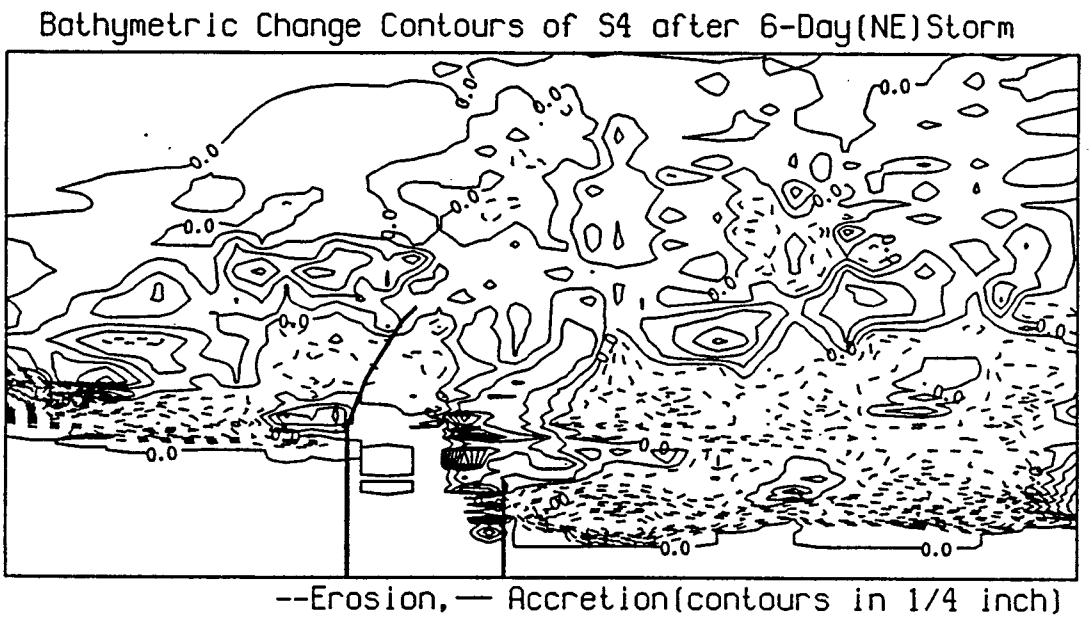

Figure I.2: Bathymetric changes for S3 and S4 in NE storm.

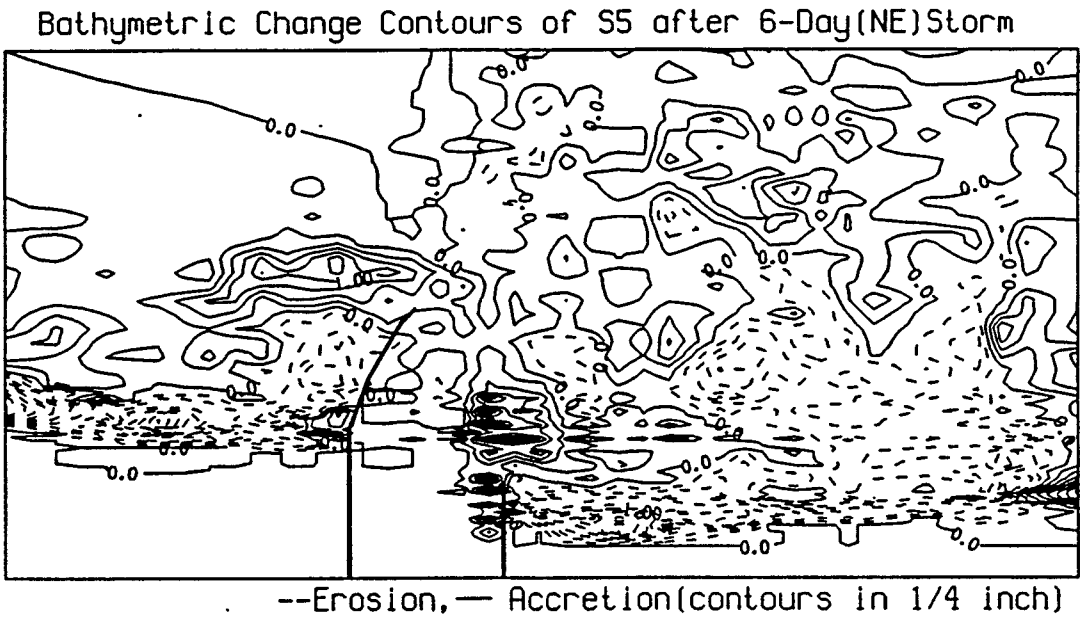

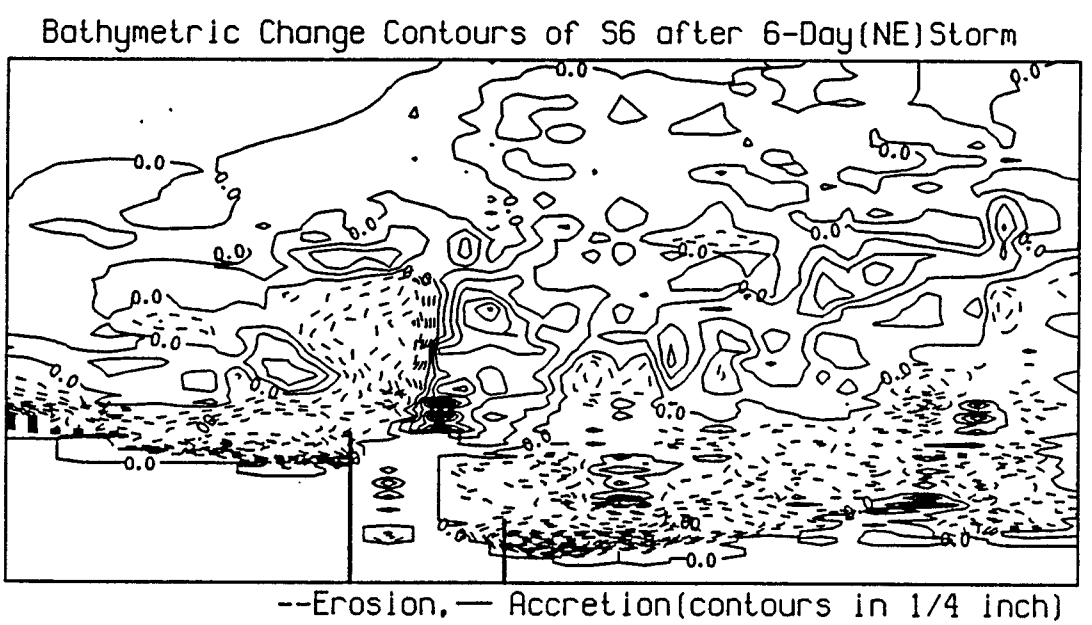

Figure I.3: Bathymetric changes for S5 and S6 in NE storm.

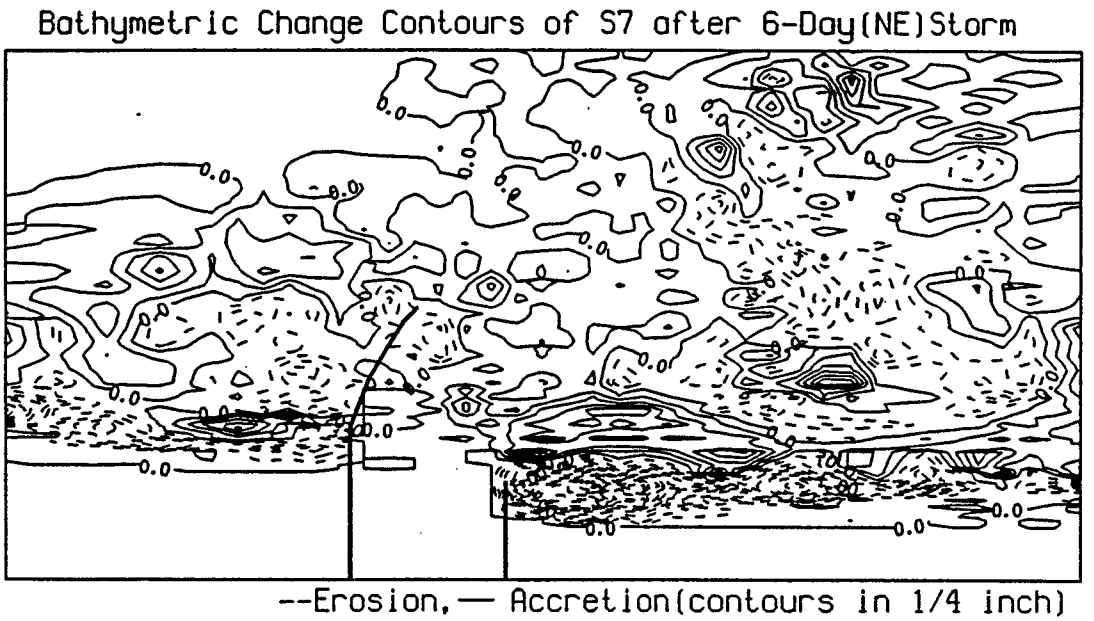

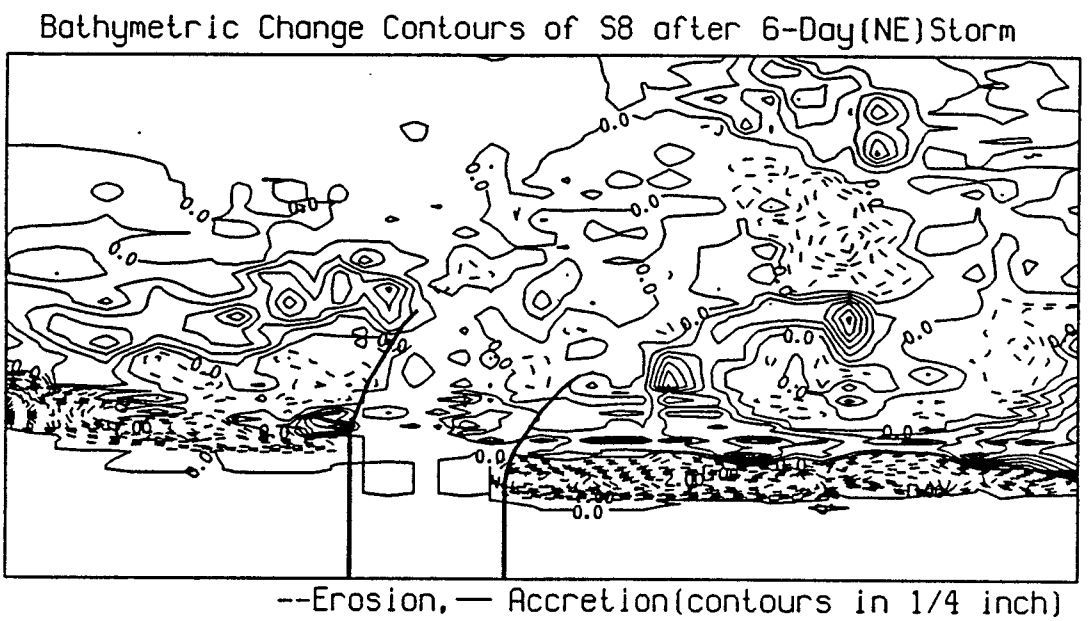

Figure I.4: Bathymetric changes for S7 and S8 in NE storm.

APPENDIX II:
Summary of Bathymetric Change Figures for S1 to S6 in 8-Day E Recovery Process.

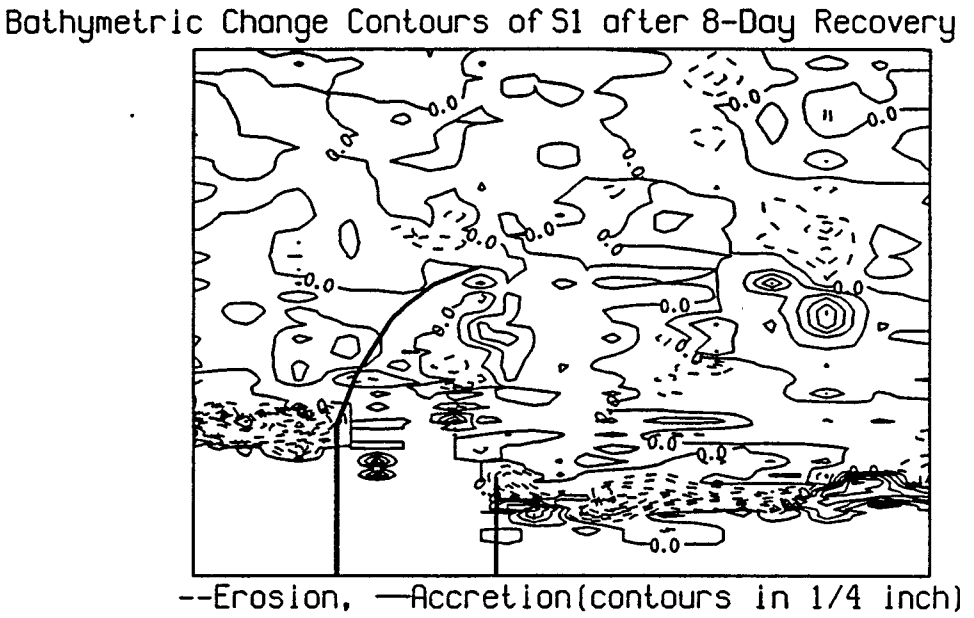

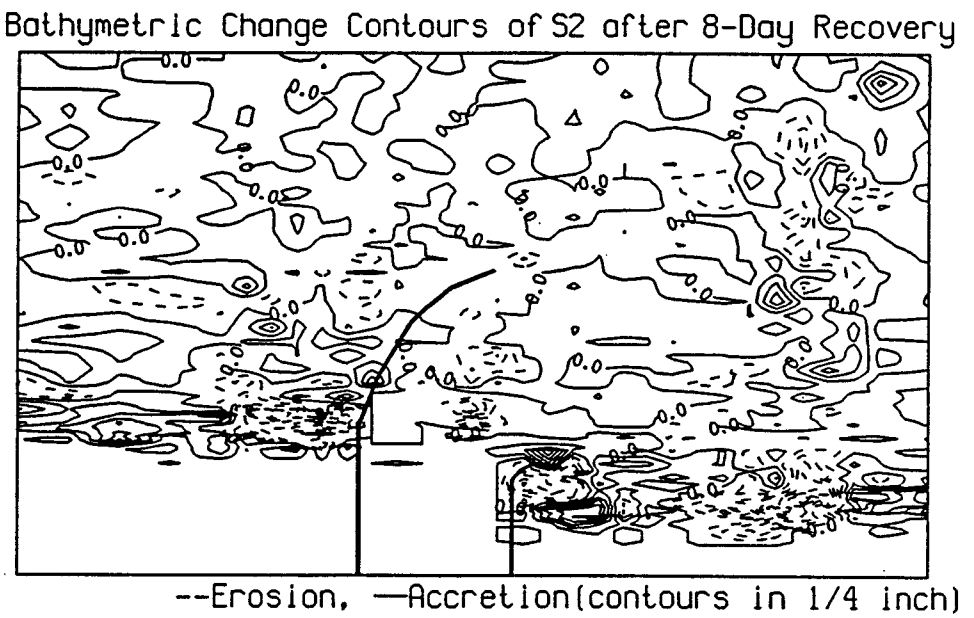

Figure II.1: Bathymetric changes for S1 and S2 in recovery process.

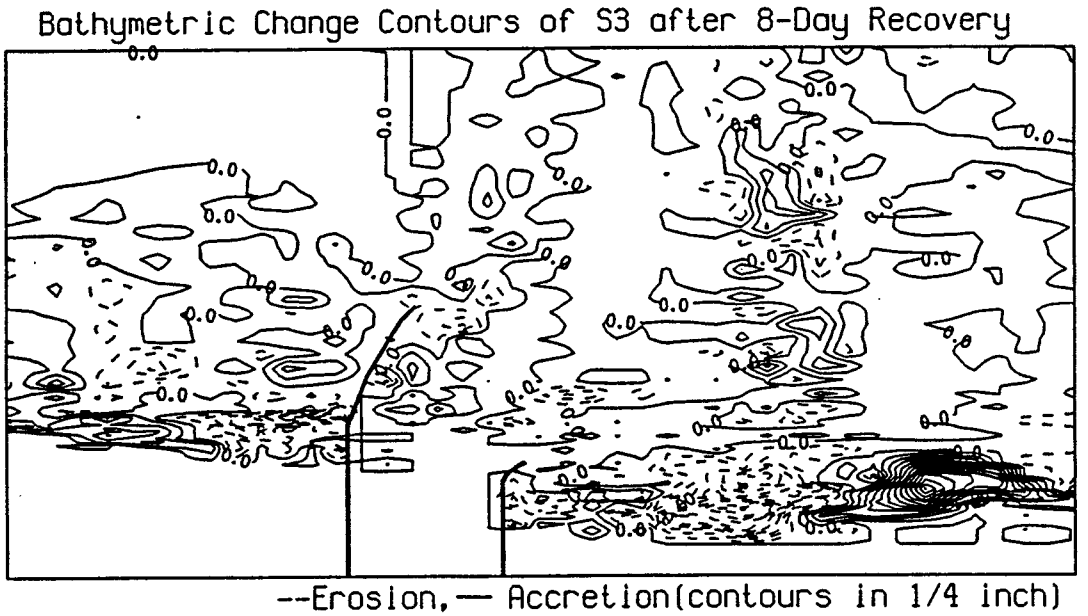

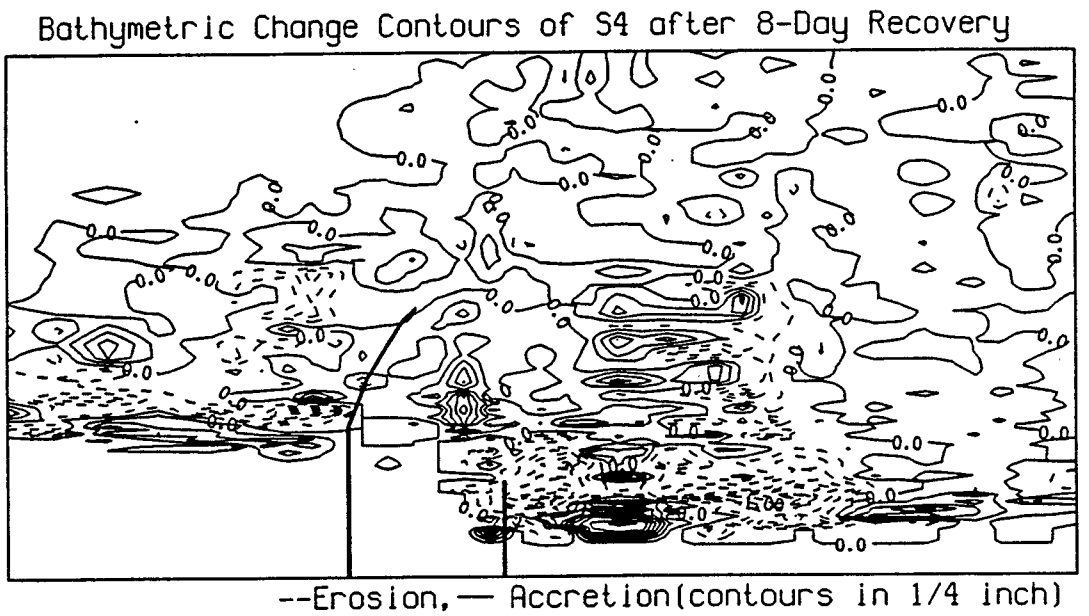

Figure II.2: Bathymetric changes for S3 and S4 in recovery process.

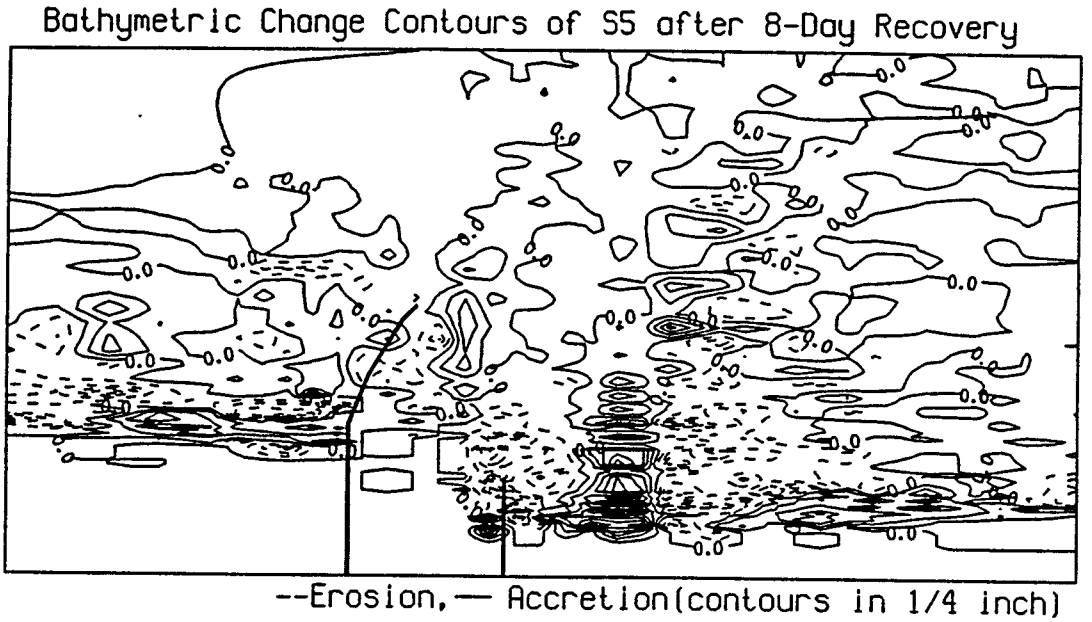

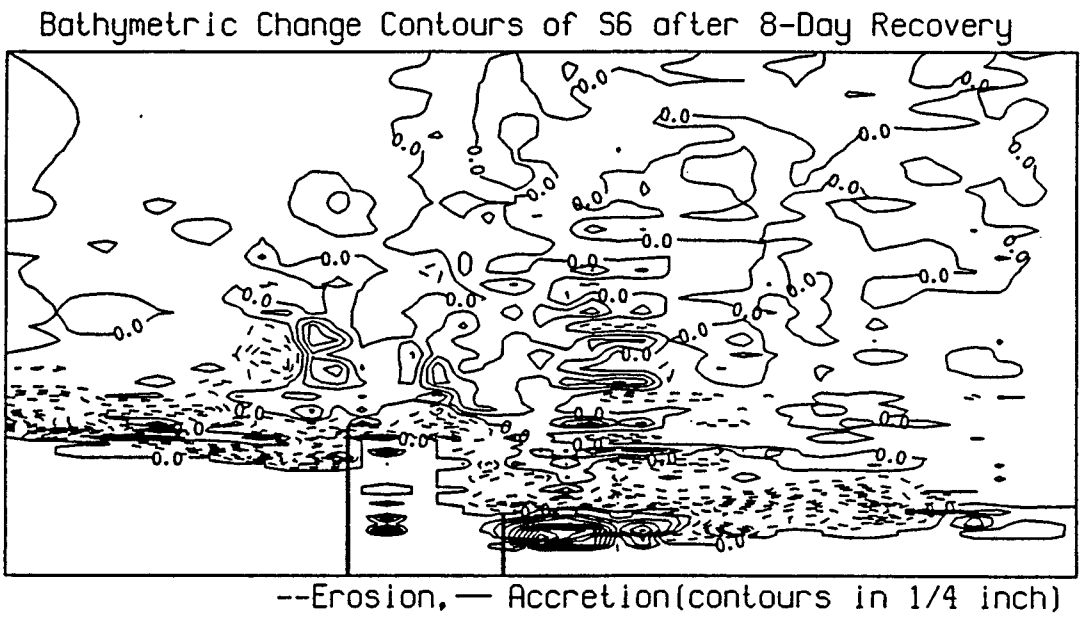

Figure II.3: Bathymetric changes for S5 and S6 in recovery process.

APPENDIX III:
Summary of Bathymetric Change Figures for S2,S4,S6 in 8-Day NE Moderate Wave Process.

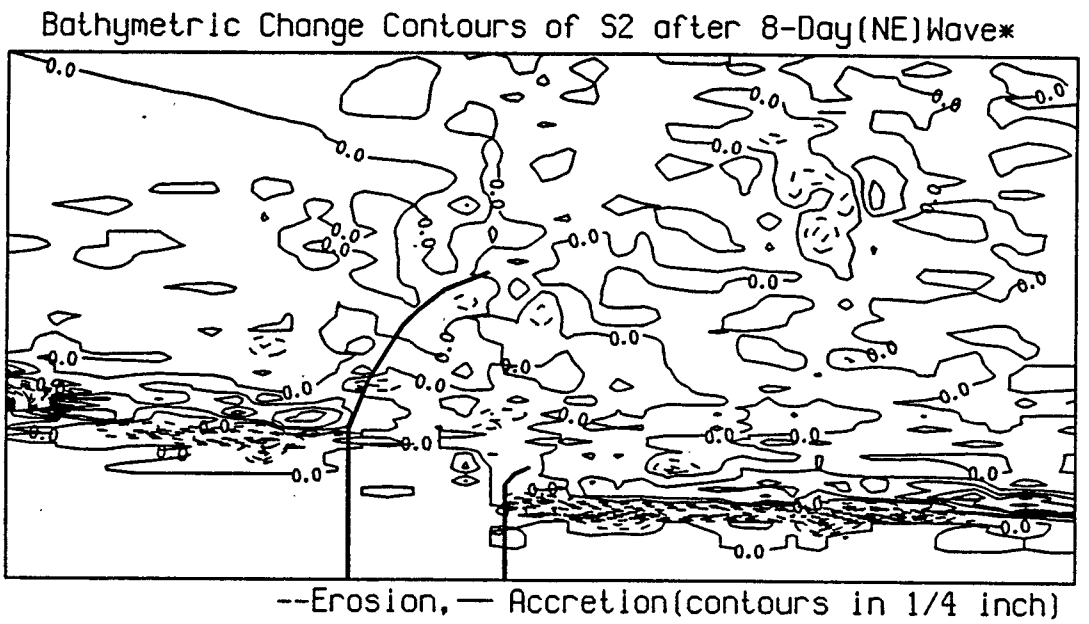

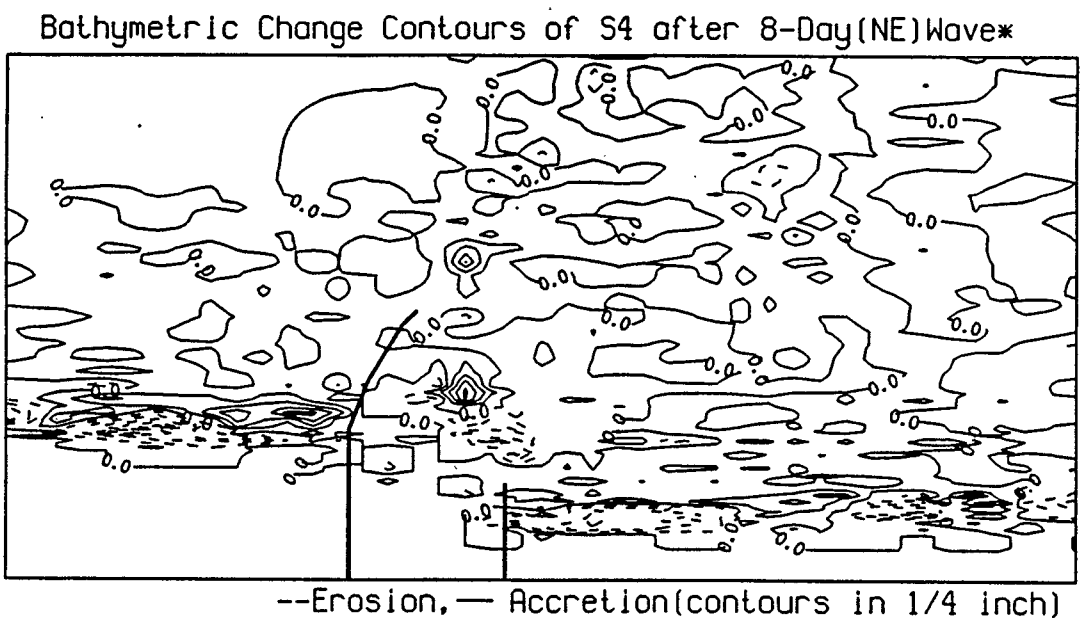

Figure III.1: Bathymetric changes for S2 and S4 under moderate waves.

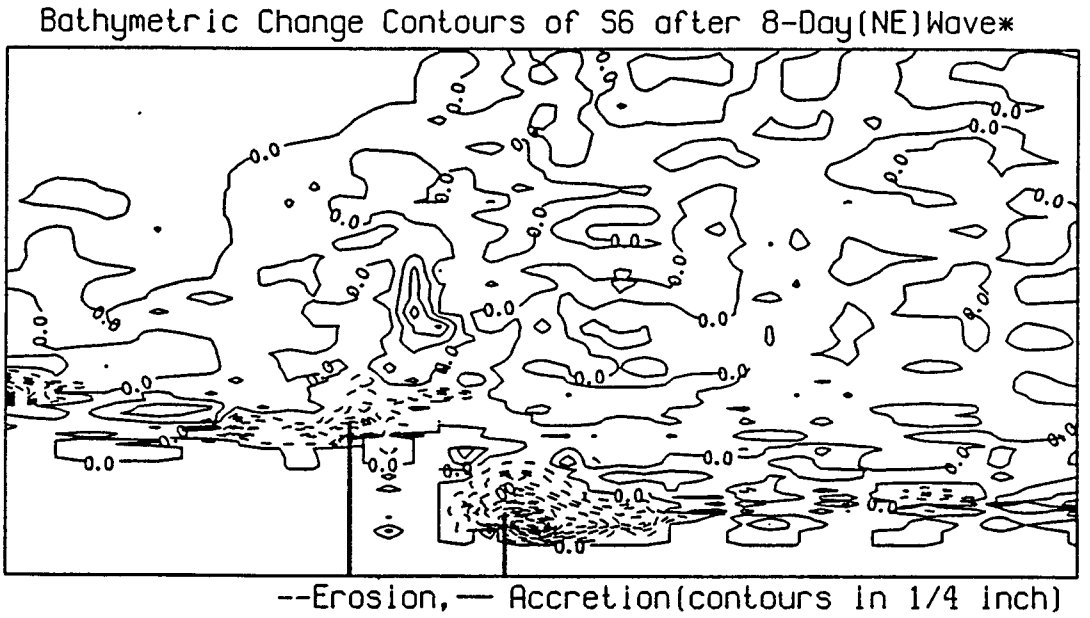

Figure III.2: Bathymetric changes for S6 under moderate waves.

APPENDIX IV:
Summary of Bathymetric Change Figures for S3 and S5 in 6-Day SE Storm Process.

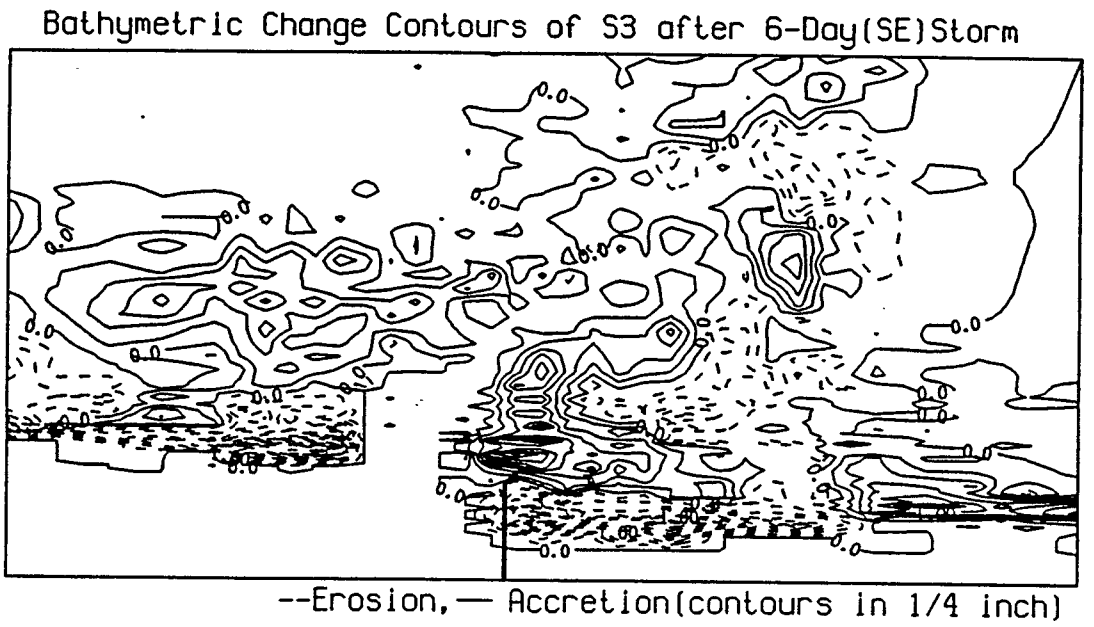

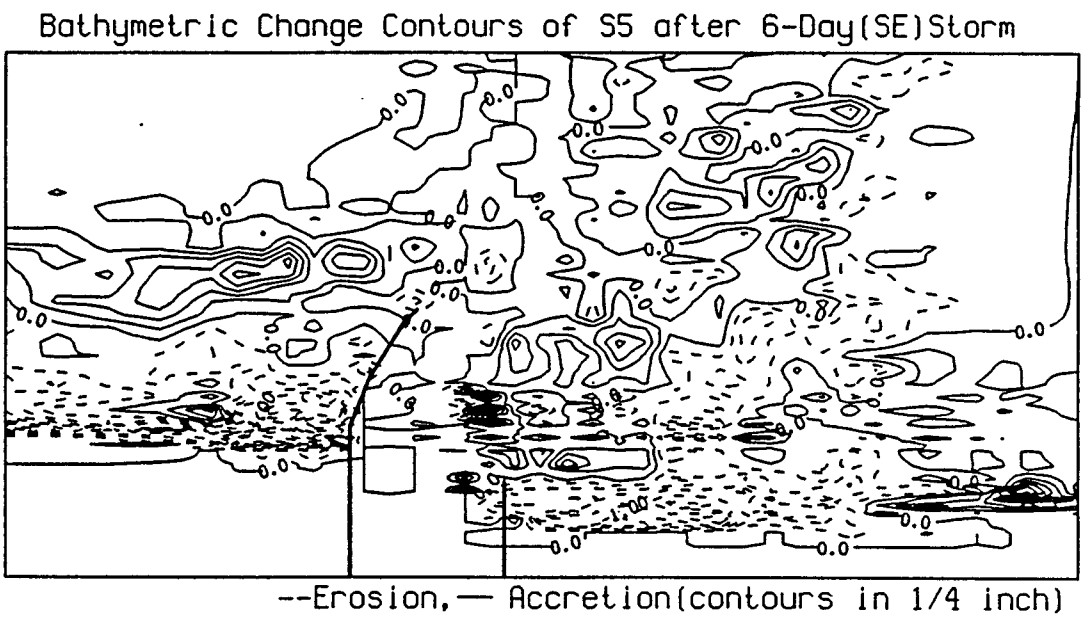

Figure IV.1: Bathymetric changes for S3 and S5 in SE storm.

APPENDIX V:
Summary of Southside Profile Changes for S1 to S8 in 6-Day NE Storm Process.

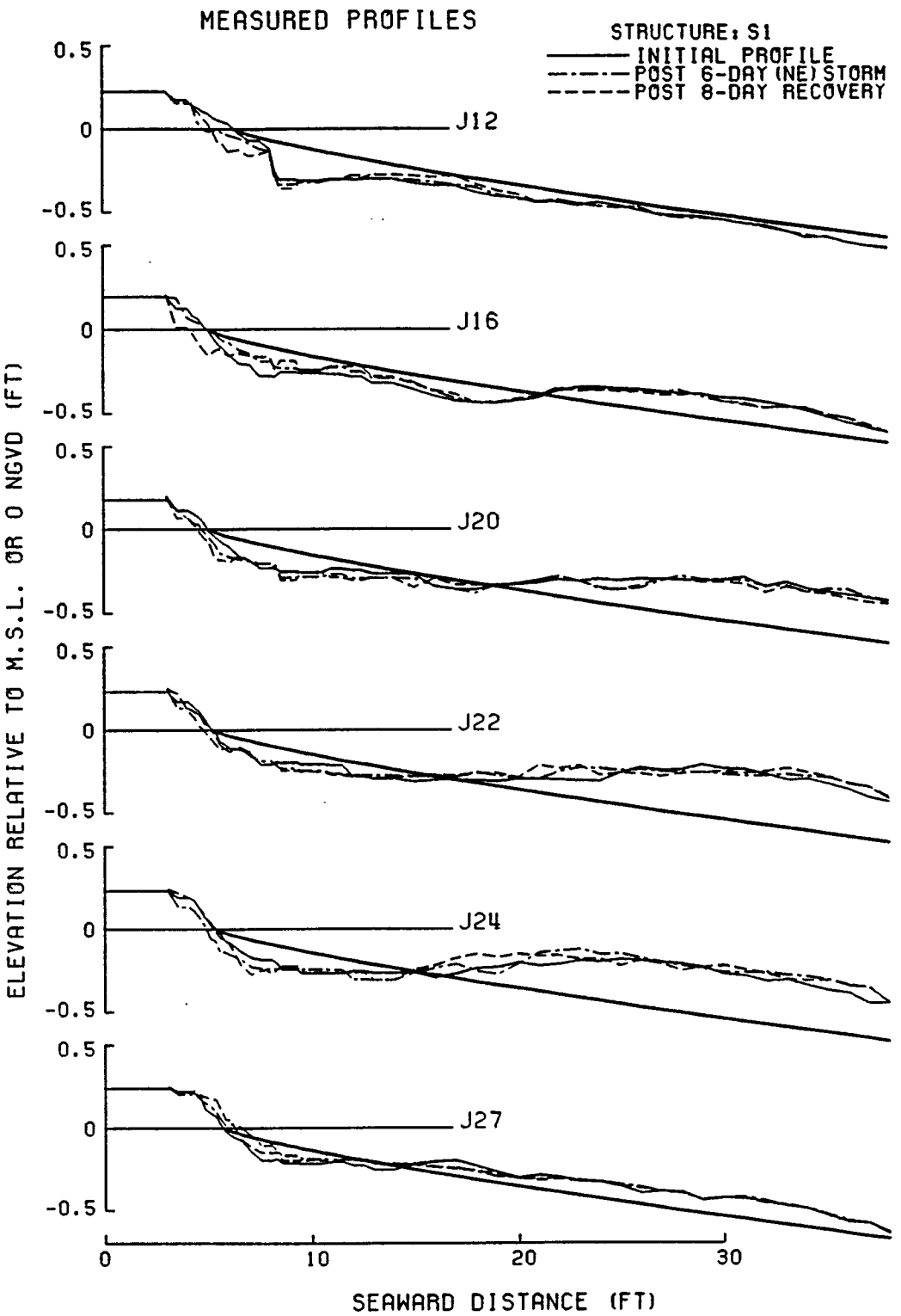

Figure V.1: Comparisons of surveyed profiles from J12 to J27 for S1.

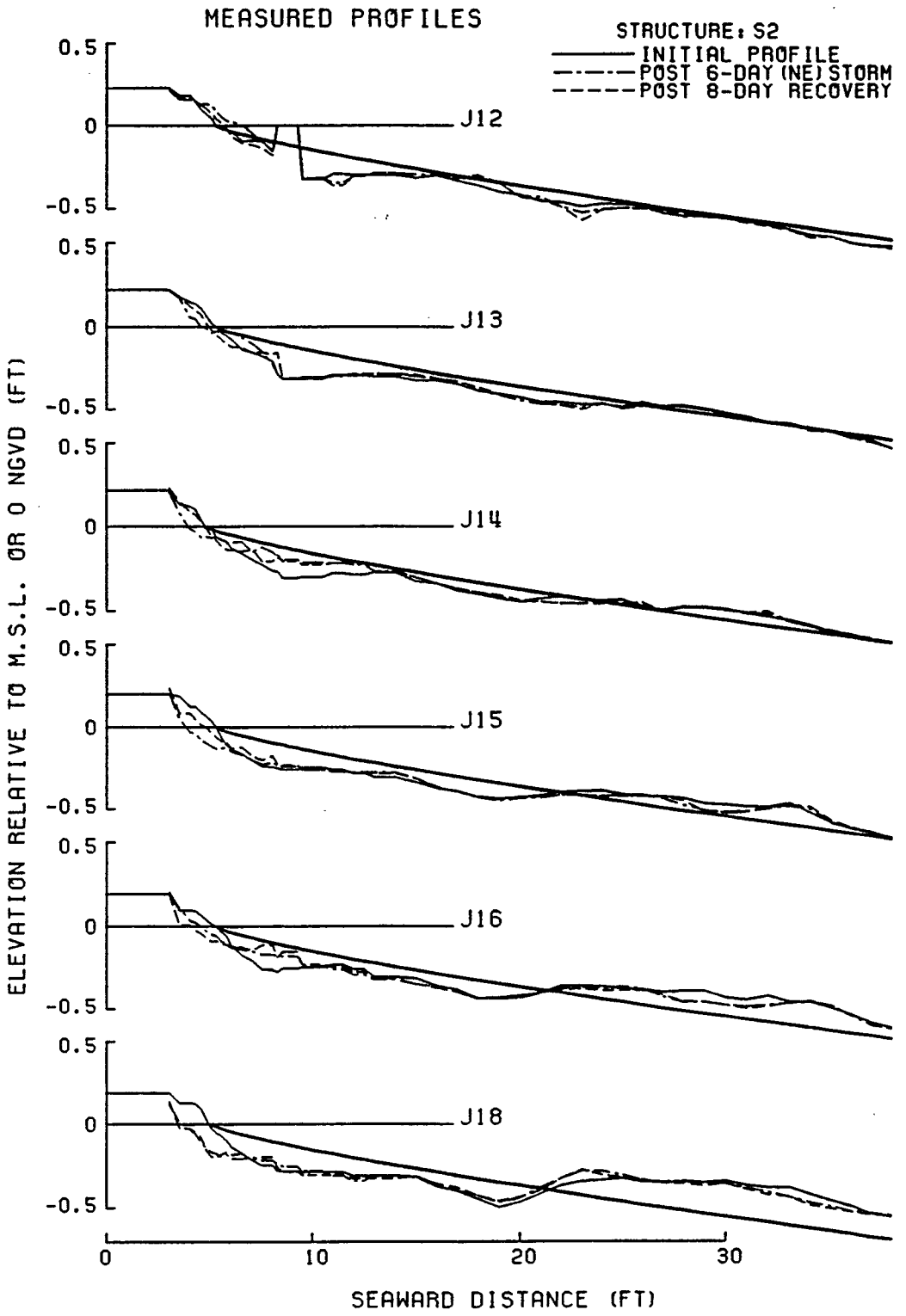

Figure V.2: Comparisons of surveyed profiles from J12 to J18 for S2.

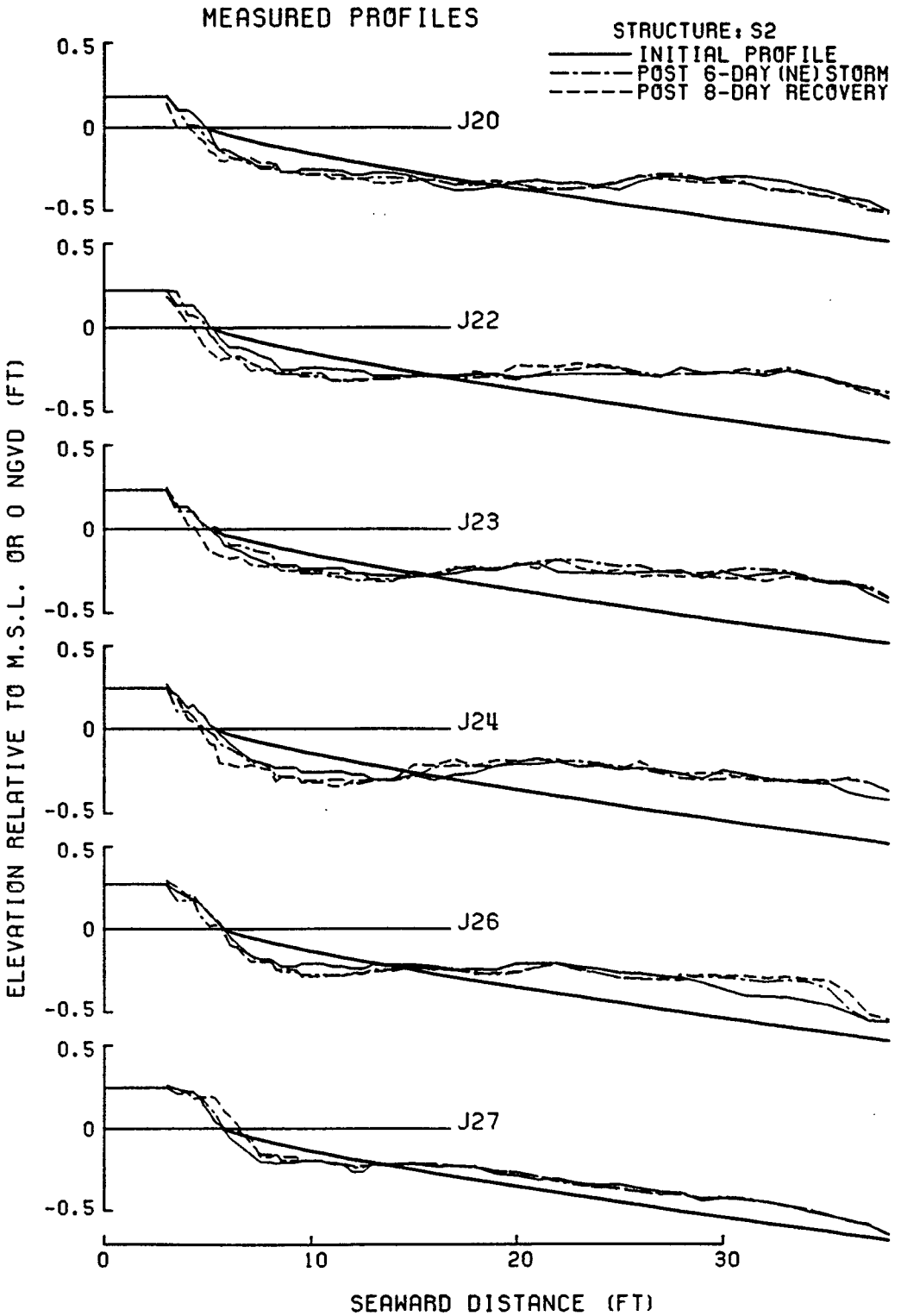

Figure V.3: Comparisons of surveyed profiles from J20 to J27 for S2.

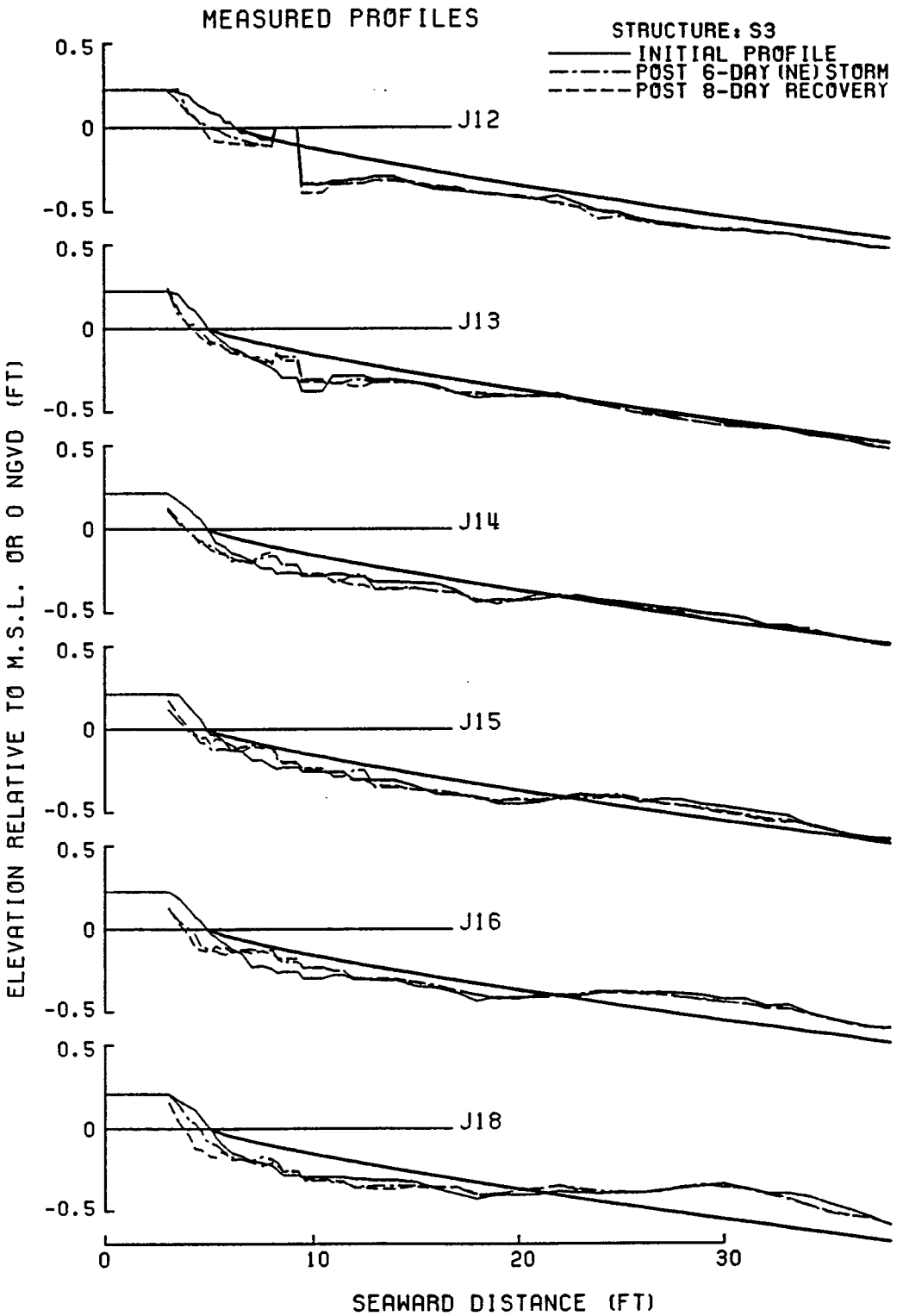

Figure V.4: Comparisons of surveyed profiles from J12 to J18 for S3.

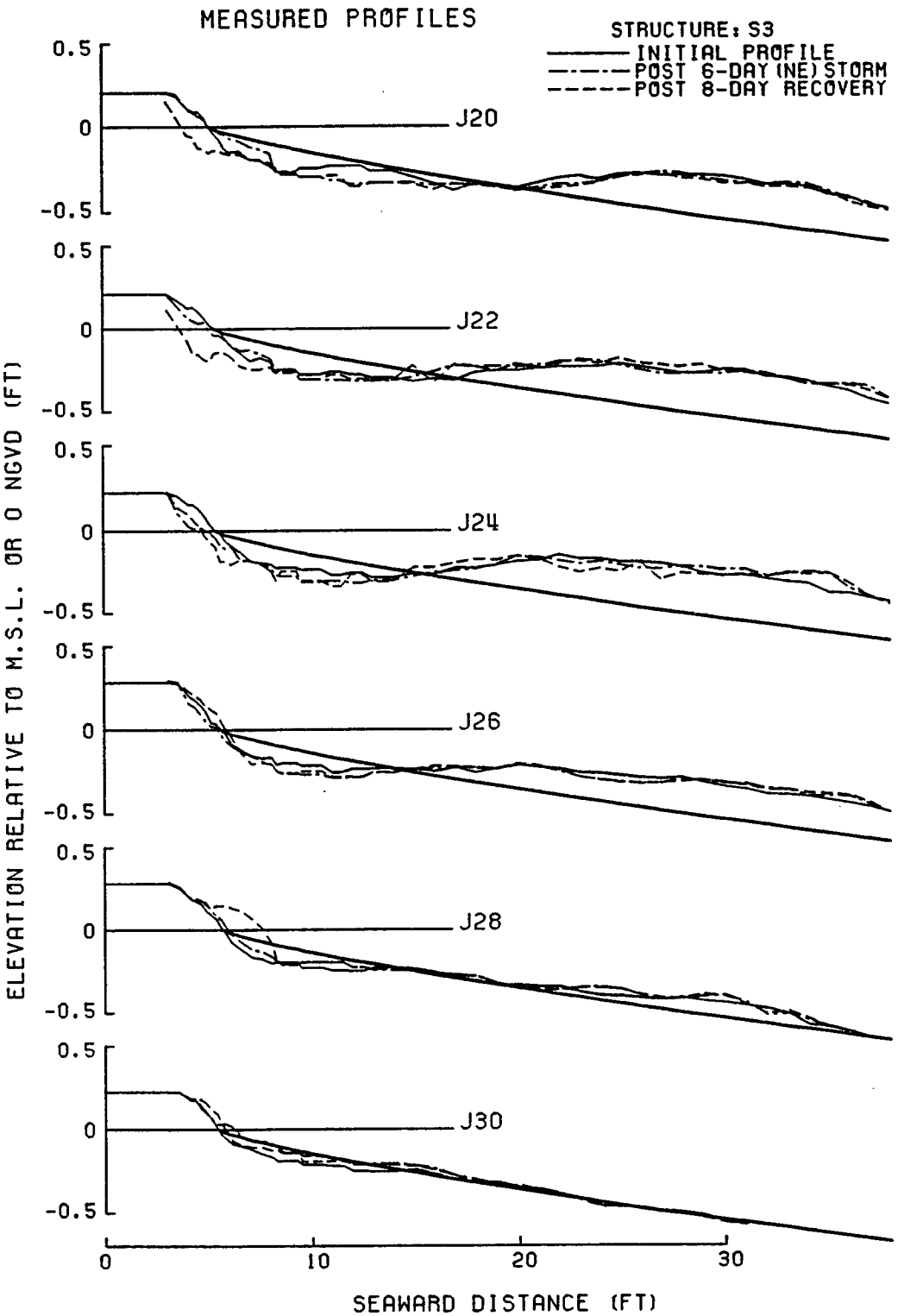

Figure V.5: Comparisons of surveyed profiles from J20 to J30 for S3.

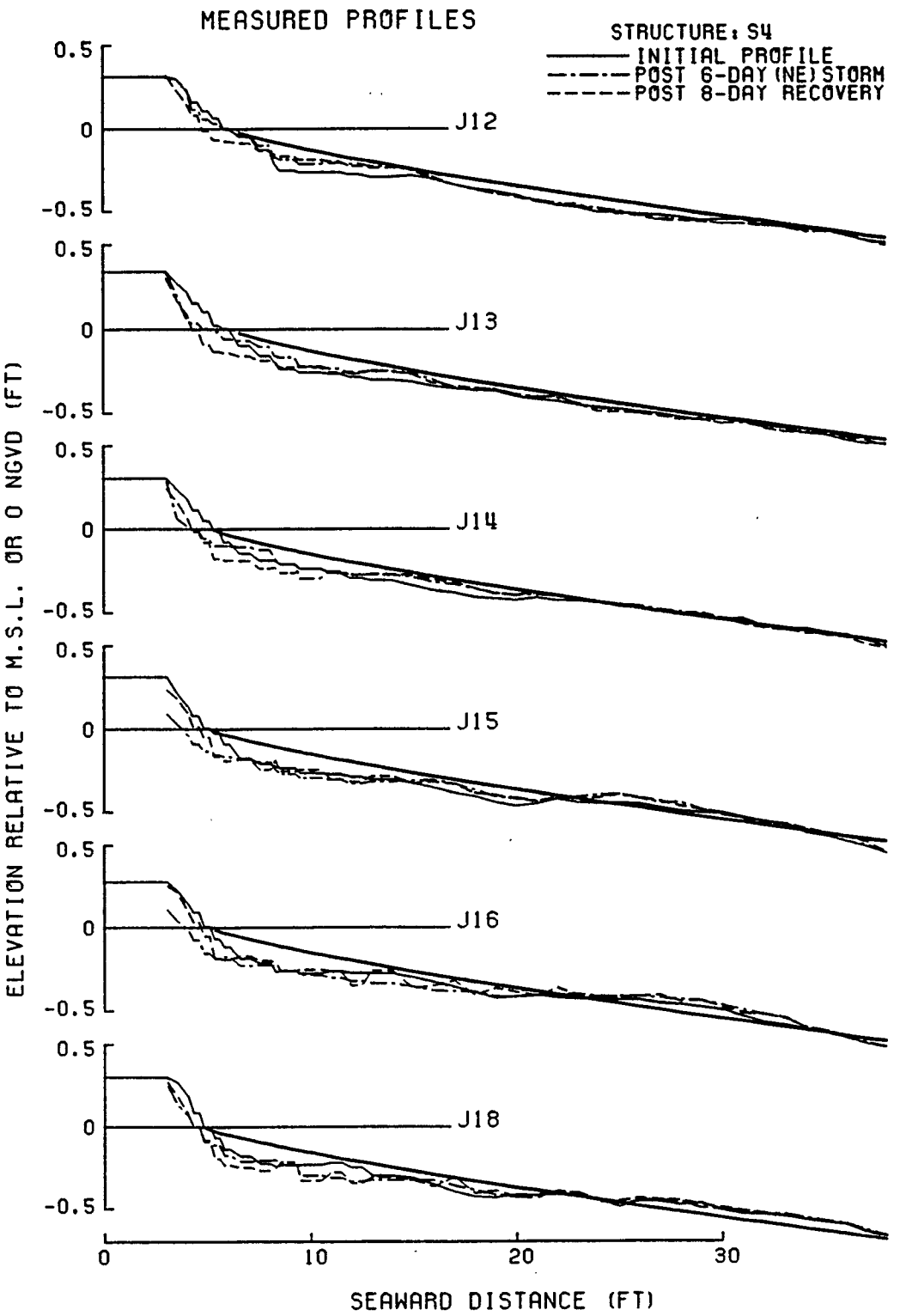

Figure V.6: Comparisons of surveyed profiles from J12 to J18 for S4.

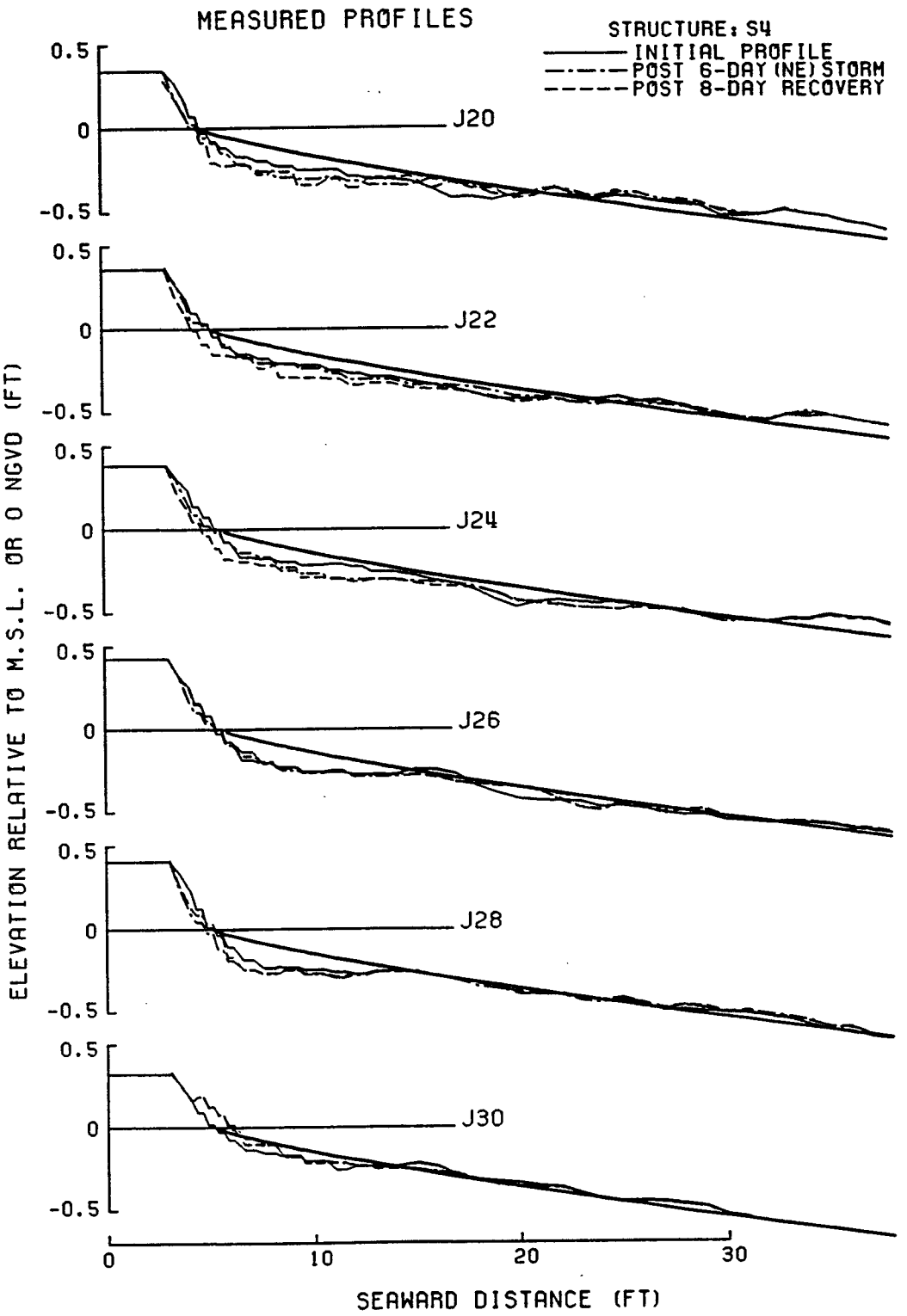

Figure V.7: Comparisons of surveyed profiles from J20 to J30 for S4.

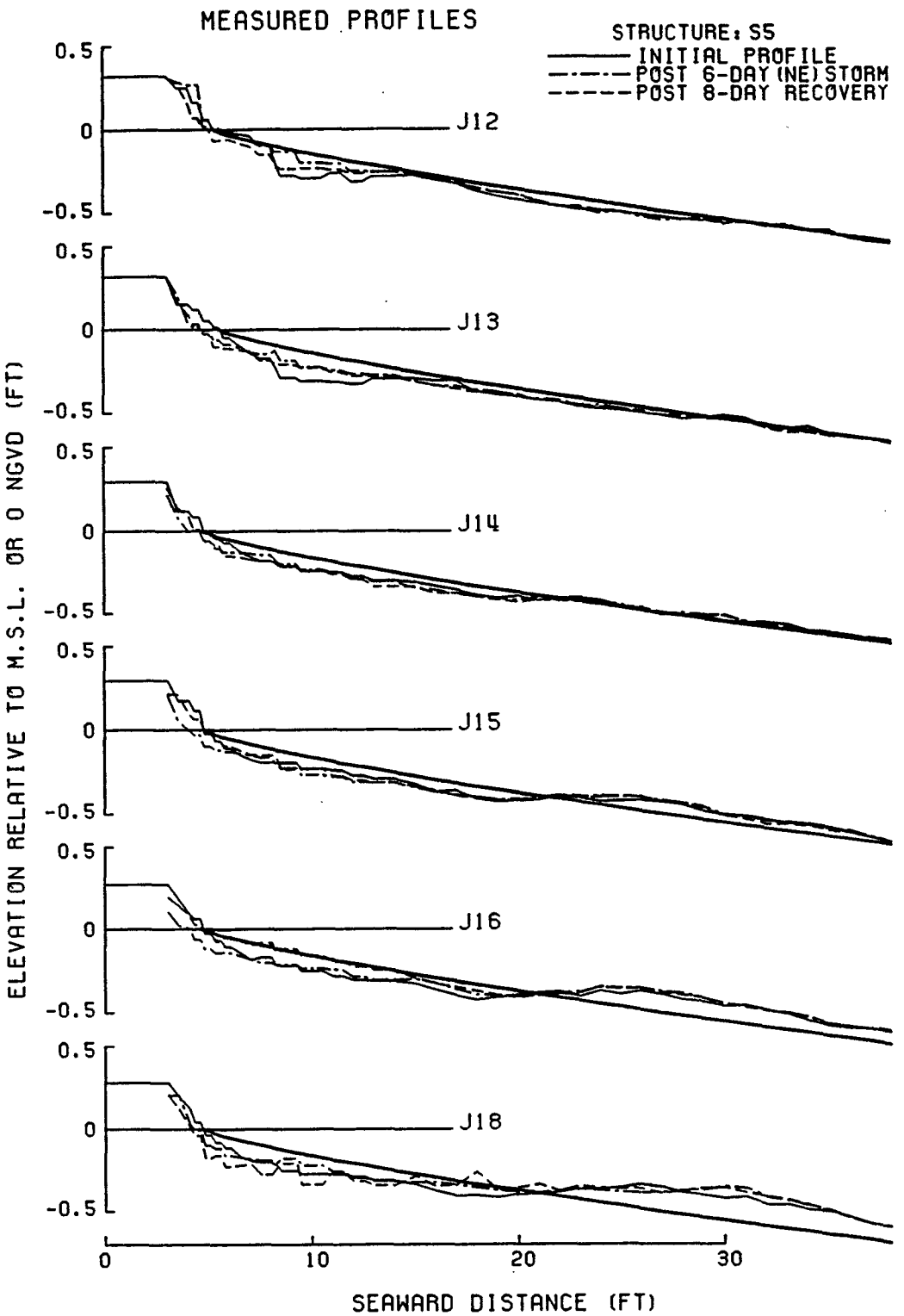

Figure V.8: Comparisons of surveyed profiles from J12 to J18 for S5.

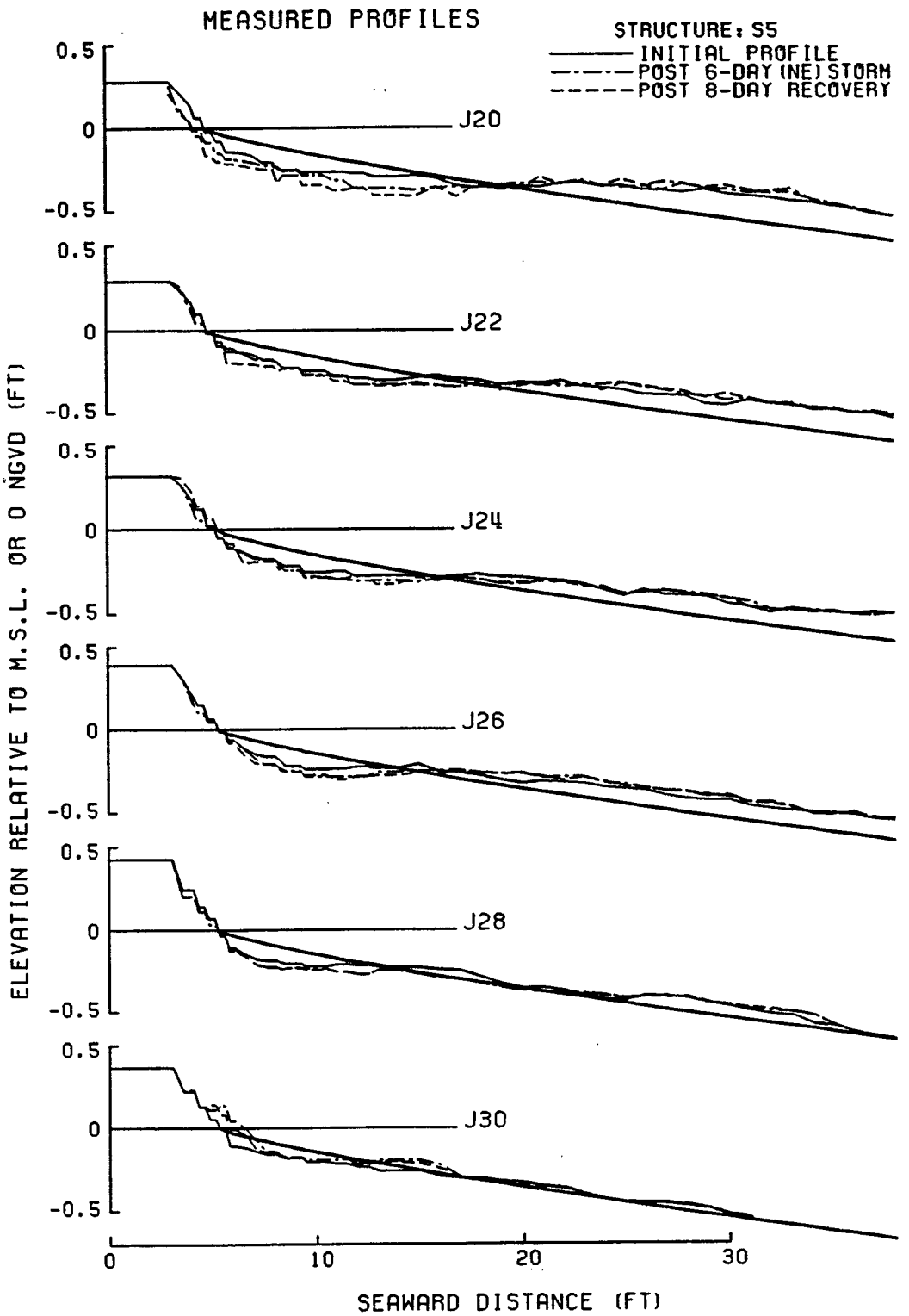

Figure V.9: Comparisons of surveyed profiles from J20 to J30 for S5.

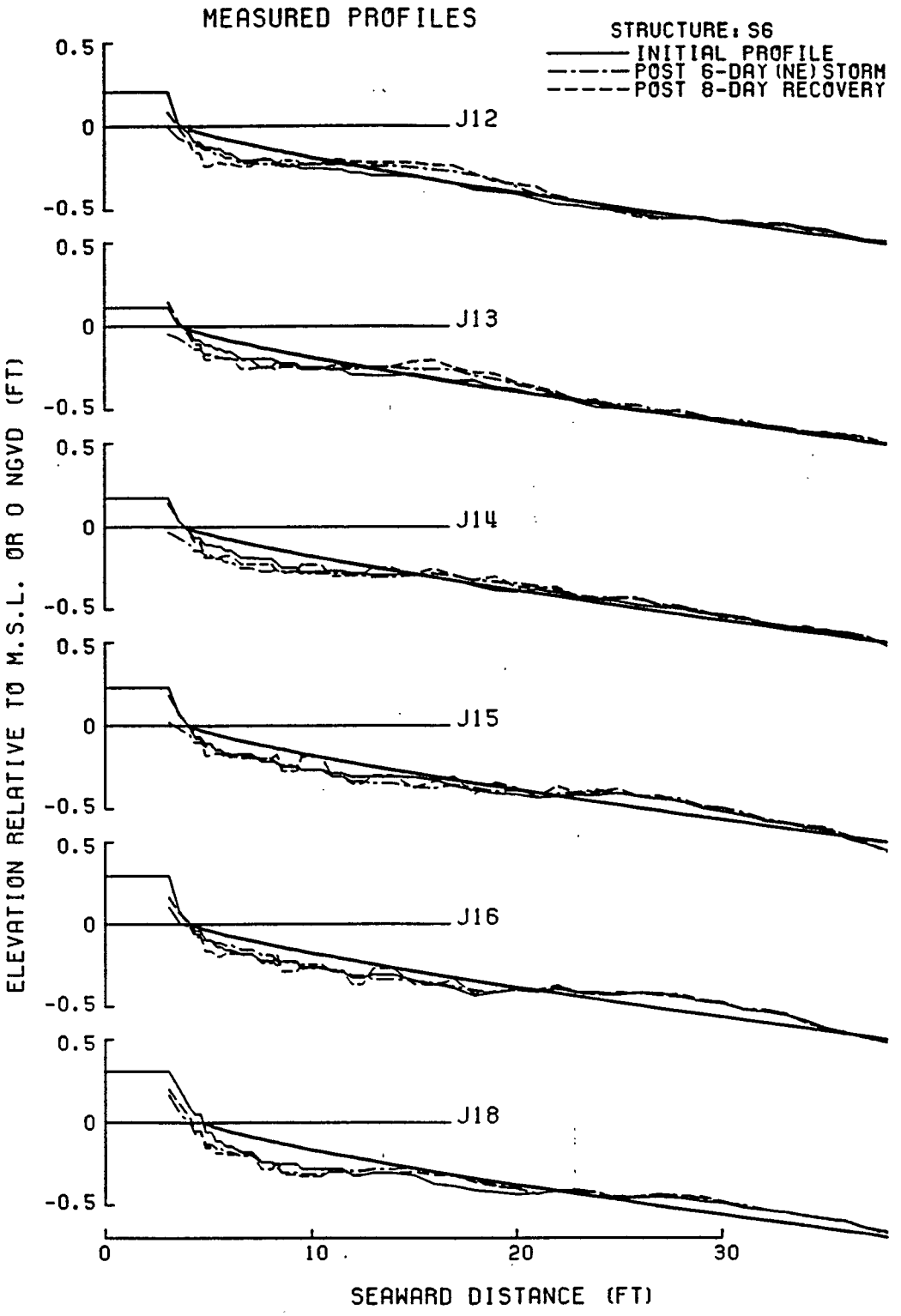

Figure V.10: Comparisons of surveyed profiles from J12 to J18 for S6.

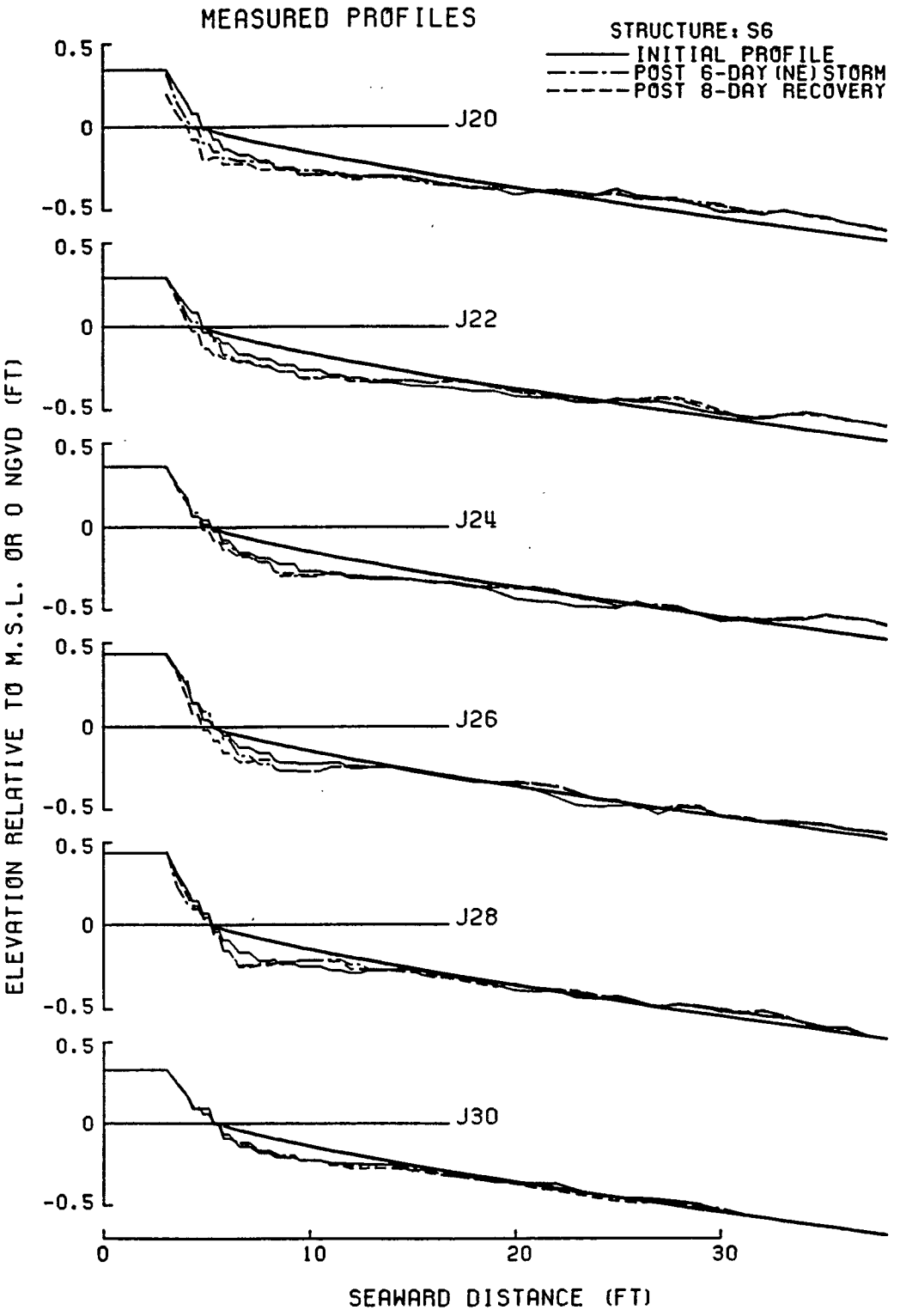

Figure V.11: Comparisons of surveyed profiles from J20 to J30 for S6.

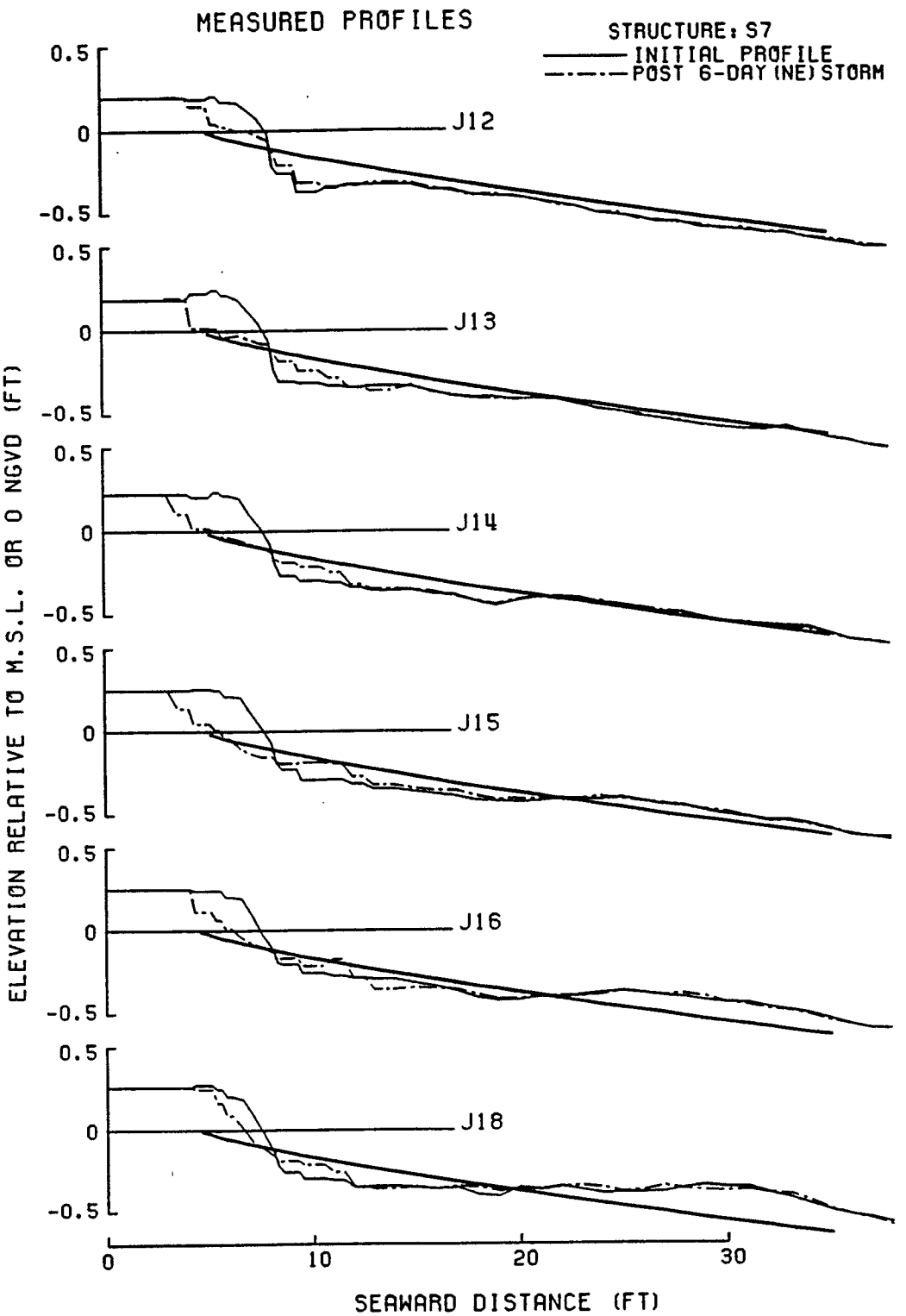

Figure V.12: Comparisons of surveyed profiles from J12 to J18 for S7.

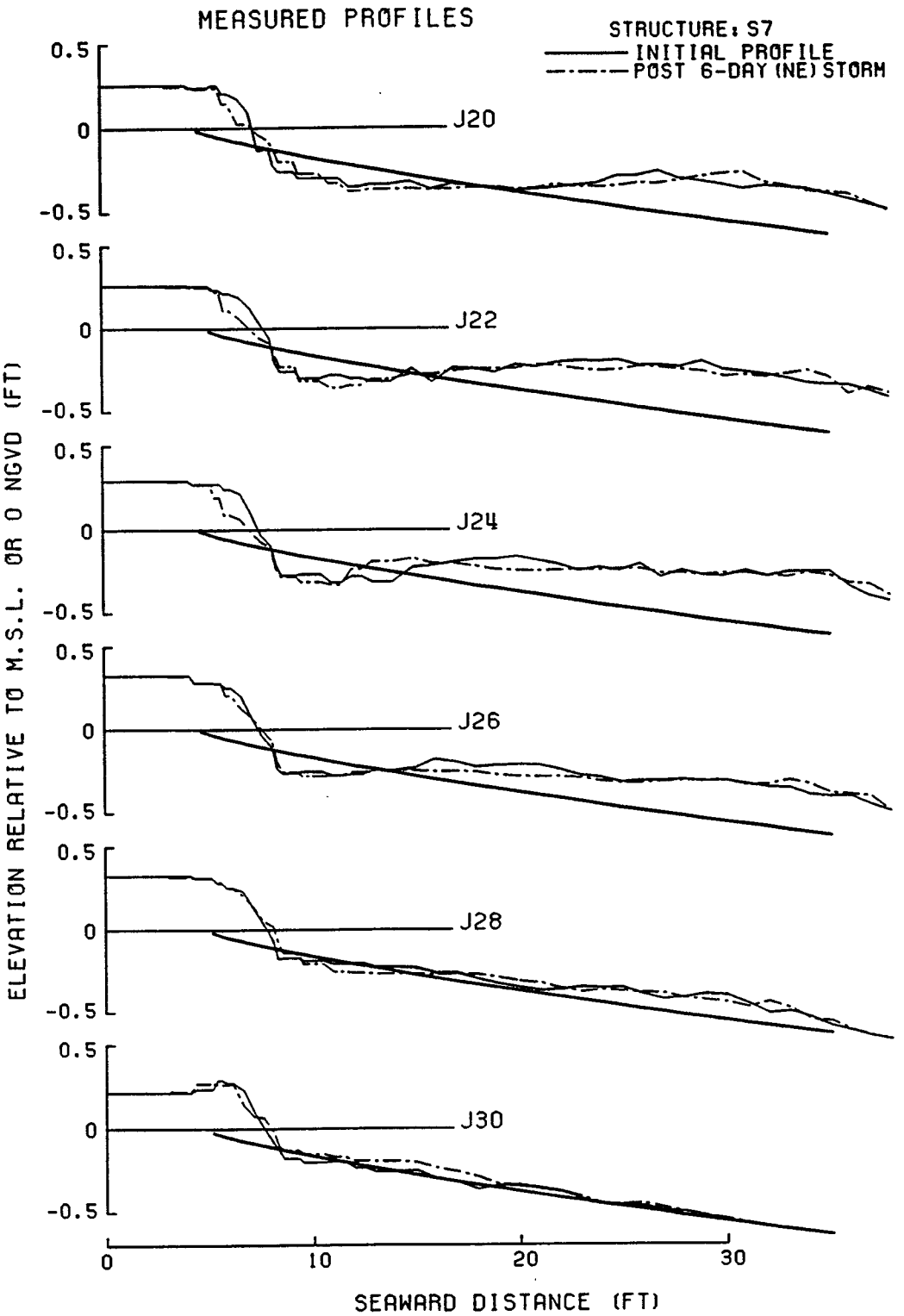

Figure V.13: Comparisons of surveyed profiles from J20 to J30 for S7.

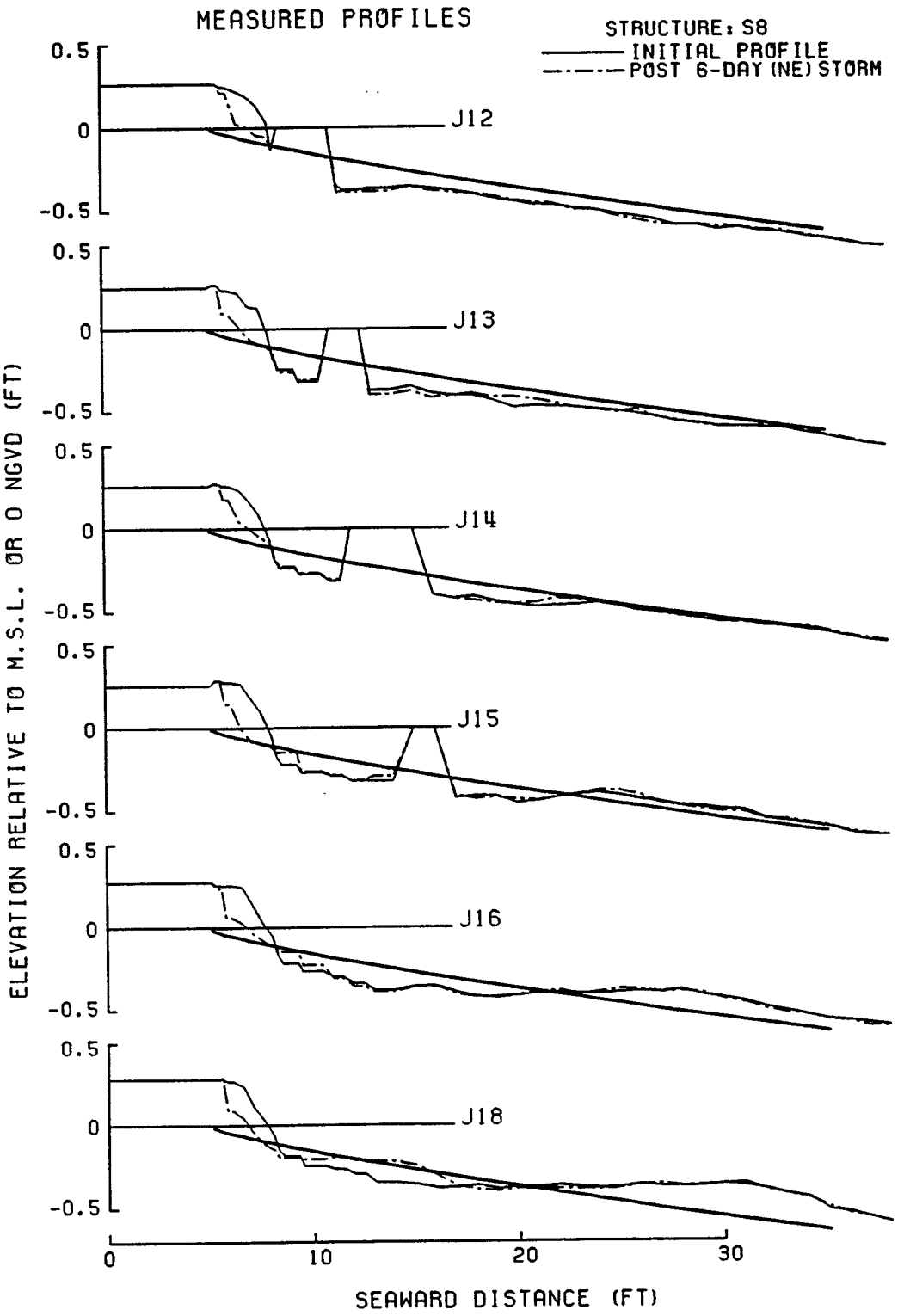

Figure V.14: Comparisons of surveyed profiles from J12 to J18 for S8.

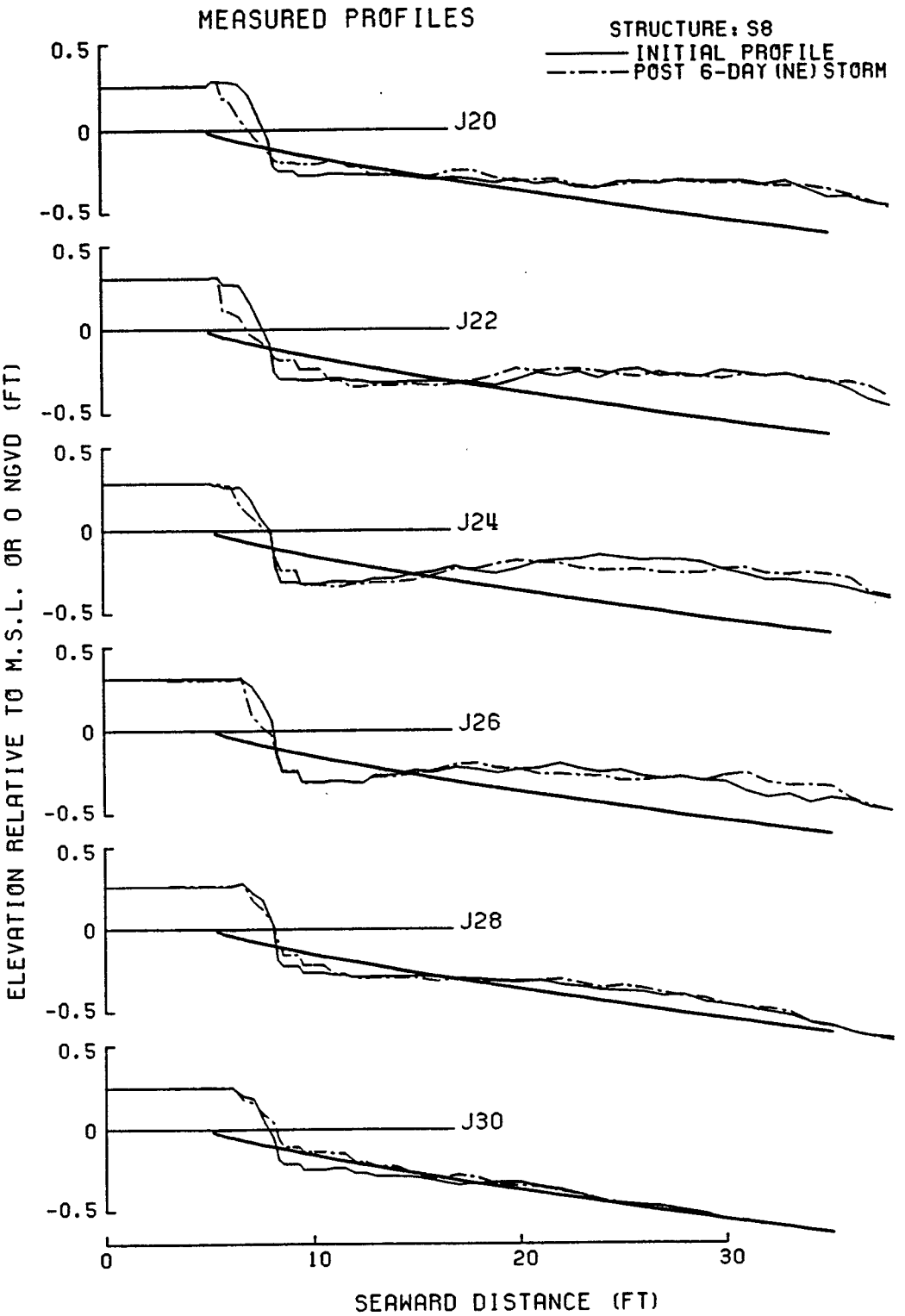

Figure V.15: Comparisons of surveyed profiles from J20 to J30 for S8.

APPENDIX VI:
Histogram Presentation of Sand Budget Based on Laboratory Experiment Results.

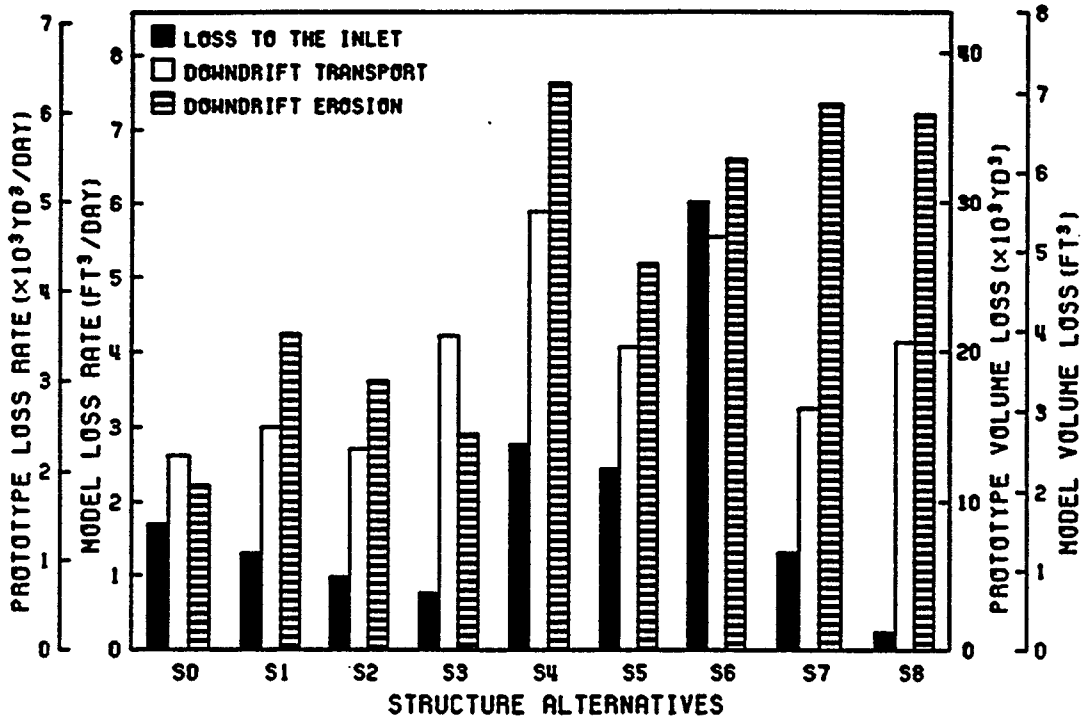

Figure VI.1: Sand budget from 6-day NE storm.

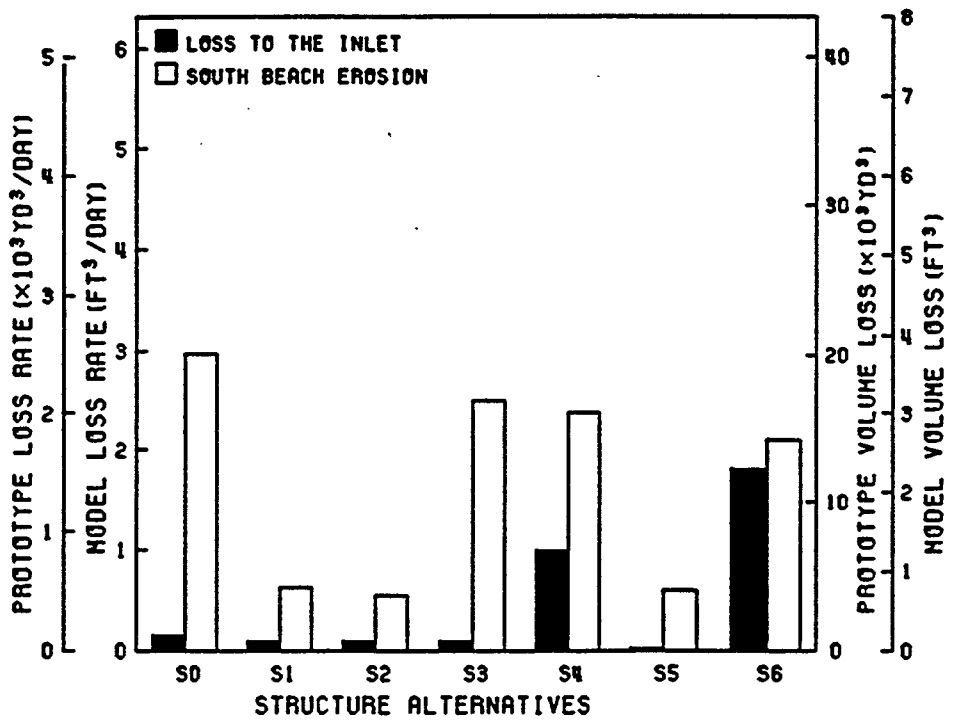

Figure VI.2: Sand budget from 8-day E recovery process.

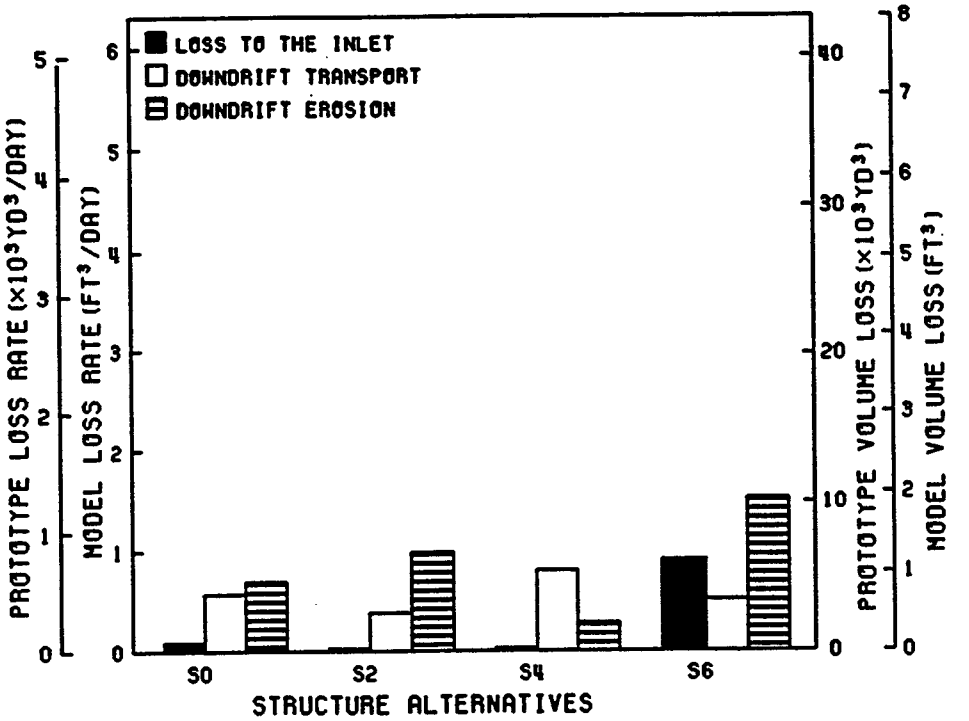

Figure VI.3: Sand budget from 8-day NE moderate wave process.

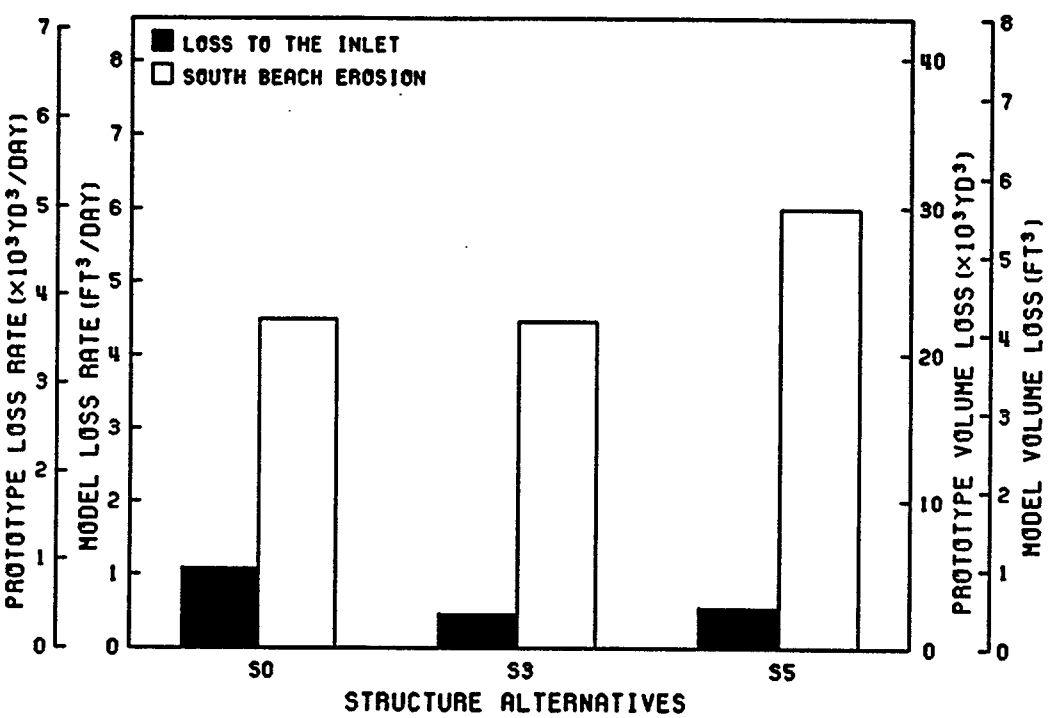

Figure VI.4: Sand budget from 6-day SE storm.